

**INVESTIGATION OF THE ADSORPTION KINETICS OF
SOME RADIOISOTOPES ON CLAY MINERALS IN
TURKEY AND EVALUATION OF THERMODYNAMIC
PARAMETERS OF ADSORPTION**

BERNA YILDIZ

**Submitted to Institute of Science of Hacettepe University
as a partial fulfillment for the requirements for the award of the degree of
DOCTOR OF PHILOSOPHY
in CHEMISTRY**

2007

**BAZI RADYOİZOTOPLARIN TÜRKİYE'DEKİ KİLLER
ÜZERİNDEKİ ADSORPSİYON KİNETİĞİNİN İNCELENMESİ
VE ADSORPSİYONA AİT TERMODİNAMİK
BÜYÜKLÜKLERİN BULUNMASI**

**INVESTIGATION OF THE ADSORPTION KINETICS OF
SOME RADIOISOTOPES ON CLAY MINERALS IN
TURKEY AND EVALUATION OF THERMODYNAMIC
PARAMETERS OF ADSORPTION**

BERNA YILDIZ

**Submitted to Institute of Science of Hacettepe University
as a partial fulfillment for the requirements for the award of the degree of**

DOCTOR OF PHILOSOPHY

in CHEMISTRY

2007

to my mummy,
TUNA YILDIZ

INVESTIGATION OF THE ADSORPTION KINETICS OF SOME RADIOISOTOPES ON CLAY MINERALS IN TURKEY AND EVALUATION OF THERMODYNAMIC PARAMETERS OF ADSORPTION

Berna Yıldız

ABSTRACT

In the scope of the thesis, the main subject is to investigate the zeolite and clay-radioisotope interactions by radiotracer method. Either zeolite and clay can be proposed as a sorption material in order to use in geological barriers against the leakage and spread of radioactive waste from the repositories. ⁶⁵Zinc ($t_{1/2}=245$ days) , ¹³³Barium ($t_{1/2}=10.7$ years), ⁶⁰Cobalt ($t_{1/2}=5.271$ years), ¹³⁷Caesium ($t_{1/2}=30.15$ years) and ⁹⁰Strontium ($t_{1/2}=28.1$ years) were used as radioisotope cause of their most abundance in the radioactive wastes. Sorption experiments were carried out by natural Bentonite (Çankırı), Zeolite (Balıkesir-Bigadiç) and Kaolin (Bilecik-Bigadiç) at different temperatures and at different concentrations. Measurement were taken with a NaI crystal gamma counter and end window Geiger Müller counter. Samples were characterized; chemical compositions were determined by Induced coupled plasma technique, the particle size distribution was found out by laser sizer, the surface areas of the particles were performed by BET (Brunauer, Emmett and Teller method) the structure analysis were made by using X-ray diffraction. According to very high uptake results; clay and zeolite can be proposed as a good adsorbent to contribute to the waste management. By the increase of temperature adsorption amount increases at all systems. Desorption of the sorbed amount does not occur significantly. Thermodynamic parameters of adsorption were investigated; for all types of adsorbent-radioisotope systems it was found highly negative value for Gibbs energy, ΔG° , indicating that adsorption process is spontaneous, positive enthalpy of adsorption, ΔH° , indicating the process is endothermic, and positive entropy, ΔS° .

Keywords: Clay, Bentonite, Kaolin, Zeolite, Radioactive waste disposal, Strontium-90, Zinc-65, Barium-133, Caesium-137, Cobalt-60.

Advisor: Prof.Dr. Mehmet KIŞ, Hacettepe University, Department of Chemistry, Physical Chemistry Section,

Co-advisor: Prof.Dr. Hasan ERTEN, Bilkent University, Department of Chemistry.

BAZI RADYOİZOTOPLARIN TÜRKİYE'DEKİ KİLLER ÜZERİNDEKİ ADSORPSİYON KİNETİĞİNİN İNCELENMESİ VE ADSORPSİYONA AİT TERMODİNAMİK BÜYÜKLÜKLERİN BULUNMASI

Berna Yıldız

ÖZ

Tez kapsamında, esas konu zeolit ve kil ile radyoizotop etkileşimlerini radyotracer yöntemiyle takip etmektir. Hem zeolit hem kil radyoaktif atıkların depolardan sızması ve yayılmasına karşın jeolojik engellerde kullanmak amacıyla tutulma malzemesi olarak önerilebilir.

Radyoaktif atıklarda bol miktarda bulunmaları nedeniyle ⁶⁵Çinko ($t_{1/2}=245$ gün) , ¹³³Baryum ($t_{1/2}=10.7$ yıl), ⁶⁰Kobalt ($t_{1/2}=5.271$ yıl), ¹³⁷Sezyum ($t_{1/2}=30.15$ yıl) and ⁹⁰Stronsyum ($t_{1/2}=28.1$ yıl) radyoizotop olarak kullanıldı. Tutulma deneyleri doğal bentonit (Çankırı), zeolit (Balıkesir-Bigadiç) ve kaolen (Bilecik-Bigadiç) ile değişik konsantrasyon ve sıcaklıklarda gerçekleştirildi. Ölçümler NaI kristalli gamma sayıcısı ve Geiger Müller sayıcısı ile yapıldı. Kil numuneleri karakterize edildi; kimyasal bileşimleri ICP plazma tekniğiyle, parçacık boyut dağılımı lazer ile, partiküllerin yüzey alanları BET (Brunauer, Emmett ve Teller metodu) ile, yapı analizi X-ışınları difraksiyonu kullanılarak tespit edildi. Yüksek tutulma sonuçlarına göre; kil ve zeolit atıkların bertarafı için iyi adsorbent olarak önerilebilir. Bütün sistemlerde adsorpsiyon miktarı sıcaklık artışıyla artmaktadır. Adsorpsiyon işlemi temelde iyon-değişimine dayanır. Tutulan miktarlar önemli oranlarda geri salınmaz. Adsorpsiyona ait termodinamik büyüklükler takip edildi; tüm adsorbent-radyoizotop türleri için Gibbs enerjisi, ΔG° , için adsorpsiyon işleminin kendiliğinden olduğunu gösteren yüksek negatif değerler, adsorpsiyon entalpisi, ΔH° , için işlemin endotermik olduğunu gösteren pozitif değerler, entropi, ΔS° , için pozitif değerler bulunmuştur.

Anahtar Kelimeler: Kil, Bentonit, Kaolen, Zeolit, Radyoaktif atık depolama, Stronsyum-90, Çinko-65, Baryum-133, Sezyum-137, Kobalt-60.

Danışman: Prof.Dr. Mehmet KIŞ, Hacettepe Üniversitesi, Kimya Bölümü, Fizikokimya Anabilim Dalı.

Eş Danışman: Prof.Dr. Hasan ERTEN, Bilkent Üniversitesi, Kimya Bölümü.

ACKNOWLEDGMENT

In my doctorate studies I used 2500 experiment tubes and 2500 counting tubes. I managed to study in a new research area in a laboratory that I organized again from the beginning. Especially, during one year, I went to my laboratory every day for experiments, even every national & religious feast days and new year's day. I succeeded in these difficult working conditions with a big patience. I supplied my power from my dear family. I am very grateful to my mother TUNA YILDIZ and my brother MUTLU YILDIZ for their support.

I would like to thank Dean of Faculty of Science at Bilkent University Prof.Dr. HASAN ERTEN who suggested the subject of my thesis. I get this research field due to his valuable guidance.

Prof.Dr. ÖZGEN BİRGÜL, from Department of Physics, is very important name in my thesis. He made possible γ -counting system in my laboratory for me. He solved my technical difficulties. He came to my laboratory whenever I called him to help me, even at week-end.

I am very grateful to HAKAN DÜNDAR who helped me in grinding procedure of the samples, to ÖMÜRDEN GENÇ for laser sizer, to ABDULLAH OBUT for BET experiments and his suggestions, to ÖZEN ÖZGEN for X-rays studies, to NICHOLE BARRE from Paris-Sud XI for repeat results of BET, to SOLMAZ KARABULUT for her moral support.

I am indebted to our great leader ATATÜRK for attaining our national freedom and offering us the woman rights; as a consequence of which we are dealing with science freely...

BERNA YILDIZ

INDEX

	<u>Page</u>
ÖZ	i
ABSTRACT	ii
ACKNOWLEDGEMENTS	iii
INDEX	iv
FIGURE INDEX	vii
TABLE INDEX	xiii
LIST OF ABBREVIATIONS	xiv
1. INTRODUCTION	1
2.THEORETICAL BACKGROUND	4
2.1. Radioactive decays and ionisation rays	4
2.1.1 α decay	4
2.1.2. β^- decay	4
2.1.3. Gamma rays	5
2.1.3.1. Shielding	5
2.1.4. Some examples of decay processes	6
2.1.4.1. The radioactive decay of the nuclide ^{90}Sr	6
2.1.4.2. The radioactive decay of the nuclide ^{137}Cs	6
2.1.4.3. The radioactive decay of the nuclide ^{60}Co	6
2.1.5. Origin of radioactive waste	7
2.1.6. Classification of radioactive waste	7
2.1.7. Management of radioactive waste	8
2.2. Clay Minerals	11
2.2.1. Kaolin	11
2.2.2. Smectite	12
2.2.3. Ion exchange properties of clays	13
2.3. Zeolites	14
2.4. Uses of Clays and Zeolites in Radioactive Waste Management	16
2.4.1. Uses of bentonites	16
2.4.2. Uses of zeolites	19
2.4.3. Uses of kaolins	21
3. EXPERIMENTAL STUDIES	23
3.1. Characterization of the Samples	23
3.2. Radioisotopes	30
3.2.1. Preparation of radioisotope solutions	30
3.2.2. Preparation of synthetic groundwater	31

3.3. Radiotracer method	31
3.4. The Distribution Ratio	32
3.5. The Experiments	34
4. RESULTS AND DISCUSSION	38
4.1. The results of ⁶⁵ zinc ion adsorption behaviours on bentonite, kaolin and zeolite	38
4.2. The results of ¹³⁷ caesium ion adsorption behaviours on bentonite, kaolin and zeolite	42
4.3. The results of ⁶⁰ cobalt ion adsorption behaviours on bentonite, kaolin and zeolite	49
4.4. The results of ¹³³ barium ion adsorption behaviours on bentonite, kaolin and zeolite	53
4.5. The results of ⁹⁰ strontium ion adsorption behaviours on bentonite, kaolin and zeolite	58
4.6. The effect of temperature on ⁶⁵ zinc ion adsorption behaviours on bentonite, kaolin and zeolite	62
4.7. The effect of temperature on ¹³⁷ caesium ion adsorption behaviours on bentonite, kaolin and zeolite	67
4.8. The effect of temperature on ⁶⁰ cobalt ion adsorption behaviours on bentonite, kaolin and zeolite	72
4.9. The effect of temperature on ¹³³ barium ion adsorption behaviours on bentonite, kaolin and zeolite	77
4.10. The effect of temperature on ⁹⁰ strontium ion adsorption behaviours on bentonite, kaolin and zeolite	82
4.11. Freundlich isotherms of zinc adsorption at 5°C	88
4.12. Freundlich isotherms of barium adsorption at 5°C	89
4.13. Freundlich isotherms of cobalt adsorption at 5°C	90
4.14. Freundlich isotherms of caesium adsorption at 5°C	91
4.15. Freundlich isotherms of strontium adsorption at 5°C	92
4.16. Desorption behaviours of zinc ion 5°C, 25°C on bentonite, kaolin	

and zeolite	94
4.17. Desorption behaviours of barium ion at 5°C, 25°C on bentonite, kaolin and zeolite	95
4.18. Desorption behaviours of cobalt ion at 5°C, 25°C on bentonite, kaolin and zeolite	97
4.19. Desorption behaviours of strontium ion bentonite, kaolin and zeolite	98
4.20. Desorption behaviours of caesium ion at 5°C on bentonite, kaolin and zeolite	99

FIGURE INDEX

	<u>Page</u>
Figure 1.1. One type of low-level waste disposal facility	1
Figure 1.2. Cross section of tunnel with deposition hole of the Swedish disposal program for nuclear waste	2
Figure 2.1. An example of disposal facility and pit for high-level radioactive wastes	9
Figure 2.2. Image of “self-sealing” of buffer material and applied stress to facility by swelling of buffer and backfill materials after submergence of ground water ..	10
Figure 2.3. Parts of the deep disposal system and their most important safety functions	10
Figure 2.4. The structure of kaolinite	12
Figure 2.5. Structure of montmorillonite mineral	13
Figure 2.6. The sodalite unit and the framework structures of the zeolites	16
Figure 3.1. Particle size distribution curves of the samples used in the sorption experiments	23
Figure 3.2. X-ray diffractograms of the samples used in sorption studies	24
Figure 3.3. X-Ray Diffraction Patterns of the Clay Fraction of Bentonite Sample Following Different Treatments	25
Figure 3.4. X-Ray Diffraction Patterns of the Clay Fraction of Kaolin Sample Following Different Treatments	26
Figure 3.5. X-Ray Diffraction Patterns of the Clay Fraction of Zeolite Sample Following Different Treatments	27
Figure 3.6. Schematic presentation of the experimental procedure	35
Figure 3.7. Schematic diagram of counting system	36
Figure 4.1. Counted activity-time plot of $^{65}\text{Zn}^{2+}$ uptake on bentonite. The effect of cation concentration on sorption was investigated at 5°C	38
Figure 4.2. $^{65}\text{Zn}^{2+}$ uptake on bentonite. The effect of cation concentration on sorption was investigated at 5°C	39
Figure 4.3. Counted activity-time plot of $^{65}\text{Zn}^{2+}$ uptake on zeolite. The	

effect of cation concentration on sorption was investigated at 5°C	39
Figure 4.4. $^{65}\text{Zn}^{2+}$ uptake on zeolite. The effect of cation concentration on sorption was investigated at 5°C	40
Figure 4.5. Counted activity- time plot of $^{65}\text{Zn}^{2+}$ uptake on kaolin. The effect of cation concentration on sorption was investigated at 5°C	41
Figure 4.6. $^{65}\text{Zn}^{2+}$ uptake on kaolin. The effect of cation concentration on sorption was investigated at 5°C	41
Figure 4.7. Counted activity- time plot of $^{137}\text{Cs}^+$ uptake on bentonite. The effect of cation concentration on sorption was investigated at 5°C	42
Figure 4.8. $^{137}\text{Cs}^+$ uptake on bentonite. The effect of cation concentration on sorption was investigated at 5°C	42
Figure 4.9. Counted activity- time plot of $^{137}\text{Cs}^+$ uptake on zeolite. The effect of cation concentration on sorption was investigated at 5°C	43
Figure 4.10. $^{137}\text{Cs}^+$ uptake on zeolite. The effect of cation concentration on sorption was investigated at 5°C	43
Figure 4.11. Counted activity- time plot of $^{137}\text{Cs}^+$ uptake on kaolin. The effect of cation concentration on sorption was investigated at 5°C	45
Figure 4.12. $^{137}\text{Cs}^+$ uptake on kaolin. The effect of cation concentration on sorption was investigated at 5°C	45
Figure 4.a. Structure of 1:1 clay mineral (a) and 2:1 clay mineral (b)	47
Figure 4.b. A qualitative description of the binding mechanism of hydrated metal onto clay minerals surfaces	48
Figure 4.c. Schematic representation of possible interactions between silica faces and hydrated ions	48
Figure 4.13. Counted activity- time plot of $^{60}\text{Co}^{2+}$ uptake on bentonite. The effect of cation concentration on sorption was investigated at 5°C	49
Figure 4.14. $^{60}\text{Co}^{2+}$ uptake on bentonite. The effect of cation concentration on sorption was investigated at 5°C	49
Figure 4.15. Counted activity- time plot of $^{60}\text{Co}^{2+}$ uptake on zeolite. The effect of cation concentration on sorption was investigated at 5°C	50
Figure 4.16. $^{60}\text{Co}^{2+}$ uptake on zeolite. The effect of cation concentration on sorption was investigated at 5°C	50
Figure 4.17. Counted activity- time plot of $^{60}\text{Co}^{2+}$ uptake on kaolin. The	

effect of cation concentration on sorption was investigated at 5°C	51
Figure 4.18. $^{60}\text{Co}^{2+}$ uptake on kaolin. The effect of cation concentration on sorption was investigated at 5°C	51
Figure 4.19. Counted activity- time plot of $^{133}\text{Ba}^{2+}$ uptake on bentonite. The effect of cation concentration on sorption was investigated at 5°C	53
Figure 4.20. $^{133}\text{Ba}^{2+}$ uptake on bentonite. The effect of cation concentration on sorption was investigated at 5°C	53
Figure 4.21. Counted activity- time plot of $^{133}\text{Ba}^{2+}$ uptake on zeolite. The effect of cation concentration on sorption was investigated at 5°C	54
Figure 4.22. $^{133}\text{Ba}^{2+}$ uptake on zeolite. The effect of cation concentration on sorption was investigated at 5°C	54
Figure 4.23. Counted activity- time plot of $^{133}\text{Ba}^{2+}$ uptake on kaolin. The effect of cation concentration on sorption was investigated at 5°C	56
Figure 4.24. $^{133}\text{Ba}^{2+}$ uptake on kaolin. The effect of cation concentration on sorption was investigated at 5°C	56
Figure 4.25. Counted activity- time plot of $^{90}\text{Sr}^{2+}$ uptake on bentonite. The effect of cation concentration on sorption was investigated at 5°C	58
Figure 4.26. $^{90}\text{Sr}^{2+}$ uptake on bentonite. The effect of cation concentration on sorption was investigated at 5°C	58
Figure 4.27. Counted activity- time plot of $^{90}\text{Sr}^{2+}$ uptake on zeolite. The effect of cation concentration on sorption was investigated at 5°C	59
Figure 4.28. $^{90}\text{Sr}^{2+}$ uptake on zeolite. The effect of cation concentration on sorption was investigated at 5°C	60
Figure 4.29. Counted activity- time plot of $^{90}\text{Sr}^{2+}$ uptake on kaolin. The effect of cation concentration on sorption was investigated at 5°C	60
Figure 4.30. $^{90}\text{Sr}^{2+}$ uptake on kaolin. The effect of cation concentration on sorption was investigated at 5°C	61
Figure 4.31. Counted activity- time plot of $^{65}\text{Zn}^{2+}$ uptake on bentonite at constant cation concentration ($1 \times 10^{-6}\text{M}$). The effect of temperature on sorption was investigated	62
Figure 4.32. $^{65}\text{Zn}^{2+}$ uptake on bentonite at constant cation concentration ($1 \times 10^{-6}\text{M}$). The effect of temperature on sorption was investigated	63
Figure 4.33. Counted activity- time plot of $^{65}\text{Zn}^{2+}$ uptake on zeolite at constant cation concentration ($1 \times 10^{-6}\text{M}$). The effect of temperature	

on sorption was investigated	64
Figure 4.34. $^{65}\text{Zn}^{2+}$ uptake on zeolite at constant cation concentration ($1 \times 10^{-6}\text{M}$). The effect of temperature on sorption was investigated	65
Figure 4.35. Counted activity- time plot of $^{65}\text{Zn}^{2+}$ uptake on kaolin at constant cation concentration ($1 \times 10^{-6}\text{M}$). The effect of temperature on sorption was investigated	66
Figure 4.36. $^{65}\text{Zn}^{2+}$ uptake on kaolin at constant cation concentration ($1 \times 10^{-6}\text{M}$). The effect of temperature on sorption was investigated	66
Figure 4.37. Counted activity- time plot of $^{137}\text{Cs}^{+}$ uptake on bentonite at constant cation concentration ($1 \times 10^{-6}\text{M}$). The effect of temperature on sorption was investigated	67
Figure 4.38. $^{137}\text{Cs}^{+}$ uptake on bentonite at constant cation concentration ($1 \times 10^{-6}\text{M}$). The effect of temperature on sorption was investigated	68
Figure 4.39. Counted activity- time plot of $^{137}\text{Cs}^{+}$ uptake on zeolite at constant cation concentration ($1 \times 10^{-6}\text{M}$). The effect of temperature on sorption was investigated	69
Figure 4.40. $^{137}\text{Cs}^{+}$ uptake on zeolite at constant cation concentration ($1 \times 10^{-6}\text{M}$). The effect of temperature on sorption was investigated	69
Figure 4.41. Counted activity- time plot of $^{137}\text{Cs}^{+}$ uptake on kaolin at constant cation concentration ($1 \times 10^{-6}\text{M}$). The effect of temperature on sorption was investigated	71
Figure 4.42. $^{137}\text{Cs}^{+}$ uptake on kaolin at constant cation concentration ($1 \times 10^{-6}\text{M}$). The effect of temperature on sorption was investigated	71
Figure 4.43. Counted activity- time plot of $^{60}\text{Co}^{2+}$ uptake on bentonite at constant cation concentration ($1 \times 10^{-6}\text{M}$). The effect of temperature on sorption was investigated	72
Figure 4.44. $^{60}\text{Co}^{2+}$ uptake on bentonite at constant cation concentration ($1 \times 10^{-6}\text{M}$). The effect of temperature on sorption was investigated	73
Figure 4.45. Counted activity- time plot of $^{60}\text{Co}^{2+}$ uptake on zeolite at constant cation concentration ($1 \times 10^{-6}\text{M}$). The effect of temperature on sorption was investigated	74
Figure 4.46. $^{60}\text{Co}^{2+}$ uptake on zeolite at constant cation concentration ($1 \times 10^{-6}\text{M}$). The effect of temperature on sorption was investigated	74
Figure 4.47. Counted activity- time plot of $^{60}\text{Co}^{2+}$ uptake on kaolin at constant cation concentration ($1 \times 10^{-6}\text{M}$). The effect of temperature on sorption was investigated	75

Figure 4.48. $^{60}\text{Co}^{2+}$ uptake on kaolin at constant cation concentration ($1 \times 10^{-6}\text{M}$). The effect of temperature on sorption was investigated	76
Figure 4.49. Counted activity- time plot of $^{133}\text{Ba}^{2+}$ uptake on bentonite at constant cation concentration ($1 \times 10^{-6}\text{M}$). The effect of temperature on sorption was investigated	77
Figure 4.50 $^{133}\text{Ba}^{2+}$ uptake on bentonite at constant cation concentration ($1 \times 10^{-6}\text{M}$). The effect of temperature on sorption was investigated	77
Figure 4.51. Counted activity- time plot of $^{133}\text{Ba}^{2+}$ uptake on zeolite at constant cation concentration ($1 \times 10^{-6}\text{M}$). The effect of temperature on sorption was investigated	78
Figure 4.52. $^{133}\text{Ba}^{2+}$ uptake on zeolite at constant cation concentration ($1 \times 10^{-6}\text{M}$). The effect of temperature on sorption was investigated	79
Figure 4.53. Counted activity- time plot of $^{133}\text{Ba}^{2+}$ uptake on kaolin at constant cation concentration ($1 \times 10^{-6}\text{M}$). The effect of temperature on sorption was investigated	80
Figure 4.54. $^{133}\text{Ba}^{2+}$ uptake on kaolin at constant cation concentration ($1 \times 10^{-6}\text{M}$). The effect of temperature on sorption was investigated	80
Figure 4.55. Counted activity- time plot of $^{90}\text{Sr}^{2+}$ uptake on bentonite at constant cation concentration ($1 \times 10^{-6}\text{M}$). The effect of temperature on sorption was investigated	82
Figure 4.56. $^{90}\text{Sr}^{2+}$ uptake on bentonite at constant cation concentration ($1 \times 10^{-6}\text{M}$). The effect of temperature on sorption was investigated	82
Figure 4.57. Counted activity- time plot of $^{90}\text{Sr}^{2+}$ uptake on zeolite at constant cation concentration ($1 \times 10^{-6}\text{M}$). The effect of temperature on sorption was investigated	84
Figure 4.58. $^{90}\text{Sr}^{2+}$ uptake on zeolite at constant cation concentration ($1 \times 10^{-6}\text{M}$). The effect of temperature on sorption was investigated	84
Figure 4.59. Counted activity- time plot of $^{90}\text{Sr}^{2+}$ uptake on kaolin at constant cation concentration ($1 \times 10^{-6}\text{M}$). The effect of temperature on sorption was investigated	85
Figure 4.60. $^{90}\text{Sr}^{2+}$ uptake on kaolin at constant cation concentration ($1 \times 10^{-6}\text{M}$). The effect of temperature on sorption was investigated	86
Figure 4.61. $^{65}\text{Zn}^{2+}$ -Bentonite system: $n=0.7236$, $k=0.0172$	88
Figure 4.62. $^{65}\text{Zn}^{2+}$ -Zeolite system: $n=0.6524$, $k=0.0025$	88

Figure 4.63. $^{65}\text{Zn}^{2+}$ -Kaolin system: $n=0.6867$, $k=0.0055$	88
Figure 4.64. $^{133}\text{Ba}^{2+}$ -Bentonite system: $n=0.9551$, $k=0.381$	89
Figure 4.65. $^{133}\text{Ba}^{2+}$ -Zeolite system: $n=0.8493$, $k=0.072$	89
Figure 4.66. $^{133}\text{Ba}^{2+}$ -Kaolin system: $n=0.8477$, $k=0.02215$	89
Figure 4.67. $^{60}\text{Co}^{2+}$ -Bentonite system: $n=0.7238$, $k=0.0151$	90
Figure 4.68. $^{60}\text{Co}^{2+}$ -Zeolite system: $n=0.7727$, $k=0.00442$	90
Figure 4.69. $^{60}\text{Co}^{2+}$ -Kaolin system: $n=0.6883$, $k=0.00464$	90
Figure 4.70. $^{137}\text{Cs}^{+}$ -Bentonite system: $n=0.8285$, $k=0.0802$	91
Figure 4.71. $^{137}\text{Cs}^{+}$ -Zeolite system: $n=0.7911$, $k=0.07867$	91
Figure 4.72. $^{137}\text{Cs}^{+}$ -Kaolin system: $n=0.7104$, $k=0.00916$	91
Figure 4.73. $^{90}\text{Sr}^{2+}$ -Bentonite system: $n=0.8499$, $k=0.049$	92
Figure 4.74. $^{90}\text{Sr}^{2+}$ -Zeolite system: $n=0.7841$, $k=0.0159$	92
Figure 4.75. $^{90}\text{Sr}^{2+}$ -Kaolin system: $n=0.88$, $k=0.0214$	92
Figure 4.76. $^{65}\text{Zn}^{2+}$ desorption behaviours at 5°C (constant cation concentration $1 \times 10^{-6}\text{M}$)	94
Figure 4.77. $^{65}\text{Zn}^{2+}$ desorption behaviours at 25°C (constant cation concentration $1 \times 10^{-6}\text{M}$)	94
Figure 4.78. $^{133}\text{Ba}^{2+}$ desorption behaviours at 5°C (constant cation concentration $1 \times 10^{-6}\text{M}$)	95
Figure 4.79. $^{133}\text{Ba}^{2+}$ desorption behaviours at 25°C (constant cation concentration $1 \times 10^{-6}\text{M}$)	96
Figure 4.80. $^{60}\text{Co}^{2+}$ desorption behaviours at 5°C (constant cation concentration $1 \times 10^{-6}\text{M}$)	97
Figure 4.81. $^{60}\text{Co}^{2+}$ desorption behaviours at 25°C (constant cation concentration $1 \times 10^{-6}\text{M}$)	97
Figure 4.82. $^{90}\text{Sr}^{2+}$ desorption behaviours at 5°C (constant cation concentration $1 \times 10^{-6}\text{M}$)	98
Figure 4.83. $^{137}\text{Cs}^{+}$ desorption behaviours at 5°C (constant cation concentration $1 \times 10^{-6}\text{M}$)	99

TABLE INDEX

	<u>Page</u>
Table 2.1. Classes of clays used in the study.....	11
Table 2.2. Structures and compositions of some important natural zeolites	15
Table 3.1. The chemical analyses of the samples used in the sorption studies.....	28
Table 3.2. Properties of the radionuclide containing compounds used in the study.....	30
Table 3.3. The chemical composition of the ground water.....	31
Table 4.a. Ion radius and hydration energy of studied cations.....	44
Table 4.1. Thermodynamic parameters of ⁶⁵ Zinc-Bentonite system.....	64
Table 4.2. Thermodynamic parameters of ⁶⁵ Zinc-Zeolite system.....	65
Table 4.3. Thermodynamic parameters of ⁶⁵ Zinc-Kaolin system.....	67
Table 4.4. Thermodynamic parameters of ¹³⁷ Caesium-Bentonite system.....	68
Table 4.5. Thermodynamic parameters of ¹³⁷ Caesium-Zeolite system.....	70
Table 4.6. Thermodynamic parameters of ¹³⁷ Caesium-Kaolin system.....	72
Table 4.7. Thermodynamic parameters of ⁶⁰ Cobalt-Bentonite system.....	73
Table 4.8. Thermodynamic parameters of ⁶⁰ Cobalt-Zeolite system.....	75
Table 4.9. Thermodynamic parameters of ⁶⁰ Cobalt-Kaolin system.....	76
Table 4.10. Thermodynamic parameters of ¹³³ Barium-Bentonite system.....	78
Table 4.11. Thermodynamic parameters of ¹³³ Barium-Zeolite system.....	79
Table 4.12. Thermodynamic parameters of ¹³³ Barium-Kaolin system.....	81
Table 4.13. Thermodynamic parameters of ⁹⁰ Strontium-Bentonite system.....	83
Table 4.14. Thermodynamic parameters of ⁹⁰ Strontium-Zeolite system.....	85
Table 4.15. Thermodynamic parameters of ⁹⁰ Strontium-Kaolin system.....	86
Table 4.16. The evaluation of the thermodynamic results which are obtained....	87
Table 4.17. Freundlich parameters.....	93

LIST OF ABBREVIATIONS

β^-	Beta
γ	Gamma
Zn^{2+}	Zinc ion
Co^{2+}	Cobalt ion
Ba^{2+}	Barium ion
Sr^{2+}	Strontium ion
Cs^+	Caesium ion
Al^{3+}	Aluminum ion
Si^{4+}	Silisium ion
TOT	Tetrahedra octahedra tetrahedra sheet
ΔG°	Gibbs free energy
ΔH°	Entalphy
ΔS°	Entropy

1. INTRODUCTION

The nuclear wastes are one of the most important environmental problems for the world. A widely used qualitative classification system separates radioactive waste into three classes: low level waste (LLW), intermediate level waste (ILW) and high level waste (HLW). Many countries must address the disposal of very large quantities of waste containing long-lived natural radionuclides. Such waste typically contains natural radionuclides like uranium, thorium, and radium and is frequently generated from uranium/thorium mining and milling or similar activities (Radwass programme of International Atomic Agency, 1994).

After storage of the radioactive waste, clays can be used as a backfilling material in order to construct a geological barrier against reaching of the waste to the biosphere with the aid of groundwater, which can damage human being and other living creatures. To overcome this problem, especially clays are used as good type backfilling materials due to their high sorption properties.

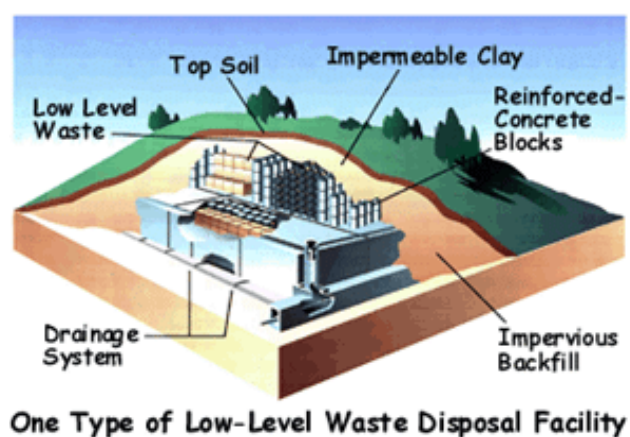


Figure 1.1. One type of low-level waste disposal facility.

The fact that radionuclides encountered as radioactive wastes have a harmful impact on the biosphere that pushes investigators to study on the sorption characteristics of natural clay minerals against radionuclides. In the reprocessing of nuclear fuels, disposition of the radioactive waste is a serious problem. For the

longterm disposal of nuclear waste, deep geological shafts with multibarrier protection were engineered in last years (Erten 1988).

Bentonite has recently attracted increasing attention as a backfilling (buffer) material for high-level nuclear waste due to its ability to expand and completely fill up openings (Xu et al. 2004).

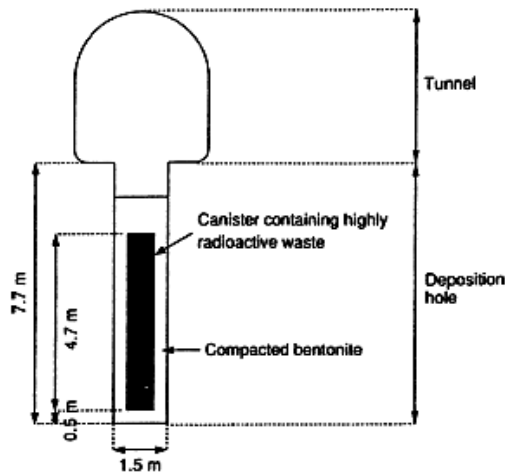


Figure 1.2. Cross section of tunnel with deposition hole of the Swedish disposal program for nuclear waste (Xu et al., 2004).

The main objective of this study is to investigate the adsorption characteristics of zinc-65, barium-133, cobalt-60, caesium-137 and strontium-90 radioisotopes on natural bentonite, zeolite and kaolin samples in order to propose a backfill material for using in natural barriers. The removal of ^{65}Zn ($t_{1/2}=244$ days), ^{133}Ba ($t_{1/2}=10.7$ years), ^{60}Co ($t_{1/2}=5.271$ years), ^{137}Cs ($t_{1/2}=30.15$ years) and ^{90}Sr ($t_{1/2}=28.1$ years) from aqueous solutions by natural bentonite (Çankırı), zeolite (Balıkesir) and kaolin (Bilecik) at different temperatures and concentrations were investigated by using the radiotracer method. The sorption data were given as ratios of radioactivity uptaken by the sorbents and remained in the solution, as distribution ratio (R_D), which means the ratio of sorbate (radionuclide) concentration on solid phase to its concentration in liquid phase. The difference of this thesis from the earlier studies is the experimental temperature. In the literature the experiments were carried out above the room temperature but in my thesis, we studied at lower temperatures.

Batch sorption experiments were done; the natural sorbents as a stationary phase and the synthetic groundwater as a mobile phase. Before performing batch experiments, the samples were characterized by mainly chemical and x-ray diffractometer analyses. Other techniques (surface area, size distribution, etc.) were also used for physico-chemical characterization of the samples. The desorption experiments were also carried out.

Finally, using the sorption/desorption counts versus time, the kinetic behaviours of the radioisotope-clay systems were revealed for different temperatures. According to the experimental results, thermodynamic parameters of sorptions were also calculated.


2.THEORETICAL BACKGROUND

2.1. Radioactive decays and ionisation rays

Radioactive decay is the process in which an unstable atomic nucleus loses energy by emitting radiation in the form of particles or electromagnetic waves. The SI unit of radioactive decay is the becquerel (Bq). One Bq is defined as one transformation (or decay) per second. Another unit of decay is the curie, which was originally defined as the radioactivity of one gram of pure radium, and is equal to 3.7×10^{10} Bq.


2.1.1 α decay

The emission of an α particle, or ${}^4\text{He}$ nucleus, is a process called α decay. Since α particles contain two protons and two neutrons, they must come from the nucleus of an atom.

 <p>Alpha particle:- 2 protons and 2 neutrons</p>	<p>Alpha particles are made of 2 protons and 2 neutrons.</p> <p>This means that they have a charge of +2, and a mass of 4 (the mass is measured in "atomic mass units", where each proton & neutron=1 amu)</p> <p>Alpha particles are relatively slow and heavy.</p> <p>They have a low penetrating power - you can stop them with just a sheet of paper.</p>
--	--

Though the most massive and most energetic of radioactive emissions, the alpha particle is the shortest in range because of its strong interaction with matter.


2.1.2. β^- decay

 <p>Beta particle:- the same as an electron</p>	<p>Beta particles have a charge of minus 1, that beta particles are the same as an electron.</p> <p>They are fast, and light.</p> <p>Beta particles have a medium penetrating power - they are stopped by a sheet of aluminium</p> <p>Beta particles ionise atoms that they pass, but not as strongly as alpha particles do.</p>
--	--

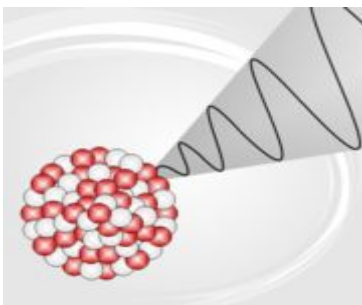
2.1.3. Gamma rays

The emission of γ -radiation generally follows some other nuclear-decay process. It is not itself a primary nuclear-decay process, but is emitted when a transition occurs between an excited state of a nucleus and a lower nuclear-energy state. These excited states are associated with the daughter nucleus formed after α -particle or β -particle decay processes. Generally, the lifetimes of excited states are extremely short so that γ -ray emission immediately follows the decay process which led to the production of the excited states (Andrews and Hornsey 1972).

Gamma rays are generally characterized as electromagnetic radiation, (EMR) having the highest frequency and energy, and also the shortest wavelength, within the electromagnetic radiation spectrum. Due to their high energy content, they are able to cause serious damage when absorbed by living cells.

 <p>Gamma ray:- not a particle, but a burst of high-frequency waves</p>	<p>Gamma rays are waves, not particles. This means that they have no mass and no charge.</p> <p>Gamma rays have a high penetrating power - it takes a thick sheet of metal such as lead, or concrete to reduce them significantly.</p> <p>Gamma rays do not directly ionise other atoms, although they may cause atoms to emit other particles which will then cause ionisation.</p> <p>We don't find pure gamma sources - gamma rays are emitted alongside alpha or beta particles. Gamma emission isn't 'radioactive decay' because it doesn't change the state of the nucleus, it just carries away some energy.</p>
---	---

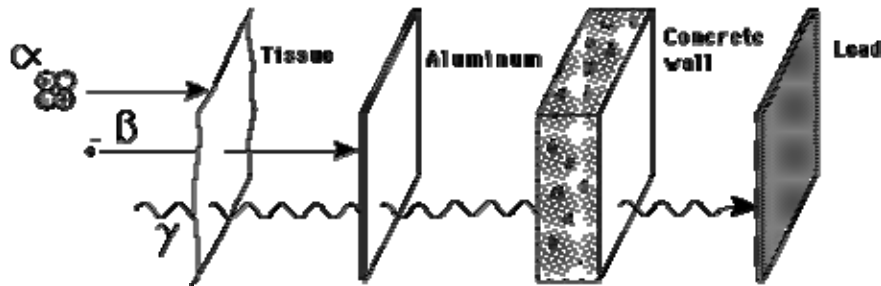
2.1.3.1. Shielding



Gamma rays.

The material used for shielding takes into account that gamma rays are better absorbed by materials with high atomic number and high density. Also, the higher the energy of the gamma rays, the thicker the shielding required.

The electromagnetic gamma ray is extremely penetrating, even penetrating considerable thicknesses of concrete.

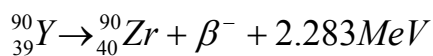
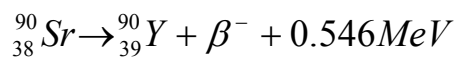


Particles that ionise other atoms strongly have a low penetrating power, because they lose energy each time they ionise an atom.

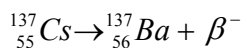
2.1.4. Some examples of decay processes

2.1.4.1. The radioactive decay of the nuclide ^{90}Sr

Sr-90 undergoes beta decay with a half-life time of 28.74 years. Once the strontium-90 decays to yttrium-90, a further beta decay occurs immediately and emits a minimum ionizing particle with energy of 2.283 MeV.

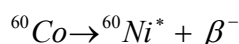


2.1.4.2. The radioactive decay of the nuclide ^{137}Cs

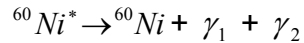


2.1.4.3. The radioactive decay of the nuclide ^{60}Co

The nuclide ^{60}Co is unstable and decays by the process of β^{-} emission to a stable isotope of the element ^{60}Ni . The half-life of ^{60}Co is 5.27 years. This decay process can be written as follows: First ^{60}Co decays to excited $^{60}\text{Ni}^*$ by beta decay:



Then the $^{60}\text{Ni}^*$ drops down to the ground state emitting two gamma rays in succession:



Gamma rays of 1.17 MeV and 1.33 MeV are produced.

2.1.5. Origin of radioactive waste

Radioactive waste basically originates from (Warnecke and Brennecke, 2002):

- 1) the process of light-water reactors and progressive reactors;
- 2) the operation of spent fuel elements from nuclear power plants;
- 3) investigations at nuclear research centers;
- 4) other research centers; universities, industrial research and development or medical applications of radioisotopes;
- 5) uranium enrichment;
- 6) other waste producers, e.g., the army.

2.1.6. Classification of radioactive waste

In the publication within the radwast programme of the International Atomic Energy Agency (1994) classification of radioactive waste was made as below:

Low and intermediate level waste (LILW): Low level waste can be defined as radioactive waste that does not require shielding during handling and transportation. Radioactive waste which required shielding but needed little or no provision for heat dissipation was classified as intermediate level. A contact dose rate of 2 mSv/h was generally used to distinguish between the two classes of waste. Low and intermediate level may be subdivided into short-lived and long-lived waste according to their half-life.

The high level waste (HLW): This waste contains large concentrations both of short and long-lived radionuclides, so that a high degree of isolation from the biosphere by means of geological disposal is needed to get disposal safety.

2.1.7. Management of radioactive waste

Geological formations that contain clay minerals are used as depository for the radioactive wastes as natural barriers against their leakage. The use of clays is chosen because of their low permeability, good adsorption/ion exchange characteristics, and wide availability (Shahwan et al., 2000; Missana and Adell 2000; Horseman 1996). Thus, several sorption studies investigating how the interactions between the clays and the radionuclides are affected by various factors that control the sorption process became quite important (Gupta and Harrison, 1980; Erten and Gokmenoglu, 1994; Shahwan et al., 2000; Krumhansl et al., 2001; Shahwan and Erten, 2002; Akar et al., 2005; Başçetin and Atun, 2006; Missana 1999). Among such factors the concentration of radionuclides in the groundwater, the period of contact, the temperature, pH, the size of clay particles, the liquid-solid ratio, etc. Mishra and Tiwary, 1999 studied on the waste disposal problem by hydrous ferric hydroxide.

The need for disposal of nuclear wastes is the cause of the investigation in the adsorption behavior of fission products and some activation product nuclides on minerals of proposed repositories. The typical repository consists of a chemical system with a stationary solid phase and a mobile groundwater phase. The composition of both phases has effect on the transport of radionuclides from their disposal sites. pH, redox potential and temperature can be shown as other factors. Adsorption data are required for the estimation of transport rates of these nuclides in the case of water penetration into the repository (Erten and Gökmenoğlu, 1994). In order to provide the protection for the environment, nuclear wastes could be disposed of geological repositories in which clay minerals have been proposed as suitable backfilling materials because of their ability in retarding or delaying the migration of radionuclides to the biosphere (Jedinakova-Krizova, 1996).

Montes-H et al. (2005) reported that bentonite backfill barrier essentially consists of compacted clay blocks because of the hydrodynamic and surface properties. Buffer material, due to swelling characteristics, fills up the spaces between the canisters containing the waste and the surrounding ground and to construct a better impermeable zone for the contour of high-level radioactive waste. This event

is called as 'self-sealing'. If the presence amount of montmorillonite in this clay mineral is high; in the radioactive waste repository the engineered barrier gains an perfect performance because of its swelling property. Na/Ca-montmorillonite to Ca-montmorillonite conversion is from medium-swelling clay to low-swelling clay.

Swedish disposal program for nuclear waste is shown in Fig. 2.1. and 2.2. Komine (2004) and Xu et al. (2004) mentioned about the reports of the Atomic Energy of Canada, 1994 and Swedish Nuclear Fuel and Waste Management Technical Report, 1992. The deposition hole is planned to construct to a depth of several hundred meters, and backfill material, generally compacted bentonite, is projected to use as buffers in this hole. The function of the buffer material is to create an impermeable zone around the canister containing the high-level nuclear waste, since nuclear waste must be kept separate from surrounding environment. The swelling properties lead to the development of low permeability in the backfill materials (Figure 2.3.).

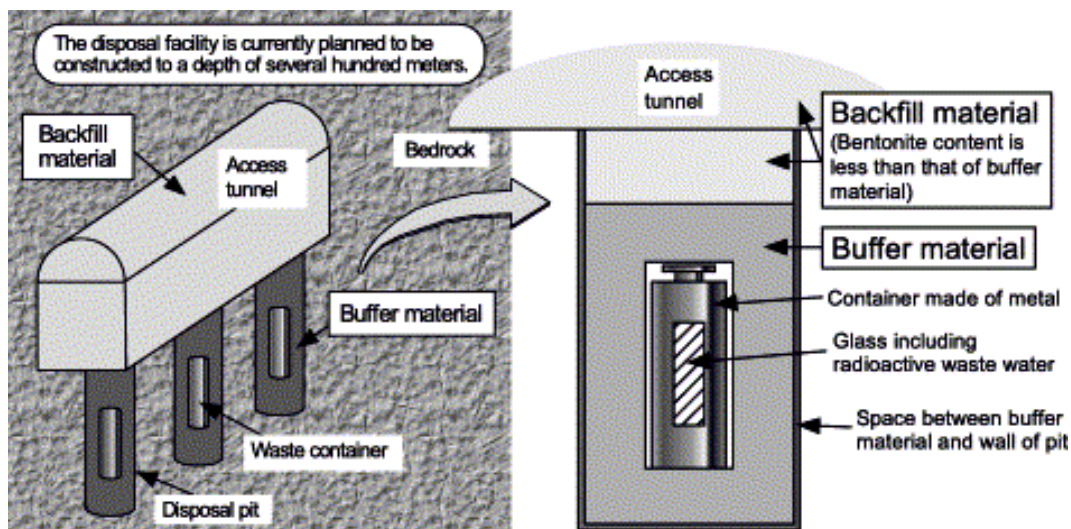


Figure 2.1. An example of disposal facility and pit for high-level radioactive wastes (vertical emplacement type) (Komine, 2004).

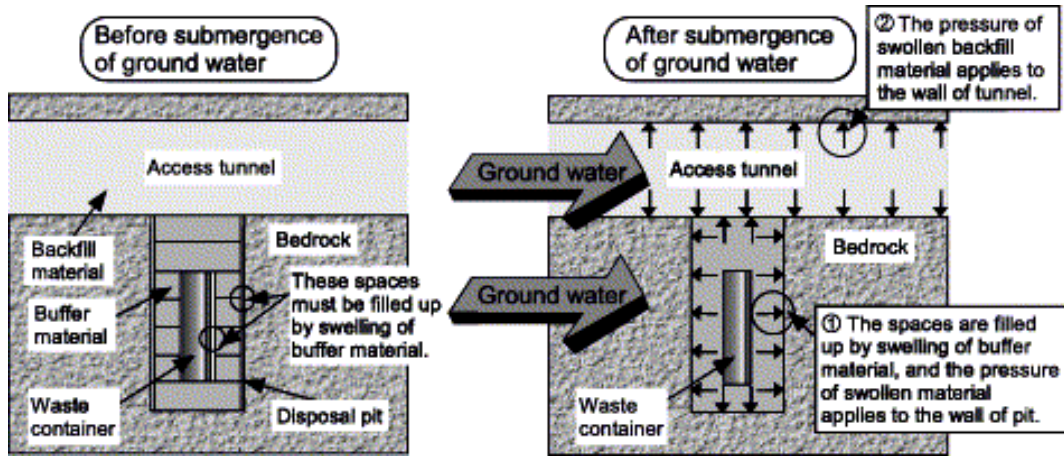


Figure 2.2. Image of “self-sealing” of buffer material and applied stress to facility by swelling of buffer and backfill materials after submergence of ground water (vertical emplacement type) (Komine, 2004).

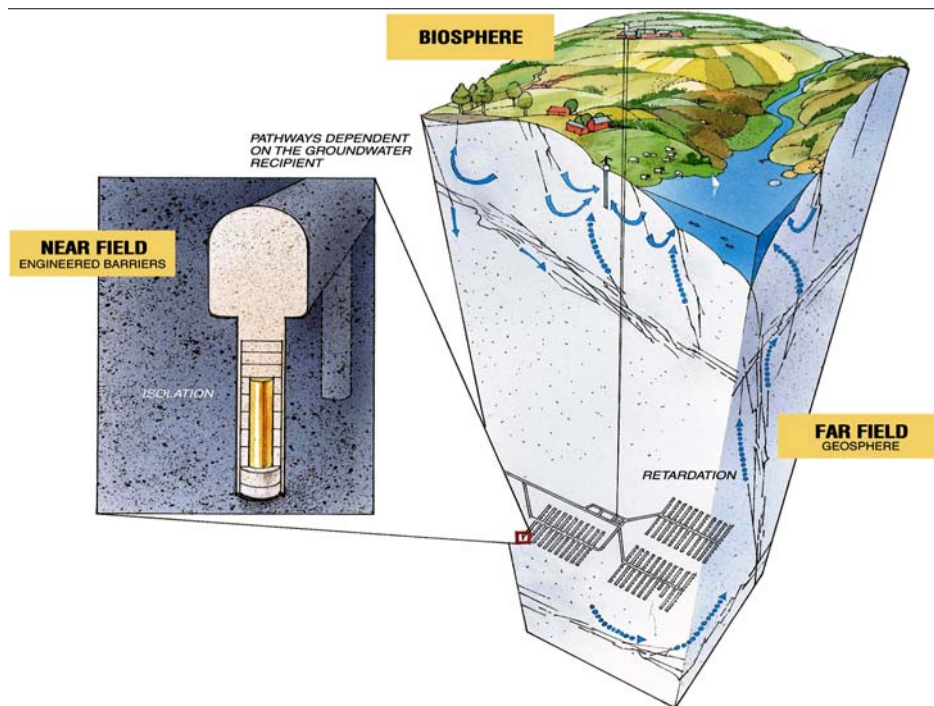


Figure 2.3. Parts of the deep disposal system and their most important safety functions (Ericsson, 1999).

^{137}Cs and ^{90}Sr are hazardous radionuclides and they should be stored in geologic formation. When radioactive waste is disposed in a geologic repository, it could be subjected to groundwater attack, however, while radionuclides are transported

along migration pathways in underground geologic formation, they may be adsorbed onto rock surfaces (Jeong, 2001).

2.2. Clay Minerals

Clay minerals are arranged in groups according to the type of silicate layer present (1:1 or 2:1), the magnitude of layer charge per formula unit and the interlayer material that compensates the layer charge. Each group is divided into subgroups on the basis of the octahedral character (dioctahedral or trioctahedral). The classes of clays which were studied in the thesis are given in Table 2.1.

Table 2.1. Classes of clays used in the study (Martin, 1991).

Layer type	Interlayer material (X: layer charge)	Group	Octahedral character	Example species
1:1	None or H ₂ O only (X~0)	Serpentine-kaolin	Trioctahedral Dioctahedral Di-trioctahedral	Lizardite, amesite, berthierine Kaolinite , dickite, nacrite Odinite
2:1	None (X~0)	Talc Pyrophyllite	Trioctahedral Dioctahedral	Talc, willemseite, kerolite Pyrophyllite, ferripyrophyllite
	Hydrated exchangeable cations (X~0.2-0.6)	Smectite	Trioctahedral Dioctahedral	Saponite, hectorite, sauconite Montmorillonite , beidelite, nontronite

2.2.1. Kaolin

Kaolin is a rock term, a clay mineral group and an industrial mineral commodity. The kaolin group minerals are hydrous aluminum silicates and have the approximate composition of Al₂O₃·2SiO₂·2H₂O. Kaolinite is the most common of the kaolin group minerals. The structure of kaolinite consists of a single silica tetrahedral sheet and a single alumina octahedral sheet combined to form the kaolinite unit layer (Figure 2.4.). These unit layers are stacked on top of each other. Variations in orientation of the unit layers in stacking cause differences in the kaolin group mineral itself and lead to the differentiation of nacrite and dickite in the kaolin group.

Kaolin is used in industry for many applications (paper, paint, ceramics, rubber, plastics, ink, catalyst and fiberglass). It is a unique industrial mineral because it is chemically inert over a relatively wide pH range.

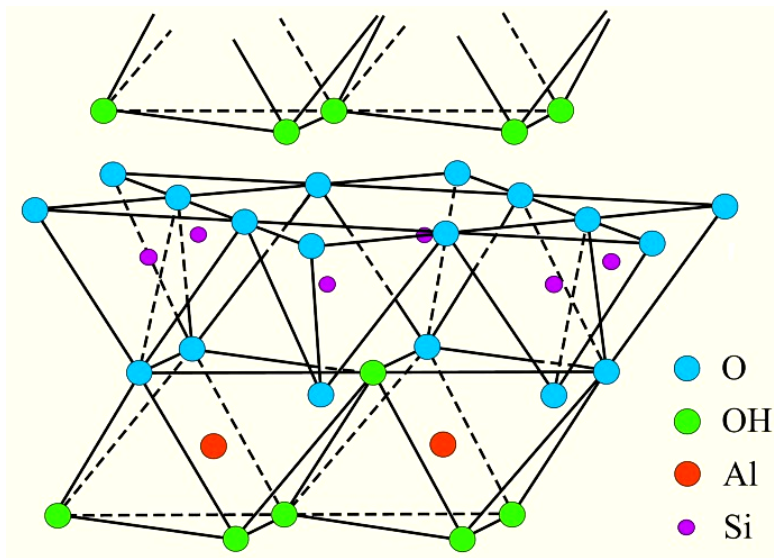


Figure 2.4. The structure of kaolinite (Murray, 2002).

2.2.2. Smectite

Smectite is the name for a group of sodium, calcium, magnesium, iron, lithium aluminum silicates, which include the individual minerals sodium montmorillonite, calcium montmorillonite, nontronite, saponite and hectorite. The rock in which these smectite minerals are usually dominant is bentonite. Smectite is composed of units consisting of two silica tetrahedral sheets with a central alumina octahedral sheet. The lattice has an unbalanced charge because of substitution of alumina for silica in the tetrahedral sheet and iron and magnesium for alumina in the octahedral sheet. Because of this, cations and polar molecules can enter between the layers and cause expansion (Figure 2.5.). Fernández et al. (2004) report that bentonites contain large quantity of montmorillonite and Missana and Adell (2000) also indicate that montmorillonite, which is the main component of bentonite, is a 2:1 layer (2 tetrahedral and 1 octahedral) clay.

The exchangeable cations present between the silica and alumina sheets have a strong influence on the use and properties of the smectite. The major uses of bentonites are in drilling muds, foundry sand bond and iron-ore pelletizing. In addition to these three major uses, bentonite is used for many miscellaneous products; including filtering agents, water impedance, cosmetics, animal feed,

pharmaceuticals, paint, ceramics, slurry trenching, catalysts, and decolorizing (Murray, 2002).

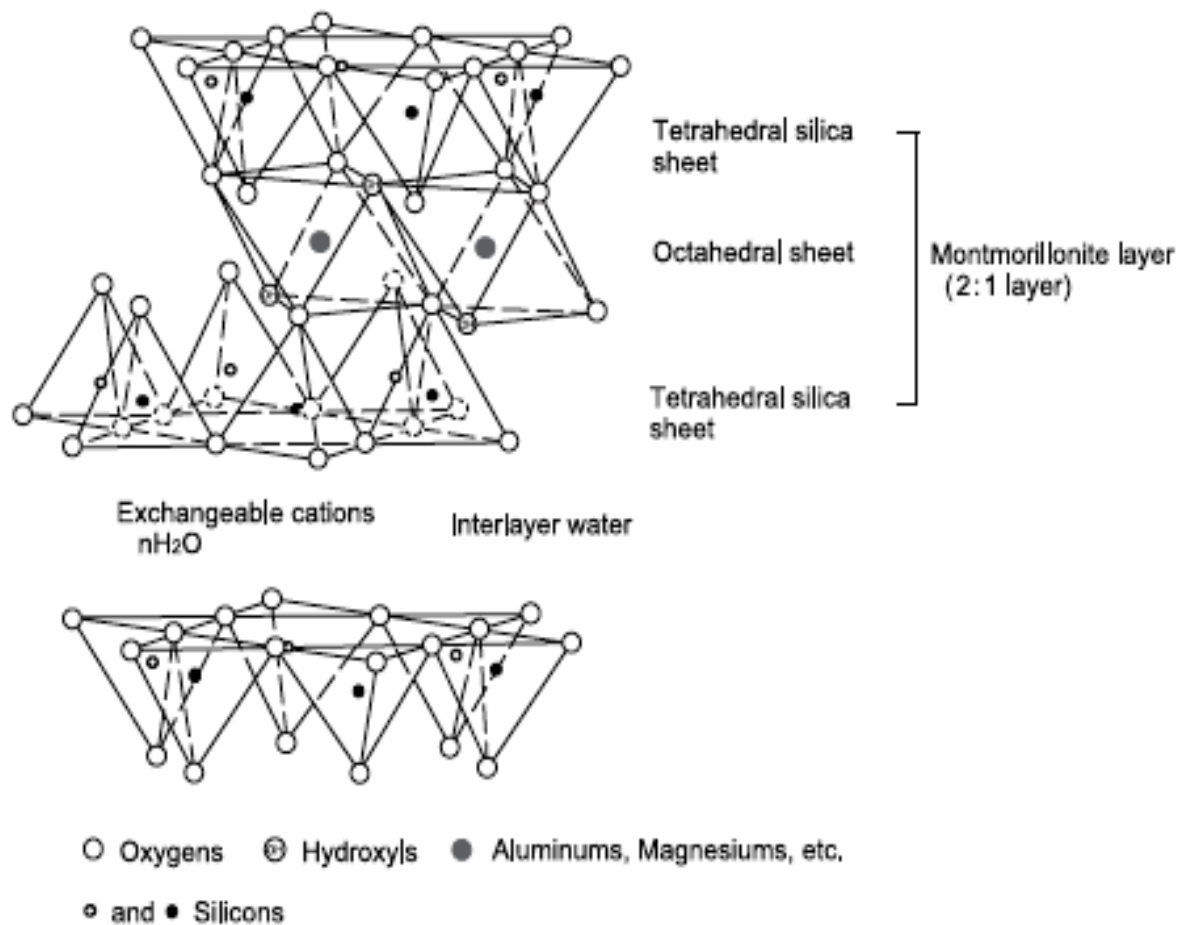


Figure 2.5. Structure of montmorillonite mineral (Komine, 2004).

2.2.3. Ion exchange properties of clays

One of the fundamental properties of clays is the electrical charge on their unit particles which means that clays uptake cations and/or anions that neutralize the layer charge, which are exchangeable. This means that they can readily be replaced other anions or cations when brought into contact with these ions in aqueous solution (Grim, 1953; van Olphen, 1977). Except under extremely acidic conditions, the layer charge is predominantly negative, a fact which may be verified by investigating the electrochemical properties of dilute, aqueous dispersions of clay (Swartzen-Allen and Matijević, 1974). This means that clays tend to sorb cations and are said to have certain cation exchange capacity (CEC) which is generally expressed as milliequivalents per hundred grams.

The main source of negative electrical charge in clay platelets is an amorphous substitution of cations in the crystal lattice by cations of lower charge, e.g. the substitution of aluminum for silicon in the tetrahedral sheet, and magnesium and/or ferrous iron for aluminum, or sometimes lithium for magnesium in the octahedral layers (Hall, 1987).

Smectites have isomorphous substitution in their structures and their CEC values are changing between 40-120 meq/100 g. Kaolinite have much less isomorphous substitution and correspondingly lower CEC values (3-15 meq/100 g). Especially for kaolinite broken bonds at clay particle edges may also participate to the exchange capacity. However, it is considerable evidence to point out that, except under fairly alkaline conditions, the charges due to edge defects are positive, it means leading to anion rather than cation adsorption at these sites. Zeolite minerals, which are occasionally found in some clays, have cation exchange capacities of the interval of 100 to 300 meq/100 g.

The negatively charged clay surfaces do not show equal affinity for all cations. In general, cation exchange selectivity increases with cation charge and for a given charge increases with ionic radius. Thus, the order of increasing affinity for the alkali metal ions is Li, Na, K, Rb, Cs, and for the alkaline earth ions Mg, Ca, Sr and Ba (Swartzen-Allen and Matijević, 1974). In both groups, increase in adsorption selectivity corresponds with decreasing polarizability and energy of hydration in aqueous solution, i.e. the cations which hold on to their hydration shells most firmly are the least strongly adsorbed by clays (Hall, 1987).

2.3. Zeolites

Zeolites are crystalline, hydrated aluminosilicates of group 1A and 2A elements with a framework structure. Their three-dimensional, polyanionic networks are built of SiO_4 and AlO_4 tetrahedra linked through oxygen atoms. Depending on the structure type, they contain regular channels or interlinked voids whose diameters are in the micropore range. These pores contain water molecules and the cations necessary to balance the negative charge of the framework. The cations, which are mobile and can be exchanged, are mainly alkali metal or alkaline earth metal

ions. There are approximately 40 natural mineral zeolites and over 150 synthetic types (Garney, 1995).

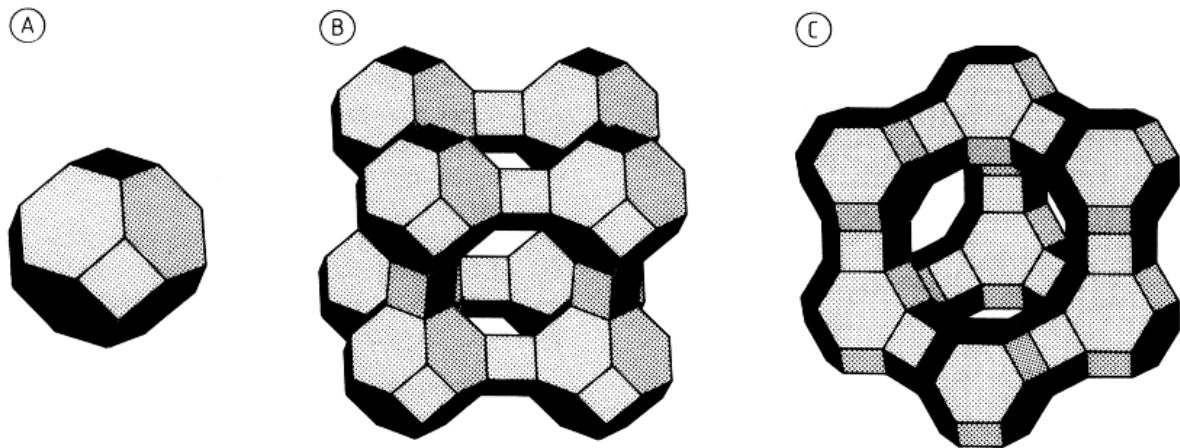
Zeolites are classified structurally as tectosilicates. The basic elements of their frameworks are TO_4 tetrahedra (T: Si and Al) linked through oxygen atoms. The typical compositions of natural zeolites are given in Table 2.2.

Table 2.2. Structures and compositions of some important natural zeolites (Roland and Kleinschmit, 2002).

Zeolite	$SiO_2/[Al_2O_3+Fe_2O_3]$	Common cations	Typical composition of unit cell
Clinoptilolite	8.0- 10.2	K > Na	$(Na,K)_6[(AlO_2)_6(SiO_2)_{30}] \cdot 24H_2O$
Heulandite	5.8- 8.0	Ca, Na	$Ca_4[(AlO_2)_8(SiO_2)_{28}] \cdot 24H_2O$
Mordenite	8.6- 10.6	Na > K	$Na_8[(AlO_2)_8(SiO_2)_{40}] \cdot 24H_2O$
Phillipsite	2.6- 6.8	K, Na, Ca	$(Ca,K_2,Na_2)_3[(AlO_2)_6(SiO_2)_{10}] \cdot 12H_2O$
Chabazite	3.4- 7.6	Ca, Na, K	$Ca_6[(AlO_2)_{12}(SiO_2)_{24}] \cdot 40H_2O$

The description of zeolites is based on the larger units known as secondary building units which consist, for example, of simple rings and prisms of various sizes. By combining such basic units the zeolite form is generated. The most seen structural units are sodalite cages (Figure 2.6.).

The most important use of synthetic zeolites based on their ion-exchange properties is in detergents. In the largest application of zeolites, the removal of undesired ions from wastewater is mainly carried out with the natural zeolites. Zeolites do not only have a high adsorption capacity but also show great selectivity, providing substances to be separated or purified. (Shelef, 1995).



A. Sodalite cage, B. Framework structure of zeolite A, C. Framework structure of faujasite with supercage

Figure 2.6. The sodalite unit and the framework structures of the zeolites (Roland and Kleinschmit, 2002).

2.4. Uses of Clays and Zeolites in Radioactive Waste Management

2.4.1. Uses of bentonites

Mellah and Chegrouche (1997) researched the effects of temperature, solid-liquid ratio, initial zinc concentration, particle size and agitation speed on the adsorption rate of zinc for 120 minutes onto natural bentonite having BET surface area of 6.43 m²/g.

Adsorption of zinc ion from aqueous solutions by natural and Na-exchanged bentonite is investigated by Kaya and Ören (2005) at different pH conditions. They evaluated their 2 days sorption data and found that the sorption fits to both Langmuir and Freundlich isotherms. They concluded most of zinc ions were adsorbed by bentonite in the first 6 hours. It is documented that bentonite is an efficient adsorbent for some heavy metals, especially for lead, Naseem and Tahir, (2001), for lead and cadmium Barbier et al. (2000), for copper and cadmium Kapoor and Viraraghavan (1998), for cadmium and zinc Gonzales-Pradas et al. (1994) are the other studies.

Sorption and diffusion behaviors of ¹³⁷Cs and ⁸⁵Sr ions on compacted bentonite were examined by Tsai et al. (2001) using batch sorption experiments with contact

time of 24 hours. Sorption and diffusion are important processes for the transport of radionuclides through buffer materials such as bentonite. These experiments give information in evaluating the retardation factor (R_d).

Shahwan et al. (2006) have a research on the adsorption of Co^{2+} ions on natural bentonite clay. The experiments were done at 25°C and 55°C using ^{60}Co as a radiotracer and HPGe detector with a multichannel PGT analyzer. The positive value of ΔH° marks the endothermic nature of sorption.

In the article of Khan et al. (1995), the sorption of Cr(III), Cr(VI) and Ag(I) from aqueous solutions on bentonite has been studied by a batch technique using multichannel γ -spectrometer for gamma counting. Their results show that sorptions of Ag^+ and Cr^{3+} on bentonite are exothermic processes, whereas the sorption of chromate (VI) ions on bentonite is an endothermic process. The values of ΔG° for the processes of Ag^+ and Cr^{3+} become less negative with increasing temperature; but the values of ΔG° become more negative with increasing temperature for chromate (VI) showing the sorption is favoured at high temperatures.

Bors et al. (1999) used organophilic bentonite which had been modified with hexadecylpyridinium cations for sorption of iodide (^{125}I), technetium ($^{95\text{m}}\text{Tc}$). They concluded that the iodide and pertechnetate sorption increase, while caesium and strontium sorption decrease with increasing HDPy⁺ saturation. They considerably found higher R_d values for Cs^+ in comparison to the bivalent Sr^{2+} . They explained this result by the lower hydration energy (larger ionic diameter) of Cs^+ .

Tahir and Naseem (2003) have the thermodynamic studies of Ni(II) adsorption onto bentonite from aqueous solution. Analysis of the results of adsorption studies performed at 298, 303, 313, and 323 K show at higher temperatures ΔG° decreases. The adsorption process is spontaneous because of positive entropy change (ΔS°). Their other study, Tahir and Naseem (2001) it was studied on the removal of Pb(II) from aqueous/acidic solutions by using bentonite as the adsorbent.

In the paper of Reyes et al. (1999), the relationship between the diffusion coefficients and temperature was examined. They pointed out that the diffusion coefficients correctly exhibit the $T^{1/2}$ dependence. The other researchers, Liu et al., (2003) searched the effect of microstructure of montmorillonite/silica sand mixture on the diffusion of strontium ions.

Börgesson et al. (2003), Kaya and Durukan (2004), Komine (2004) and Xu et al. (2004) did swelling tests on compacted bentonite for determining the swelling pressure, swelling deformation and strain, compaction characteristics, volumetric shrinkage, hydraulic conductivity of compacted bentonite. Sodium-type and a-type bentonite have different properties.

Plecas et al. (2004) investigated leaching behavior and diffusivities of ^{137}Cs and ^{60}Co at different leach rates. They found that by adding 1-5% bentonite into cement-based formulations, only 1-2% of initial radionuclides leach into the environment after 245 days. They can predict percentage of leaching during next 300 years (10 half-lives of ^{137}Cs).

Khan et al. (1995) investigated the sorption of Sr ion on bentonite. They also pointed out that the negative value of the free energy of sorption, at 298 K, showing the spontaneity. ΔG° becomes more negative with increasing temperature, which means sorption process is more favourable at higher temperatures. The positive value of heat of sorption, ΔH° , indicates that the sorption of strontium on bentonite is endothermic. In the desorption studies with groundwater denoted about 90% of Sr ion is irreversibly sorbed onto the bentonite. Shahwan and Erten (2002) researched the thermodynamic parameters of Cs^+ sorption on natural clays such as kaolinite and bentonite. All of the adsorption processes are spontaneous ($\Delta G^\circ < 0$) and exothermic ($\Delta H^\circ < 0$) in character. The negative ΔS° values corresponding to the sorption on kaolinite and bentonite indicate a stable arrangement of Cs^+ on the clay surface.

Ebina et al. (1999) studied the sorption behavior of caesium ions into the smectites. They concluded that there are two distinguishable adsorption sites.

They found that montmorillonite samples fixed approximately 50% of adsorbed Cs ions.

Sheta et al. (2003) have experiments about Zn^{2+} sorption on zeolite and bentonite sorbents. They performed batch adsorption tests for 2 hours. They researched the surface areas of two type of zeolites (clinoptilolite) and bentonite. Although the clinoptilolite-(1) including quartz, feldspar, mica as impurities has a surface area of $407.9 \text{ m}^2/\text{g}$ and the clinoptilolite-(2) having quartz and mordenite as impurities has a surface area of $428.3 \text{ m}^2/\text{g}$, the bentonite sample including quartz and mica as impurities has a surface area of $1009.0 \text{ m}^2/\text{g}$.

Başçetin and Atun (2006) have a paper on the adsorption behavior of strontium on binary mineral mixtures of montmorillonite and kaolinite. They indicate that strontium has two important isotopes, ^{90}Sr which emits β -radiation with a half life of 28 years and ^{85}Sr which is a γ -emitter with a half life of 64.8 days. ^{90}Sr , with its long half life is considered to be the more critical strontium isotope, having a tendency of strong retaining within the living organisms, mainly in the bones, being a source of long-term radiation of bone marrow.

2.4.2. Uses of zeolites

During the Chernobyl disaster thirty or forty times the radioactivity of the atomic bombs dropped on Hiroshima and Nagasaki were released. The main radioactive isotopes from the accident were ^{137}Cs , ^{134}Cs , ^{90}Sr and ^{89}Sr . The details of zeolite applications at Chernobyl remain rather obscure because of secrecy problem still remaining after disintegration of the former Soviet Union. About 500000 tons of zeolite rocks, mainly including clinoptilolite, were processed for use at Chernobyl as protective barriers and as agricultural material in polluted areas. In addition, filters of clinoptilolite tuffs were suggested to extract radionuclides from the drainage water of the encapsulated Chernobyl nuclear power plant. Filtration reduced ^{137}Cs by 95% and ^{90}Sr by 50-60% (Armbruster, 2001).

Ersoy and Çelik (2002) mentioned using the zeta potential measurements that clinoptilolite has a negative charge in water at natural pH. This negative charge results from substitutions of Al^{3+} for Si^{4+} within the clinoptilolite lattice. The cation

exchange capacity of clinoptilolite results from the unbalanced charges. The isomorphic substitutions of Al^{3+} for Si^{4+} leading to some ion exchangeable cations entering into the clinoptilolite channels to supply the positive charge deficiencies of the clinoptilolite lattice.

Singh (1999) modified the surface of the zeolite using n-octadecyltrichlorosilane for extraction of Cs^+ and Sr^{2+} from aqueous to organic phase. Kaya and Durukan (2004) utilized bentonite-embedded zeolite as clay liner. Chmielewska-Horvátová (1998) studied on the removal of ^{137}Cs and ^{134}Ba radionuclides from synthetic aqueous solutions by means of natural clinoptilolite and mordenite. They found that both Freundlich and Langmuir isotherms describe satisfactorily the caesium and barium adsorption on zeolite. They also showed that although barium can be eluted completely from loaded zeolite with the use of ammonium chloride, sodium chloride or calcium chloride solutions, caesium can not be eluted completely under the same experimental conditions.

Elizondo et al. (2000) studied the effects of solution pH and particle size on the removal of ^{137}Cs and ^{90}Sr by natural zeolite (clinoptilolite) from liquid radioactive wastes and observed that natural zeolite having particle size range between 0.25-1.00 mm is an effective filter for the radionuclides mentioned above from a liquid radioactive waste solution having a pH value of 8.

Nilchi et al. (2006) used series of different natural zeolites (clinoptilolite, analcime, mesolite) for the sorption of ^{131}I , ^{99}Mo , ^{153}Sm , ^{140}La and ^{147}Nd radionuclides from simulated waste solutions. They showed that in addition to the type of zeolite, formation of complexes, nature of chemical bond and solvent are responsible for the wide variation in the distribution coefficients for different radionuclides. They also found that the zeolites having larger pores have more efficient uptake of radioactive species from the waste solutions.

Marinin and Brown (2000) studied on the radioactive strontium removal from low-level liquid radioactive wastes by different natural (clinoptilolite) and synthetic (IE-96) zeolites.

Ören and Kaya (2006) calculated the parameters of the Langmuir and Freundlich isotherms for Zn^{2+} adsorption on two zeolites from Gördes and Bigadiç (Turkey). They investigated also the effect of grain size on the metal uptake. They reported that decrease in grain size does not increase the adsorption capacity of zeolite from Gördes, yet it increases that of zeolite from Bigadiç about 23%. According to their results, uptake of zinc was very fast in the first 6 hours, then the exchange equilibrium was established within 2 days for both materials. Negatively charged surface of zeolites can be used for adsorption of alkali earth metals, such as zinc. They researched the factors affecting adsorption characteristics of Zn^{2+} on zeolites. Their comment about the lower adsorption rates of zeolites with respect to bentonites is as the difficulty in the penetration of hydrated zinc ions into the zeolite channels. Hence, adsorption may take place at the zeolite surfaces. The lower adsorption rates for zeolites with respect to bentonites may be due to the difficulty in the penetration of hydrated zinc ions into the zeolite channels.

2.4.3. Uses of kaolins

Jeong (2001) investigated adsorption characteristics of the ^{137}Cs and ^{90}Sr onto kaolinite by batch experiments under various pH conditions (4.5 to 10.5) and concentrations of groundwater cations (Ca^{2+} , Mg^{2+} , K^+ and Na^+) and anions (HCO_3^- , CO_3^{2-} and SO_4^{2-}) ranging from 10^{-5} to 10^{-1} M. They showed that adsorption removal of ^{137}Cs and ^{90}Sr by kaolinite greatly increased as the concentrations of groundwater cations increased 10^{-5} to 10^{-1} M and in most of the experiments Cs^+ is preferentially adsorbed onto kaolinite in comparison to Sr^{2+} .

Eylem et al. (1989) studied on the sorption characteristics of barium ion on kaolinite. Atun and Başçetin (2003) studied with ^{133}Ba by means of a tracer technique in batch experiments. The sorption behavior of Ba^{2+} at different ionic strengths of solutions formed from $BaCl_2$ - $NaCl$ on montmorillonite, kaolinite and illite was investigated. Ionic strengths are ranging from $1 \times 10^{-3}M$ to $1 \times 10^{-1}M$. They reported the exchange capacity Ba^{2+} ions for all three clay minerals increased with decreasing ionic strength.

Erten et al. (1988) pointed out that for kaolinite, the Caesium-137 uptake is reversible process. In other research of Erten and Gökmenoğlu (1994) the sorption behavior of ^{60}Co , ^{65}Zn and ^{133}Ba on alumina, kaolinite and magnesite is presented. They examined the effect of liquid to solid ratio on sorption process of $^{133}\text{Ba}^{2+}$ on alumina. In the experiments they also used mixture of kaolinite-magnesite as adsorbing solid species.

Akar et al. (2005) examined the retention of strontium ions by natural kaolinite and clinoptilolite minerals with respect to kinetic and thermodynamic results. They evaluated thermodynamically the sorption process of this ion on both kaolinite and clinoptilolite was spontaneous and endothermic.

Başçetin et al. (2006) used ^{90}Sr as a radiotracer and individual and binary mineral mixtures of montmorillonite and kaolinite as a clay. β -radioactivity was measured with G-M tube. Tsai and Juyang (2000) and Rafferty (1981) studied the ^{90}Sr uptake onto montmorillonite (Cole et al. (2000)).

In the research of Yavuz et al. (2003), the kinetic and thermodynamic parameters such as enthalpy, free energy and entropy were calculated for the removal of Mn(II), Co(II), Ni(II) and Cu(II) from aqueous solutions using kaolinite. Their values show that adsorption of heavy metal on kaolinite was an endothermic process and it was favoured at high temperatures. According to their results the affinity order is Cu(II)>Ni(II)>Co(II)>Mn(II).

Ikhsan et al. (1999) did a comparative study of the adsorption of transition metals on kaolinite at 25°C in the presence of 5 mM KNO_3 . They evaluated that Zn(II)>>Co(II)≥Mn(II).

The interaction of strontium ions in aqueous solution with the surfaces of calcite and kaolinite investigated by Parkman et al. (1998) using scanning electron microscopy, X-ray absorption spectroscopy.

3. EXPERIMENTAL STUDIES

3.1. Characterization of the Samples

Inorganic sorbents used in the experimental studies are kaolin from Bozhöyük (Bilecik), bentonite from Çankırı and zeolite from Bigadiç (Balıkesir). Before using in sorption experiments, the samples are reduced in size using jaw crusher, roll crusher and grinded by ring mill then finer fractions in the samples are separated by an air separator (Alpin). The size distributions of the samples determined by Sympatec laser sizer are given below.

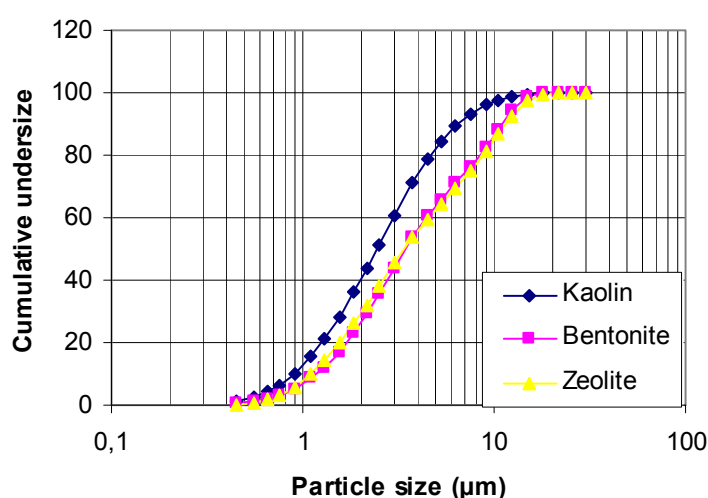


Figure 3.1. Particle size distribution curves of the samples used in the sorption experiments.

Figure 3.1. shows that kaolin has the finest, zeolite and the bentonite have nearly same particle size distribution. The whole rock x-ray diffraction patterns of the air-classified samples (Figure 3.2.) are obtained using Rigaku Dmax-2200 x-ray diffractometer operated at 40 kV and 36 mA using $\text{CuK}\alpha$ radiation. Figure 3.2. showed that all the samples are not in pure state when considering their main minerals, i.e. kaolinite in kaolin, montmorillonite in bentonite and clinoptilolite in zeolite. The type of main minerals in the samples, which is one of the most important parameter in sorption studies, are determined by xrd analyses of clay fractions separated from air-classified samples. The normal, ethylene glycolated and heated xrd patterns of the clay fractions are given in Figures 3.3., 3.4., and 3.5. These figures showed that the main mineral phases in the air classified samples are kaolinite, montmorillonite and zeolite.

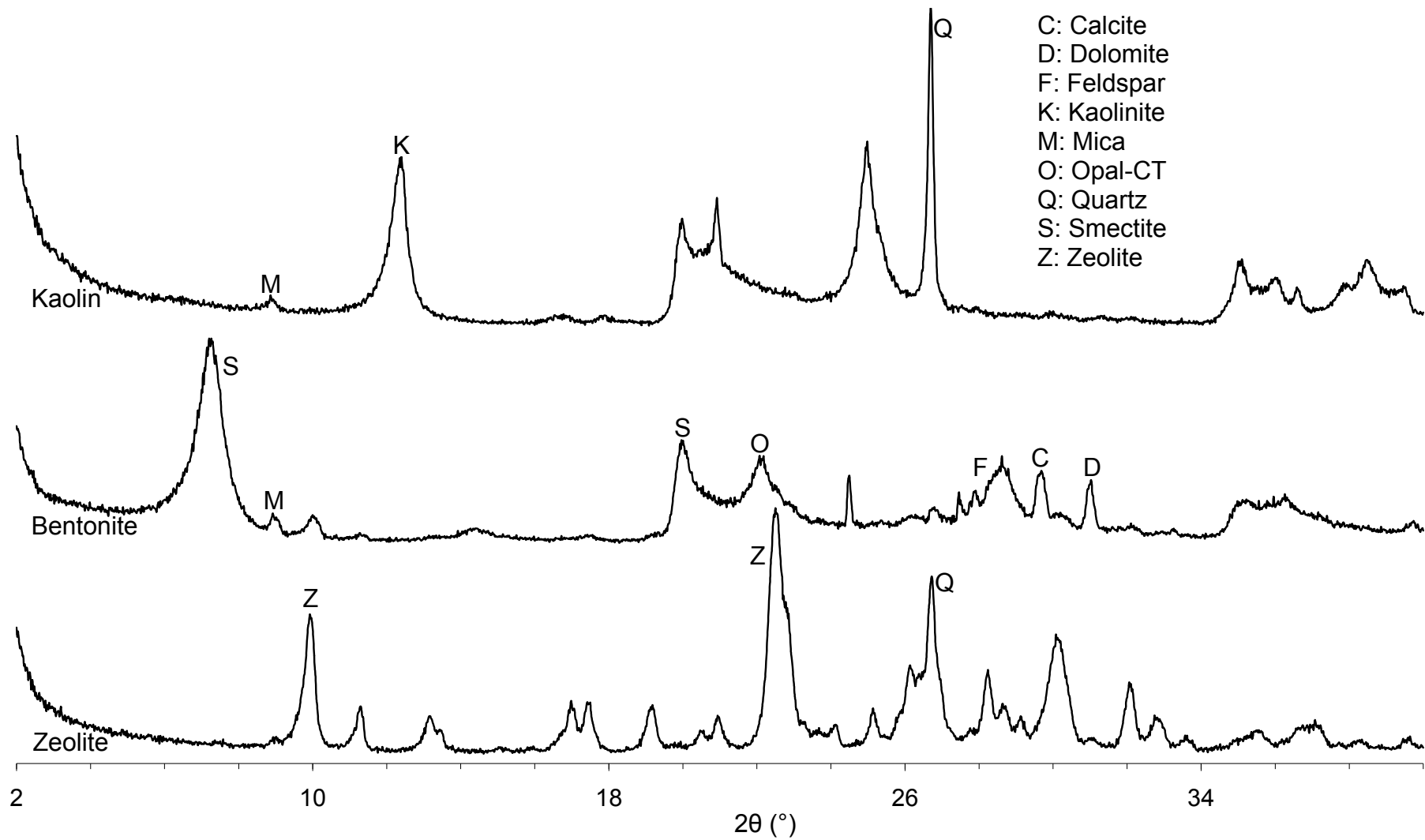


Figure 3.2. X-ray diffractograms of the samples used in sorption studies.

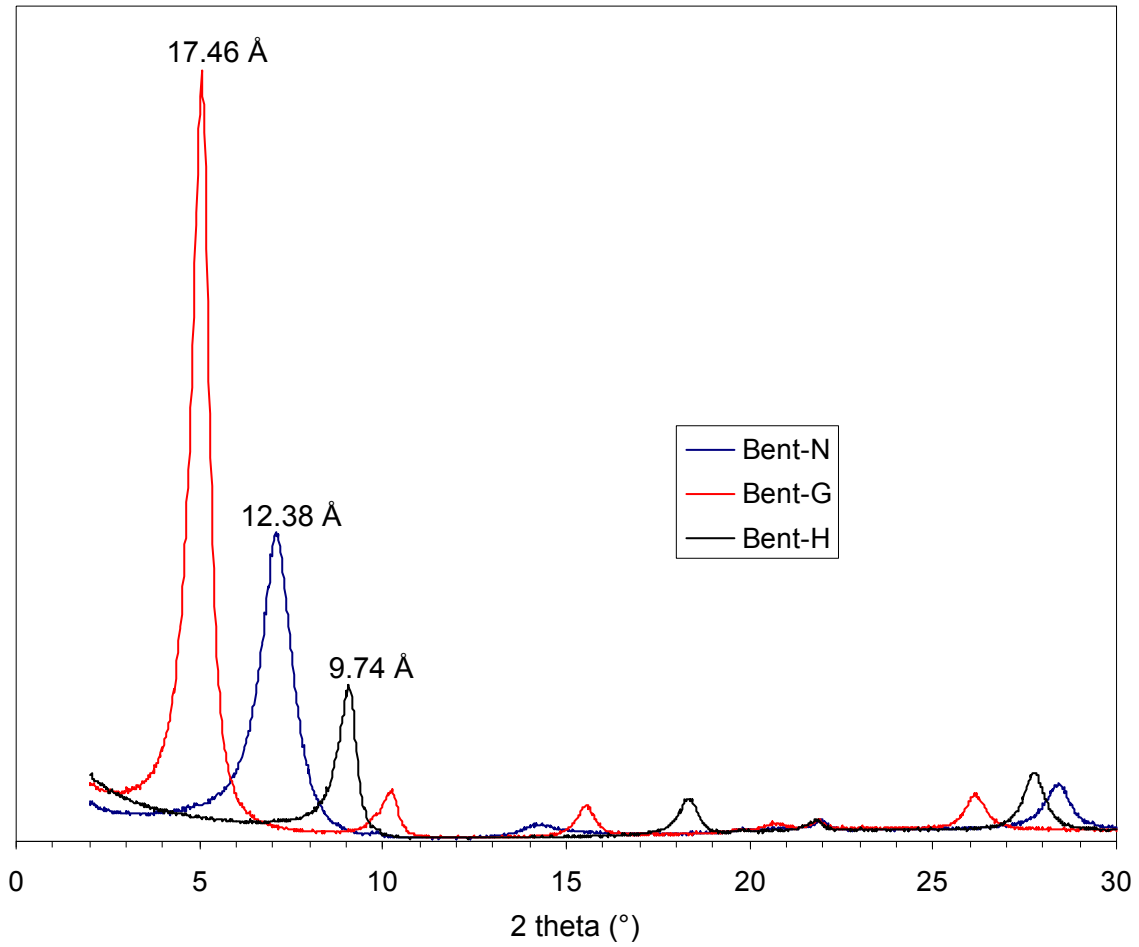


Figure 3.3. X-Ray Diffraction Patterns of the Clay Fraction of Bentonite Sample Following Different Treatments (N:Normal, G:Ethylene glycolated, H:Heated).

Sample of bentonite is purely montmorillonite mineral (Fig.3.3). The written on the peaks are the distance of interlayers of clay.

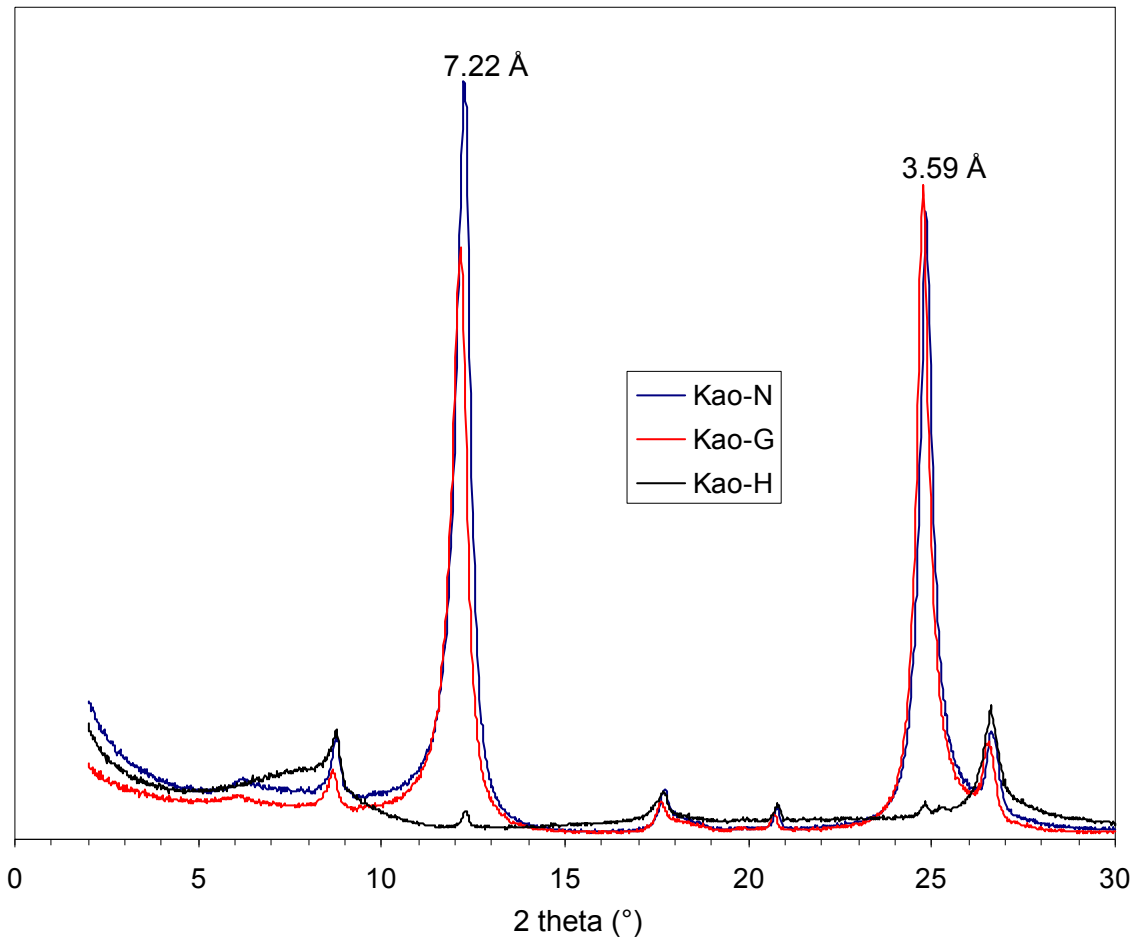


Figure 3.4. X-Ray Diffraction Patterns of the Clay Fraction of Kaolin Sample Following Different Treatments (N:Normal, G:Ethylene glycolated, H:Heated).

In the experiments the used adsorbents are not pure mineral. They are natural clay in their rock form. X-ray diffraction experiments are helping to understand whether the sample is a mixture or nearly pure. In kaolin clay, the composition is mainly kaolinite mineral which is seen in the left-hand side high peak (Fig. 3.4.). Before the high peak (7.22\AA), there is a small peak which demonstrates mika (illite). Its amount in the structure is at low ratio. The writtens on the peaks are the thicknesses of the layers of clay. Because, in kaolin structure there is no interlayer space, its structure is continous.

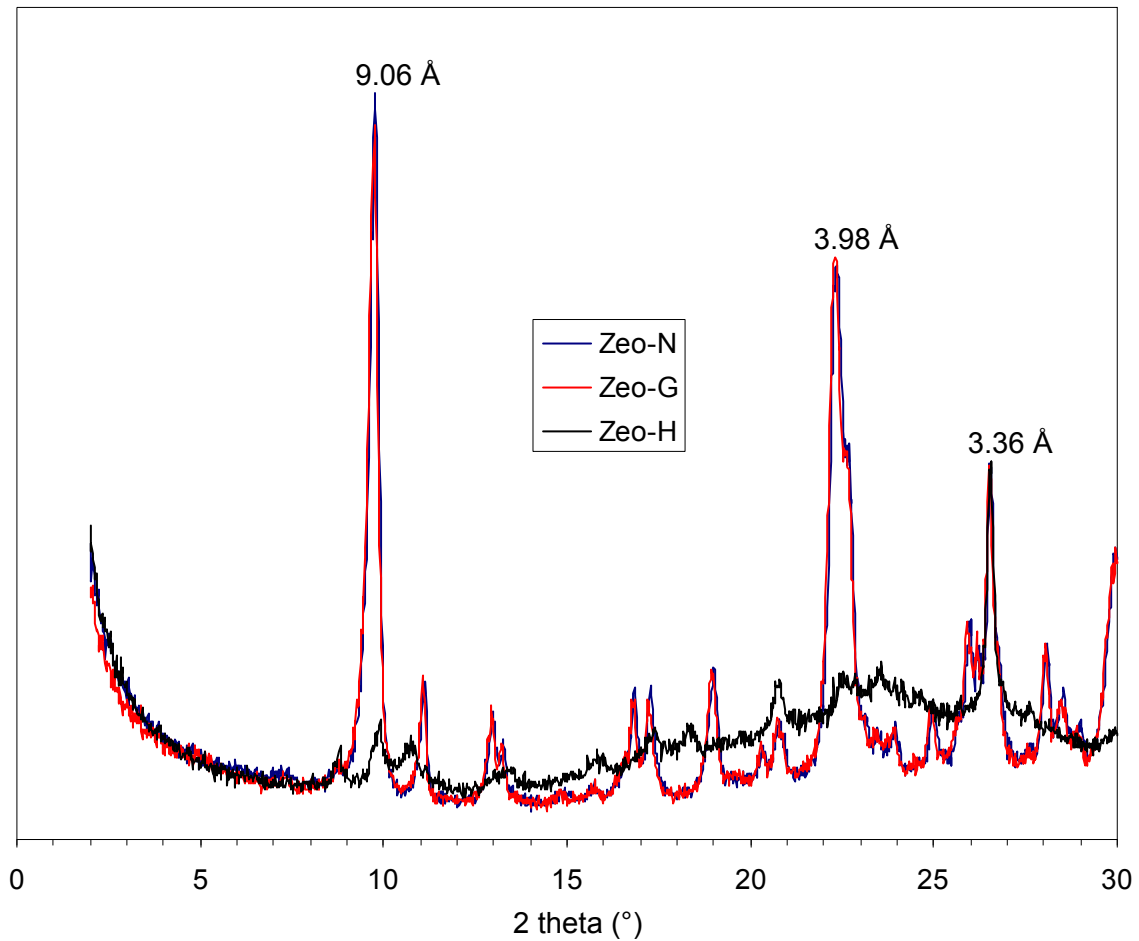


Figure 3.5. X-Ray Diffraction Patterns of the Clay Fraction of Zeolite Sample Following Different Treatments (N:Normal, G:Ethylene glycolated, H:Heated).

At the left-hand side in Figure 3.5. the peak (9.06Å) is showing that the sample is mainly composed of zeolite. In the composition of the sample there is also a little amount of mica.

Table 3.1. The chemical analyses of the samples used in the sorption studies.

SAMPLE	SiO ₂	Al ₂ O ₃	Fe ₂ O ₃	MgO	CaO	Na ₂ O	K ₂ O	TiO ₂	P ₂ O ₅	MnO	Cr ₂ O ₃
	%	%	%	%	%	%	%	%	%	%	%
Bentonite	60.47	17.08	3.39	2.11	2.29	2.36	0.68	0.30	0.11	0.07	<0.001
Zeolite	67.22	11.00	0.80	1.19	3.32	0.17	1.51	0.07	0.03	0.01	0.001
Kaolin	49.81	31.23	1.56	0.65	0.21	0.10	1.04	1.02	0.09	0.01	0.018

SAMPLE	Ba	Cu	Zn	Ni	Co	Sr	Zr	Ce	Y	Nb	Sc	Ta	LOI	TOT/C	TOT/S
	ppm	ppm	ppm	ppm	ppm	ppm	ppm	ppm	ppm	ppm	ppm	ppm	%	%	%
Bentonite	393	9	65	9	<5	724	211	76	18	13	4	11	10.9	0.56	0.02
Zeolite	331	7	22	8	<5	5071	78	34	11	16	2	<5	14.0	0.05	<0.01
Kaolin	233	31	120	45	10	231	130	63	17	20	16	11	14.2	1.08	0.03

The chemical compositions of the solid samples were also determined using ICAP-OE spectrometer and the related results are given in Table 3.1. The samples are not pure mineral, they are in their natural rock forms. According to the reference of Chmielewska (1998) mass percent of SiO₂ is 67.16 % in clinoptilolite type zeolite. In the table 3.1. our result is 67.22% SiO₂. Therefore it is closer to the type of clinoptilolite. Our samples are in their natural rock forms.

The BET surface area (Quantachrome, Monosorb) of the samples used in the sorption studies were determined as (28.85, 26.10), (40.16, 39.8), (25.23, 27.7) m²/g. for kaolin, bentonite and zeolite, respectively.

3.2. Radioisotopes

In the sorption experiments, zinc-65, strontium-90, cobalt-60, caesium-137 and barium-133 radionuclides were used. They are generated by Radioisotope Centre POLATOM in POLAND. The properties of the nuclides are given in Table 3.2.

Table 3.2. Properties of the radionuclide containing compounds used in the study.

Name and chemical formula of the compound	Half life of the radionuclide	Form of the compound	Radionuclidic puridity	Specific activity
Zinc chloride, ZnCl ₂	245 days	0.1 M HCl solution	>99.0%	>5 MBq/mg Zn
Barium chloride, BaCl ₂	10.7 years	1.0 M HCl solution	>99.0%	>1 MBq/mg Ba
Cobalt (II) chloride, CoCl ₂	5.271 years	0.1 M HCl solution	>99.0%	>250 MBq/mg Co
Caesium chloride, CsCl	30.15 years	0.1 M HCl solution	>99.5%	No carrier added
Strontium chloride, SrCl ₂	28.1 years	1.0 M HCl solution	>99.5%	>100 MBq/mg Sr, no carrier added

3.2.1. Preparation of radioisotope solutions

Radionuclides were diluted to 5 mL with pure water to form stock solutions. Then, 0.5 mL was taken from stock solutions and evaporated over a water bath to dryness in polypropylene beakers. In order to change the radionuclides to nitrous form, 17 mL of 0.1 M nitric acid solution added to dried solids and re-evaporated on the water bath. After that dry forms of radioisotopes were diluted to 100 mL (named as 1st solution) with 26.7 mL of 0.1 M HNO₃ solution and 73.3 mL of pure water.

All other experimental solutions were prepared from the 1st solution; i.e. to 3.8 mL of 1st solution, calculated amounts of Zn(NO₃)₂·6H₂O, Ba(NO₃)₂, Co(NO₃)₂·6H₂O, Sr(NO₃)₂, and CsNO₃ salts (Merck grade) are added and diluted to final volume of 500 mL with ground water (for composition see Table 3.5.) to obtain molarities between 10⁻² to 10⁻⁶ M for Zn²⁺, Sr²⁺, Co²⁺, Cs⁺ and 10⁻⁴ to 10⁻⁸ M for Ba²⁺. All of the used materials (tubes, caps, pipette, etc.) used during solution preparation and

adsorption studies are made of propylene. They are used once and stored in order to send to TAEK (Turkish Atomic Energy Authority).

3.2.2. Preparation of synthetic groundwater

The synthetic groundwater prepared using Merck grade salts were used. The anion and cation concentrations in the synthetic groundwater are given in Table 3.3.

Table 3.3. The chemical composition of the ground water*.

Anion	Concentration (meq/mL)		Cation	Concentration (meq/mL)
HCO ₃ ⁻	0.50		Na ⁺	0.50
NO ₃ ⁻	4.20		K ⁺	0.05
Cl ⁻	0.26		Ca ²⁺	0.26
SO ₄ ²⁻	0.79		Mg ²⁺	4.94

*Total equivalent values of cations and anions is equal to 5.75 meq/L and is equal to each other. For prepare the ground water NaHCO₃, KNO₃, CaCl₂, MgSO₄·7H₂O, MgNO₃·6H₂O salts used. For Ba²⁺ sorption experiments NaHCO₃ and MgSO₄·7H₂O did not used cause of precipitation.

3.3. Radiotracer method

Inorganic adsorbents were weighed at about 0.0300 g (30 mg) in polypropylene centrifuge tubes and covered with their caps. For every t time different tubes were prepared. 3 mL of groundwater was added onto sample and the suspension is ultrasonicated for 5 minutes against to the agglomeration in Bandalin sonicator and sonicated samples were equilibrated in ground water for one day at sorption/desorption temperature in Ajtator D-3 (Model 500).

After equilibration, the phases separated by centrifugation (Sigma centrifuge) at 13500 rpm for 10 minutes. The clear liquid is decanted and wet solid at the bottom of the tubes is weighed. The difference in the weights, ΔW_{pt} , is the amount of liquid remaining in the tube after centrifugation. The 3 mL of radioisotope solution added to each centrifuge tube. Sorption experiments were carried out in these

polypropylene tubes. Batch method was used; clay as solid phase and radioactive solution as mobile phase.

The tubes were taken out of the shaker after certain sorption times (i.e. 30 minutes), were centrifuged at a rate of 13500 rpm for 10 minutes. 1 mL was taken from clear supernatant by automatic pipette and transferred into 12 mm diameter polypropylene counting tubes. For each “t” time one centrifuge tube and also one counting polypropylene tubes used. For ⁹⁰Sr, instead of 1mL of counting tube, the aluminum planchets were used. 1 mL of strontium-90 solutions were dried at room temperature on these planchets, counted for 1 minute. ⁶⁵Zn, ¹³³Ba, ⁶⁰Co and ¹³⁷Cs are gamma emitters. We used a γ -counting system with NaI(Tl) crystal for the counting of gamma radiation from these radioisotopes. For the calculations, only photo-peak counts were used. Being a β -emitter, we used a sample counting system with a window type Geiger Müller counter for ⁹⁰Sr experiments.

Before starting experiments with γ -emitter isotopes, we have obtained the energy spectrums of the gammas from the ⁶⁵Zn, ¹³³Ba, ⁶⁰Co and ¹³⁷Cs to make sure that there is no contamination in these isotopes.

3.4. The Distribution Ratio

The experimental data in sorption are expressed in terms of the distribution ratio, R_D , defined as the ratio of sorbate concentration on solid phase to its concentration in liquid phase. R_D can be expressed in terms of activity.

The distribution ratio is defined by

$$R_{D,ad} = \frac{[Cs]_{s,ad}}{[Cs]_{ad}} \dots\dots\dots(1)$$

where,

$[Cs]_{s,ad}$ = concentration of Cs^+ in the solid phase after sorption,

$[Cs]_{ad}$ = concentration of Cs^+ in the solution after sorption.

Since at the beginning of sorption V mL of solution with an initial caesium concentration $[Cs]^o$ was added and at the end of sorption step $(V+\Delta W_{pt})$ mL of solution with concentration $[Cs]_{ad}$ was present.

Here ΔW_{pt} is the amount of liquid remaining in the tube after pretreatment and decantation (after pretreatment, before sorption).

The concentration of Cs^+ in the solid after sorption is given by

$$[Cs]_{s,ad} = \frac{V \cdot [Cs]^o - [Cs]_{ad} \cdot (V + \Delta W_{pt})}{W_s} \dots\dots\dots(2)$$

and R_D can be expressed in terms of activity.

The adsorption distribution ratio, $R_{D,ad}$, was calculated from the measured activities before and after shaking using the following relations;

$$[Cs]_{ad} = \frac{A_{l,ad}}{A^o} \cdot [Cs]^o \dots\dots\dots(3)$$

Substituting equations (2) and (3) into equation (1) leads to;

$$R_{D,ad} = \frac{V \cdot A^o - A_{l,ad} \cdot (V + \Delta W_{pt})}{A_{l,ad} \cdot W_s} \dots\dots\dots(4)$$

where;

A^o = initial count rate, used radioisotope activity of 1 mL,

$A_{l,ad}$ = count rate of 1 mL of solution after sorption,

W_s = weight of solid material (g),

V = volume of solution (mL),

ΔW_{pt} = amount of liquid remaining in the tube after pretreatment, before sorption.

For the desorption studies the experimental procedure used is: following the adsorption step, after 72 hours which means reaching equilibrium, 3 mL of groundwater was added to the sample tube, shaken for the desired time, centrifuged and decanted. 1 mL of the liquid phase was counted.

The distribution ratio of desorption, R_{de} ,

$$R_{de} = \frac{[Cs]_{s,de}}{[Cs]_{de}} \dots\dots\dots(5)$$

$[Cs]_{s,de}$ = concentration of Cs^+ in the solid phase after desorption,

$[Cs]_{de}$ = concentration of Cs^+ in the solution after desorption.

$$[Cs]_{de} = \frac{A_{l,de}}{A^o} \cdot [Cs]^o \dots\dots\dots(6)$$

The distribution ratio of desorption, R_{de} , was calculated from the following relation;

$$R_{D,de} = \frac{V \cdot A^o - A_{l,ad} \cdot (V + \Delta W_{pt} - \Delta W_{ad}) - A_{l,de} \cdot (V + \Delta W_{ad})}{A_{l,de} \cdot W_s} \dots\dots\dots(7)$$

where,

ΔW_{ad} = the amount of liquid remaining in the tube after adsorption and decantation,

$A_{l,de}$ = count rate of 1 mL of solution after desorption.

The rest of the terms in equation (7) have been defined earlier.

3.5. The Experiments

The adsorption experiments were carried out at 5, 10, 15, 20 and 25°C for zinc-65, strontium-90, cobalt-60, caesium-137 and barium-133 by using bentonite, zeolite and kaolin according to the flowsheet given in the Figure 3.4. Counting system was shown in Figure 3.5. R_D results calculated for every system.

All adsorption studies which were performed at 5°C, the concentrations were chosen from $1 \cdot 10^{-2}$ to $1 \cdot 10^{-6}$ M for Zn^{2+} , Sr^{2+} , Co^{2+} , Cs^+ cations and from $1 \cdot 10^{-4}$ to $1 \cdot 10^{-8}$ M for Ba^{2+} . For the other temperatures (10, 15, 20, 25°C) $1 \cdot 10^{-6}$ M cation concentration were chosen to study.

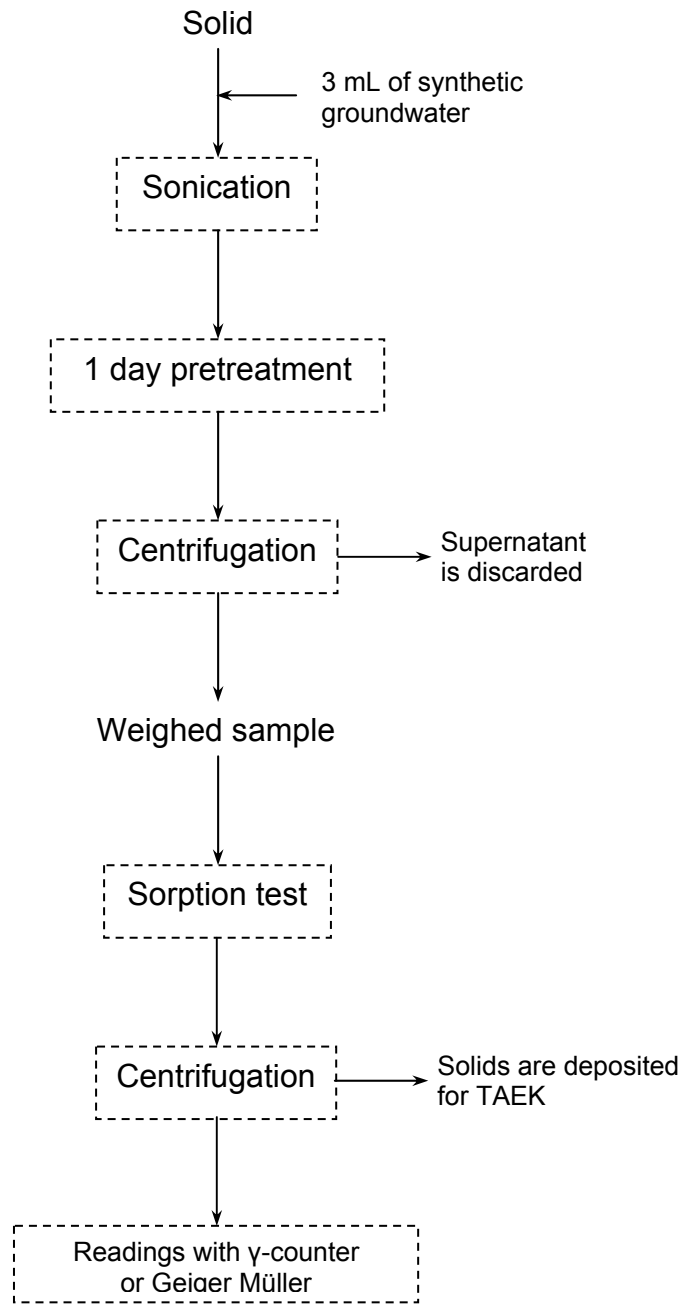


Figure 3.6. Schematic presentation of the experimental procedure.

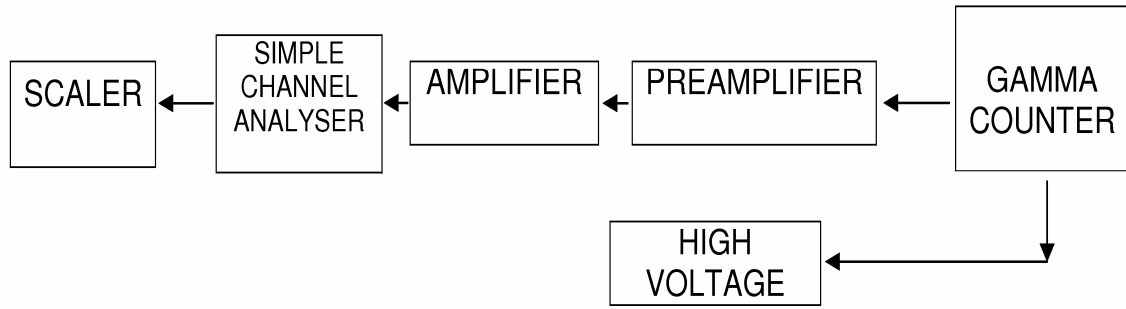


Figure 3.7. Schematic diagram of counting system.

After performing sorption studies, some of the thermodynamic and kinetic results related with adsorption of each system were evaluated.

Freundlich expression can be linearized as:

$$\log (\text{mol rad./g}_s) = \log k + n \log [C]_i \dots\dots\dots(6)$$

mol rad./g_s= no. of moles of radioisotope adsorbed per gram of solid,

[C]_i = concentration of cation remained in the solution

Plotting log(mol rad./g_s) vs log[C]_i yields n as the slope and log k as the intercept.

At equilibrium no change in Gibbs free energy occurs and the above equation reduces to:

$$\Delta G^\circ = -RT \ln R_d \dots\dots\dots(7)$$

So, using Eq. (7), it is possible to determine ΔG° of sorption directly from the R_D values at different temperatures. Gibbs free energy change can also be written in terms of enthalpy change, ΔH° , and the entropy change, ΔS° , as given below:

$$\Delta G^\circ = \Delta H^\circ - T\Delta S^\circ \dots\dots\dots(8)$$

Combining Eqs (7) and (8) the following expression result is obtained:

$$\ln R_D = \frac{-\Delta H^\circ}{R} \times \frac{1}{T} + \frac{\Delta S^\circ}{R} \dots\dots\dots(9)$$

By plotting $\ln R_D$ versus $1/T$, it is possible to determine the value of ΔH° of sorption from the slope and ΔS° of sorption from the intercept of the linear fits.

The uncertainties in the measurements stemmed principally from those of counting statistics. Other error sources of less importance were those originating from weight and volume measurements.

4. RESULTS AND DISCUSSION

(In activity graphs, the background activity is included in the activity data; it is 4750/5 min. for Ba-133, 780/5min., 540/5min. for Co-60, 1740/5min. for Cs-137, 715/5 min. for Zn-65. The total activity-time plots were drawn. In the other hand, in distribution ratios versus time (R_D -time plots) in the calculations, the background activity is subtracted from the total activity measurements).

4.1. The results of ^{65}Zn ion adsorption behaviours on bentonite, kaolin and zeolite

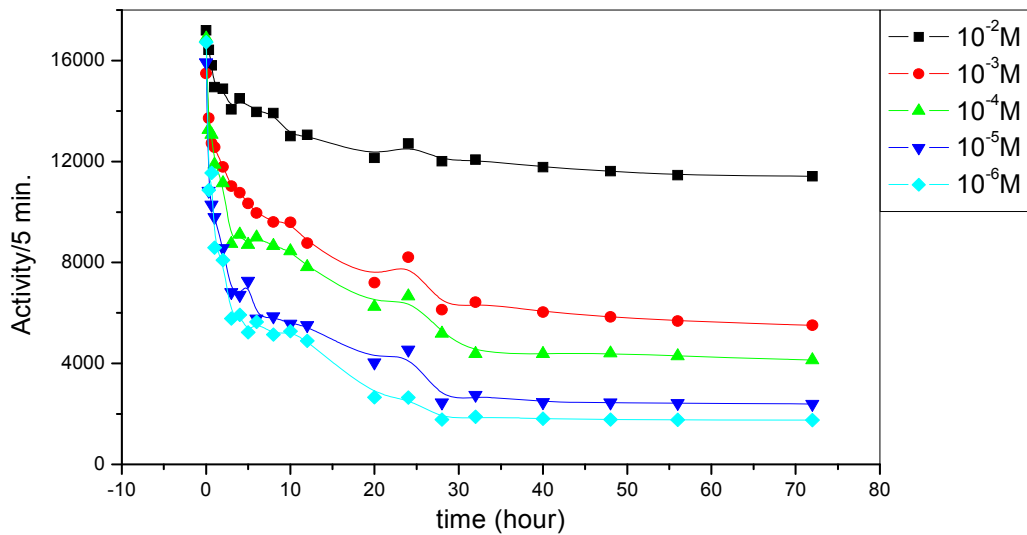


Figure 4.1. Counted activity-time plot of $^{65}\text{Zn}^{2+}$ uptake on bentonite. The effect of cation concentration on sorption was investigated at 5°C .

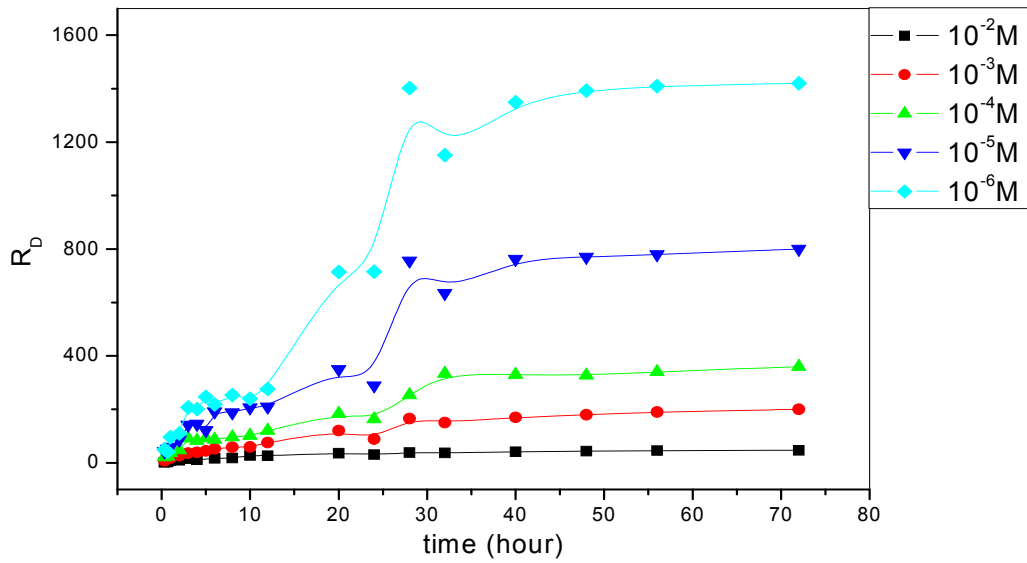


Figure 4.2. $^{65}\text{Zn}^{2+}$ uptake on bentonite. The effect of cation concentration on sorption was investigated at 5°C .

In all studies which the concentration effect was investigated it was seen a general behavior; as the concentration increases the distribution ratios decrease cause of the reaching to maximum capacity of the sites on which sorption takes place. After the sites are occupied further adsorption can not occur. Two days duration is sufficient in order to reach equilibrium at 5°C .

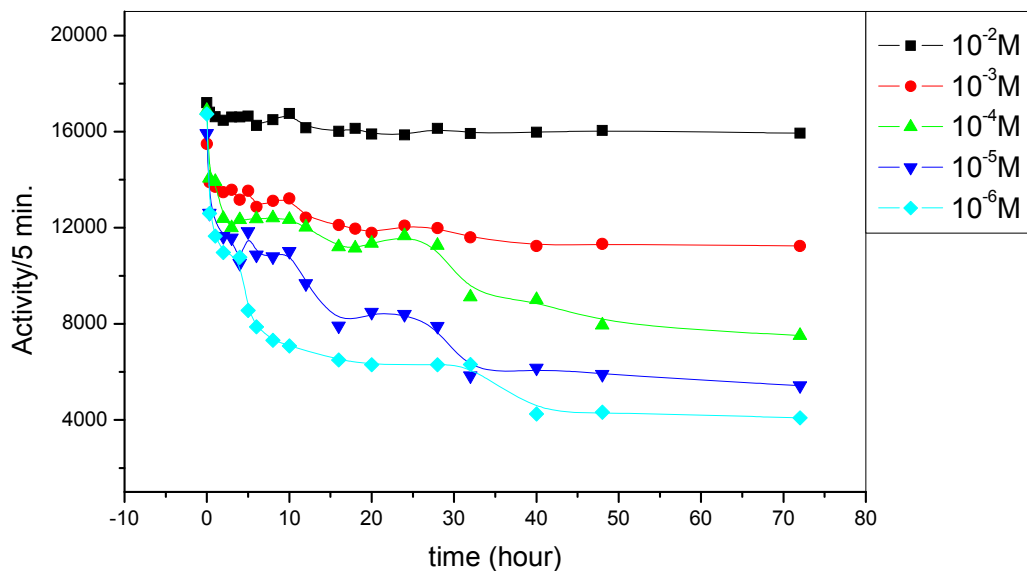


Figure 4.3. Counted activity-time plot of $^{65}\text{Zn}^{2+}$ uptake on zeolite. The effect of cation concentration on sorption was investigated at 5°C .

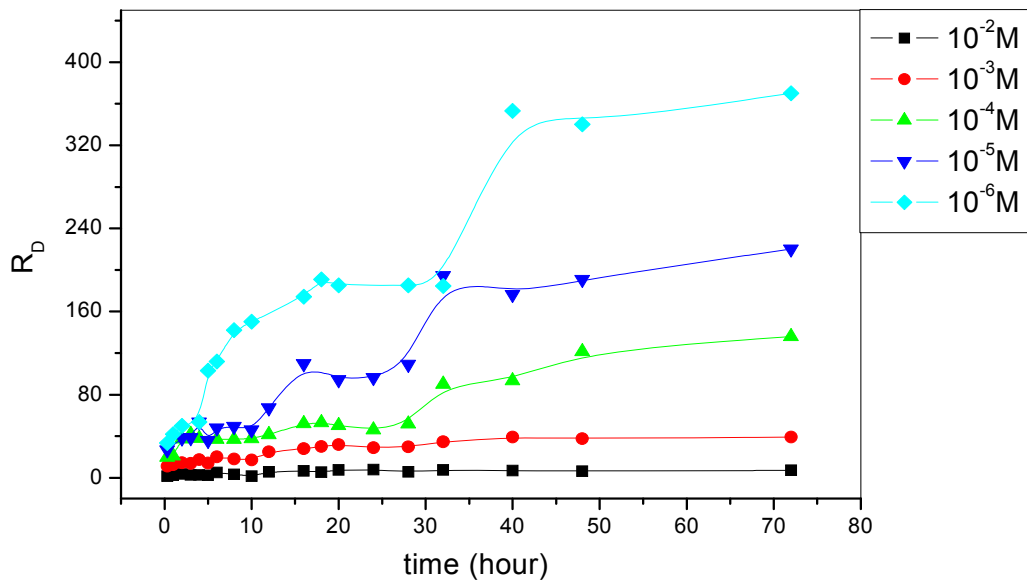


Figure 4.4. ⁶⁵Zn²⁺ uptake on zeolite. The effect of cation concentration on sorption was investigated at 5°C.

In Fig.s 4.2 and 4.4, it is clearly seen that, Zn²⁺ is highly adsorbed on bentonite than zeolite. Montmorillonite is a clay mineral type which can swell so the distances between TOT layers can increase in pretreatment step. So Zn²⁺ can diffuse easily. In Zeolite there are cavities, pores and channels in the structure. It is not easy to penetrate in the cavities. The cation exchange on the channels and the placement of cation in the hole of the structure in zeolite is difficult comparing with bentonite structure. For this reason adsorption capacity of bentonite is higher than that of zeolite.

There are one more than one pathway of uptake of cation on montmorillonite mineral in bentonite. Between the layers and also surface bonding by means of oxygen atom in silanole groups. In the reference of Abidin Kaya et al. (2005) The interaction between the zinc ion and bentonite can be given by the equilibrium:



where *m* is the exchangeable cation valence, M (Na, K, Ca, Mg) and subscripts (s) and (b) denote solution and bentonite phases, respectively.

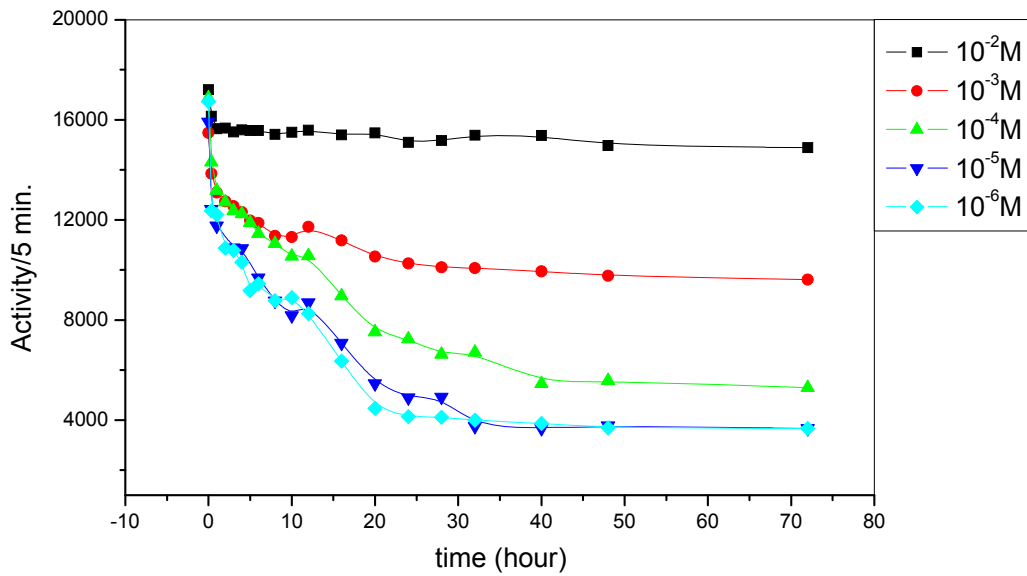


Figure 4.5. Counted activity- time plot of $^{65}\text{Zn}^{2+}$ uptake on kaolin. The effect of cation concentration on sorption was investigated at 5°C .

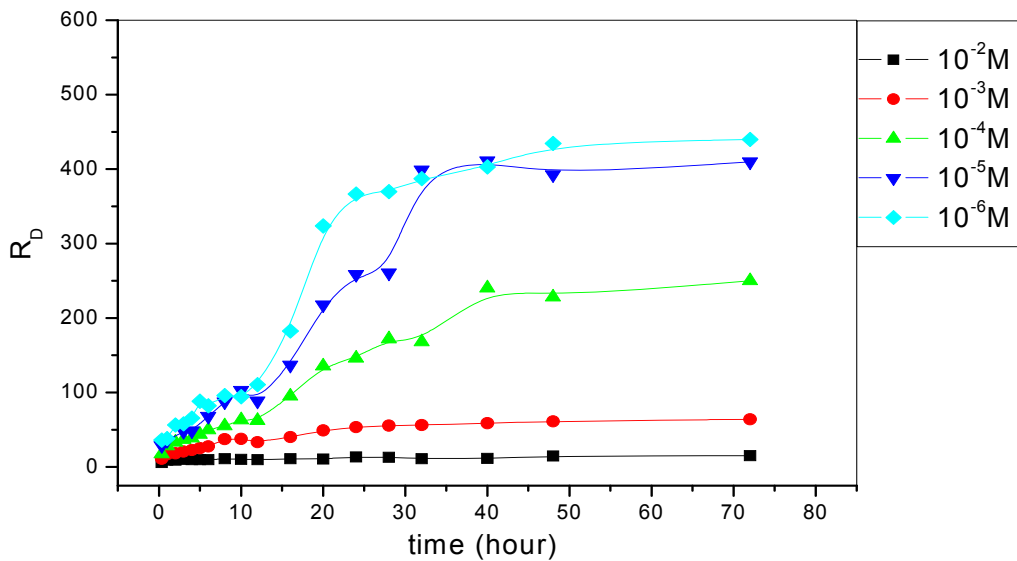


Figure 4.6. $^{65}\text{Zn}^{2+}$ uptake on kaolin. The effect of cation concentration on sorption was investigated at 5°C .

The adsorption of zinc ion on kaolin is quite less than that on bentonite because of there is no any opportunity of cation exchange between the layers in kaolinite structure (see in Figs. 4.6. and 4.2.). They bonded together very tightly. But montmorillonite layers are bonded to each other weakly; by means of van der

Waals bonds. On kaolinite, cation bonding occurs on surface. On montmorillonite exchange achieves mainly between layers rather than on surface.

4.2. The results of ^{137}Cs ion adsorption behaviours on bentonite, kaolin and zeolite

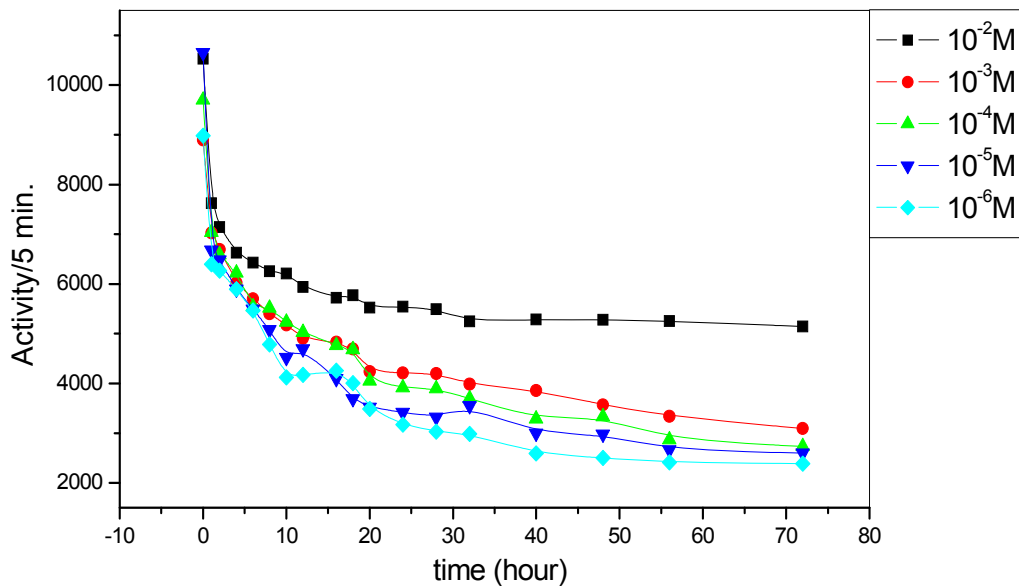


Figure 4.7. Counted activity- time plot of $^{137}\text{Cs}^+$ uptake on bentonite. The effect of cation concentration on sorption was investigated at 5°C .

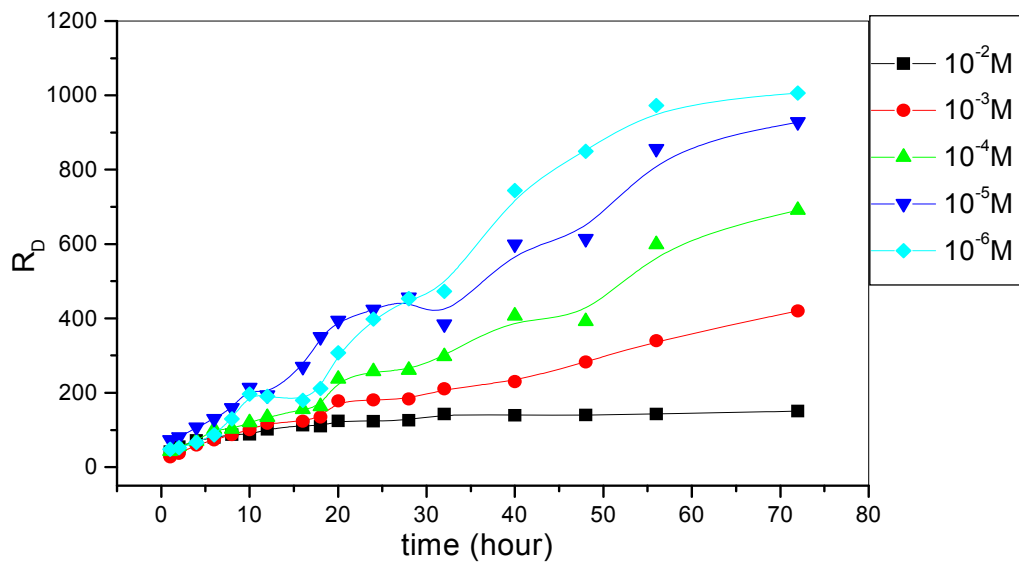


Figure 4.8. $^{137}\text{Cs}^+$ uptake on bentonite. The effect of cation concentration on sorption was investigated at 5°C .

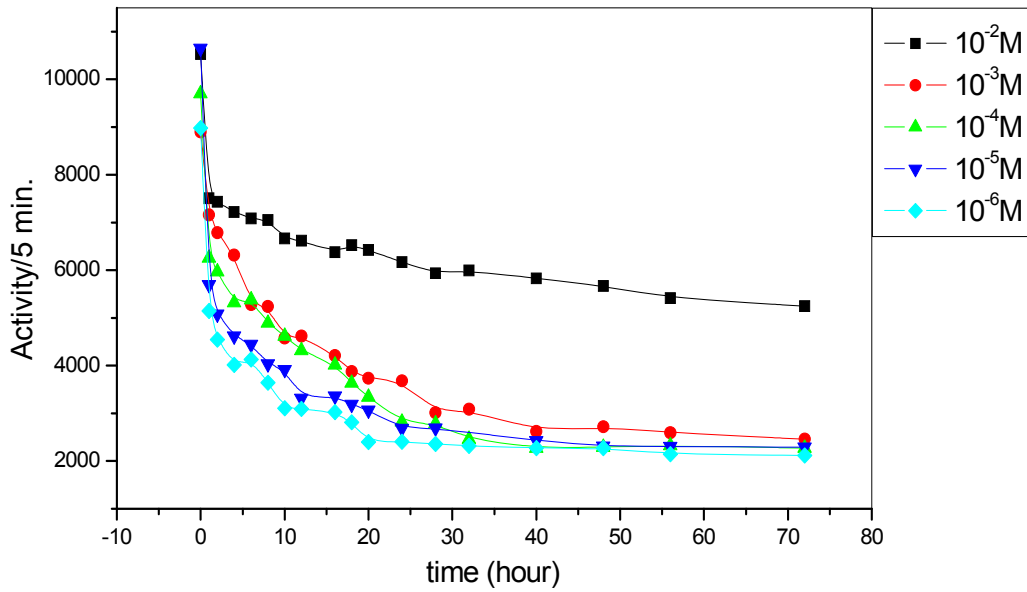


Figure 4.9. Counted activity- time plot of $^{137}\text{Cs}^+$ uptake on zeolite. The effect of cation concentration on sorption was investigated at 5°C .

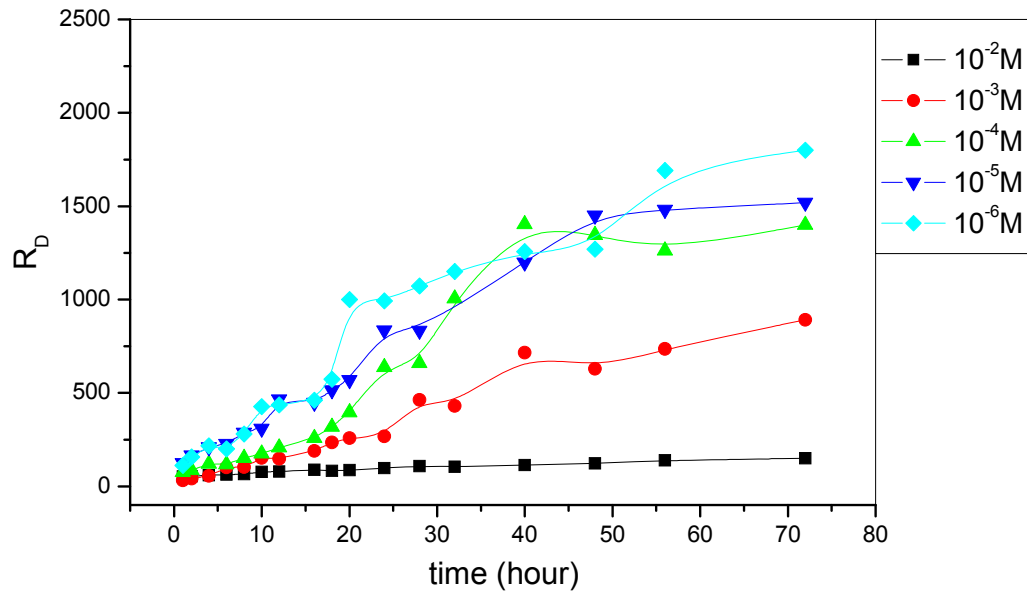


Figure 4.10. $^{137}\text{Cs}^+$ uptake on zeolite. The effect of cation concentration on sorption was investigated at 5°C .

Enthalpy of hydration, ΔH_{hyd} , of an ion is the amount of energy released when a mole of the ion dissolves in a large amount of water forming an infinite dilute solution in the process, $\text{M}^{\text{Z}^+}_{(\text{aq})}$ represents ions surrounded by water molecules and

dispersed in the solution. The hydration energies of cations are listed here. The table illustrates the point that as the numbers increases this means the ionic size increases in the same group of a periodic table, leading to a decrease in absolute values of enthalpy of hydration.

Table 4.a. Ion radius and hydration energy of studied cations.

Ion	r_{ion} (Å)	ΔH_{hyd} (kJ/mol)
Cs ⁺ (IA) group	1.67	-276
Ba ²⁺ (IIA) group	1.35	-1305
Sr ²⁺ (IIA) group	1.12	-1443
Co ²⁺ (Transition metal)	0.745	-1996
Zn ²⁺ (Transition metal)	0.74	-2046

In the results of the experiments which were shown at Figs. 4.4. and 4.10., it is obvious that the adsorptions of Cs⁺ and Zn²⁺ on zeolite are very different from each other; that of Cs⁺ is higher than that of Zn²⁺. Cs⁺ ion has larger ionic size, its hydration energy is low. Cs⁺ ion behaves likely to be adsorbed rather than be hydrated. On the other hand, Zn²⁺ ions have higher hydration energy which means that so much heat evolves during the hydration. Zn²⁺ prefers be hydrated by water molecules which are around itself. There is a sphere which made of H₂O molecules at radius 4.30 Å. (hydrated ionic radius value was taken from thesis of Güray 1997). Alkali cation-exchange selectivity is controlled by selectivity of the solution phase for the more strongly hydrated cation.

“effective” radius of the cation (i.e., the hydrated radius): A larger hydrated radius means that the cationic center of charge is farther from the clay surface so the clay-cation electrostatic interaction is weaker. The selectivity rule based on the smallest hydrated radius means that the cation with the “least negative heat of hydration” is preferred, because the more weakly hydrated ions are easier to dehydrate and therefore more likely to be specifically adsorbed to the surface (Brian and Miller 2006).

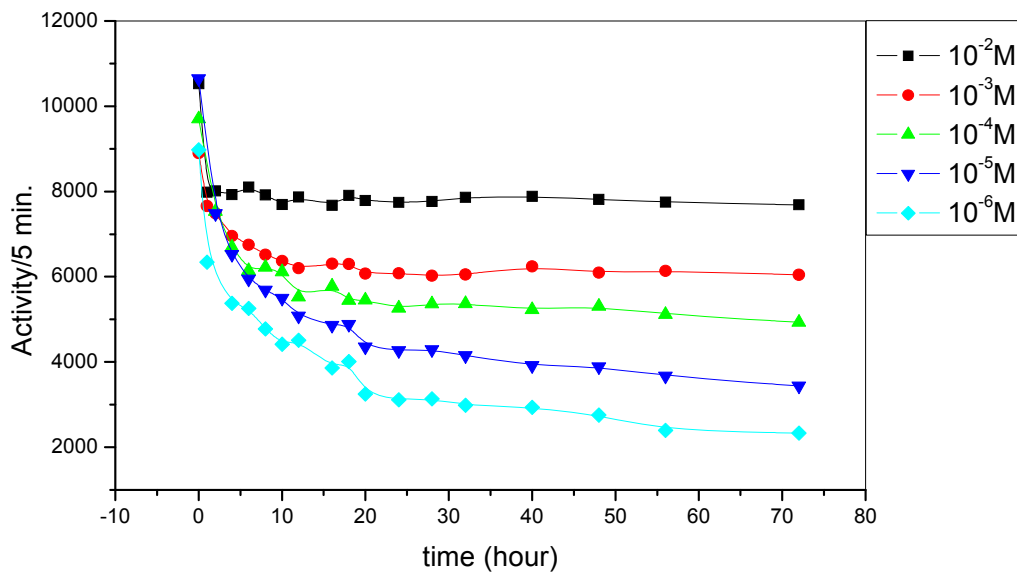


Figure 4.11. Counted activity- time plot of $^{137}\text{Cs}^+$ uptake on kaolin. The effect of cation concentration on sorption was investigated at 5°C .

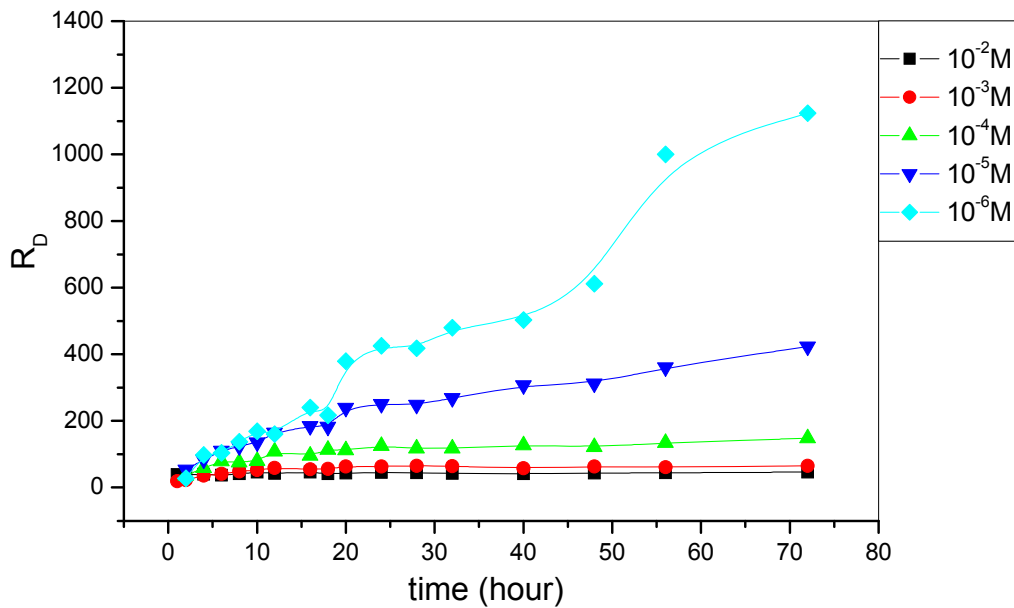


Figure 4.12. $^{137}\text{Cs}^+$ uptake on kaolin. The effect of cation concentration on sorption was investigated at 5°C .

In Figs. 4.12. and 4.6., high distribution ratio were obtained by using caesium ion on kaolin, rather than zinc cause of low hydration energy of Cs^+ . Surface

adsorption of Cs^+ ions on kaolin occurs. In Fig. 4.11. it is seen rapid decrease in activity, so Cs^+ ions adsorbed in short time.

According to the Figs. 4.8., 4.10. and 4.12 the order of adsorption capacity, in the respect of used adsorbents, is on zeolite > bentonite > kaolin. Cs^+ ions tend to sorbed on zeolite rather than be surrounded by water molecules. They can move in the channels and vacancies in the structure.

In this part in order to discuss the adsorption differences lets remember the structures: Silicon, which is 4-fold coordinated with oxygen, forms sheets. When combined with similar flat sheets of a 6-fold coordinated aluminium with oxygen and hydroxyl groups, mixed layers of silicate tetrahedra and aluminate octahedra are obtained.

Phyllosilicates constitute the principal family of clays. Their structure consists of sandwiches of layered compounds and in ideal cases they have one perfect plane of cleavage. Therefore phyllosilicates are built by arrangements of tetrahedra (T) and octahedra (O), in order to obtain infinite layers, and clays can be described by stacking of T and O sheets. As a clay layer is a combination of sheets, there is an interlayer space between two layers. The presence of ions in the interlayer space depends on the composition of the sheets (Fig.4.a). Nevertheless this presentation of phyllosilicates is idealistic and many atoms are substituted in actual solids. Some cations of octahedral or tetrahedral sheets can be replaced by others carrying a different charge. Therefore, usually the layers are charged and cations have to be present in the interlayer space to counterbalance this charge, in order to constitute a neutral compound.

Charge-imbalanced substitutions in the inorganic crystalline network (e.g., Al^{3+} for Si^{4+} in tetrahedral coordination, or Mg^{2+} for Al^{3+} in octahedral coordination, result in net negative charges, the amount of which is directly related to the amount of substitutions. The structural charges of clay are called permanent charges because they are independent of the physico-chemical conditions in the surrounding medium.

The CEC (cation exchange capacity) of kaolinite is very low, since the layers are neutral and the interlayer space does not contain cations. As for kaolinite, there are no cations in the interlayer space (Konan et al. 2007 and Salles et al. 2006), (Fig. 4.a.).

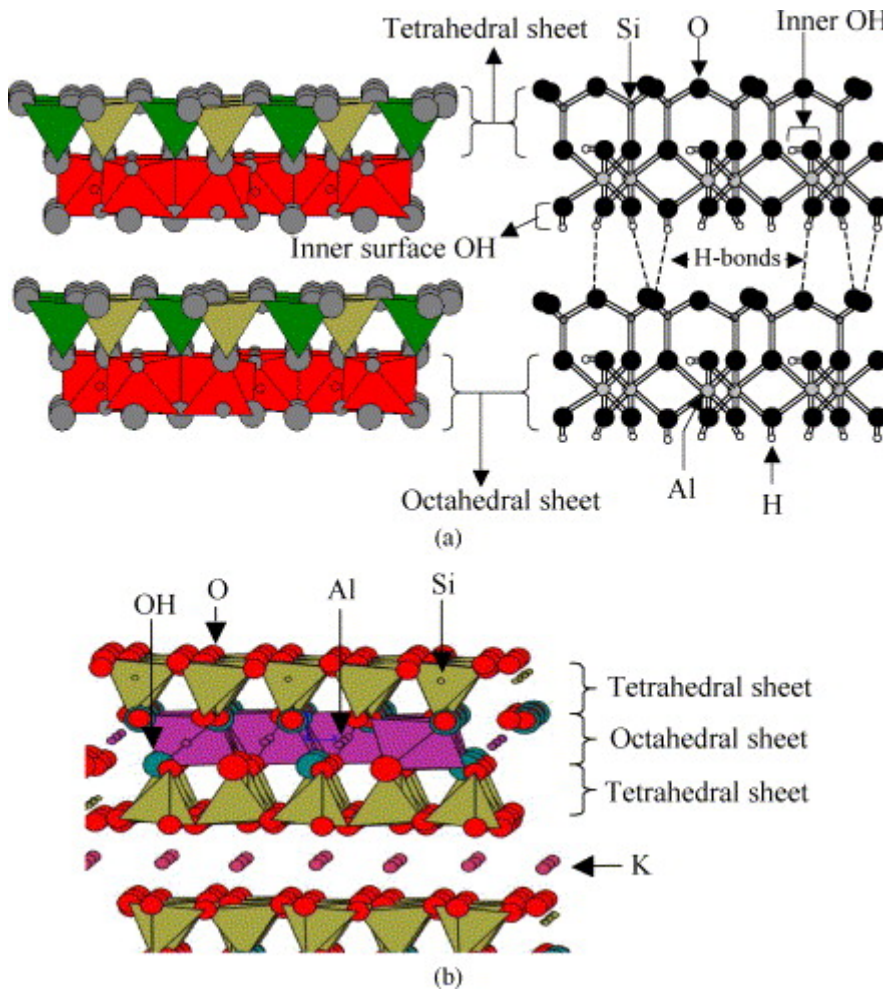


Figure 4.a. Structure of 1:1 clay mineral (a) and 2:1 clay mineral (b).(Konan et al. 2007).

On kaolinite, only surface bondings of cations occur, layers are not distinct from each other. But in montmorillonite, the layers are not close to each other. There are space that cation which comes from solution takes place. It displace here.

Surface properties of kaolinite, the water film adsorbed on the surface, can be modified by introducing various exchangeable cations, which affect these properties by changing the hydration state of the surface. The degree of the surface hydration should be related to the hydration energy of the cations. The mechanisms of water adsorption on clay minerals are (1) the hydration of exchangeable cations, (2) hydrogen bond formation with surface hydroxyls, (3) the surface dipole water dipole interactions, and (4) the dispersion forces, interactions (Janczuk 1989).

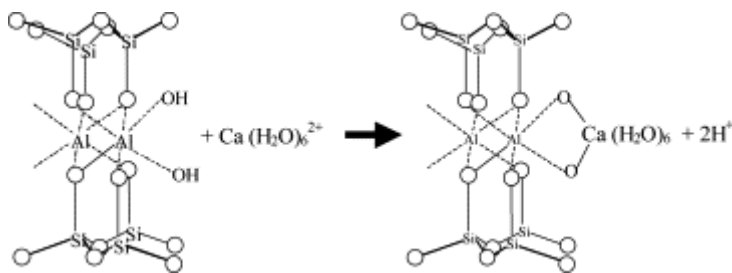


Figure 4.b. A qualitative description of the binding mechanism of hydrated metal onto clay minerals surfaces (Konan et al. 2007).

The surface interaction is formed by hydrogen bondings which were formed by the hydrogen of the water molecules present at surroundings of hydrated cations over the oxygen atom bonded to aluminium atom. This is carried out in the octahedral sheet of the clay (Fig.4.b.).

or ; in tetrahedra sheets the hydrogen bondings occurs by the hydrated cation (Figure 4.c.).

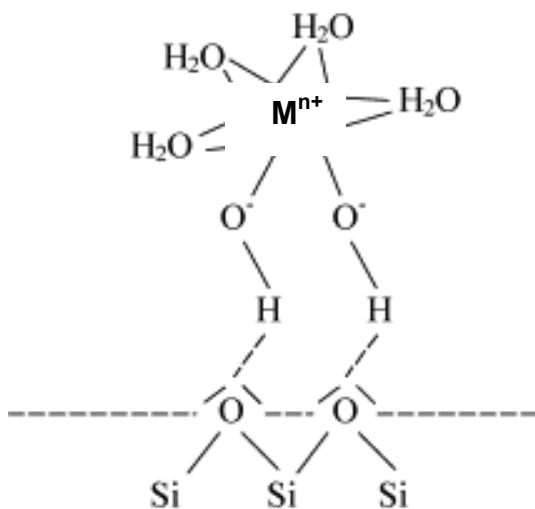


Figure 4.c. Schematic representation of possible interactions between silica faces and hydrated ions. (Konan et al. 2007).

4.3. The results of ^{60}Co ion adsorption behaviours on bentonite, kaolin and zeolite

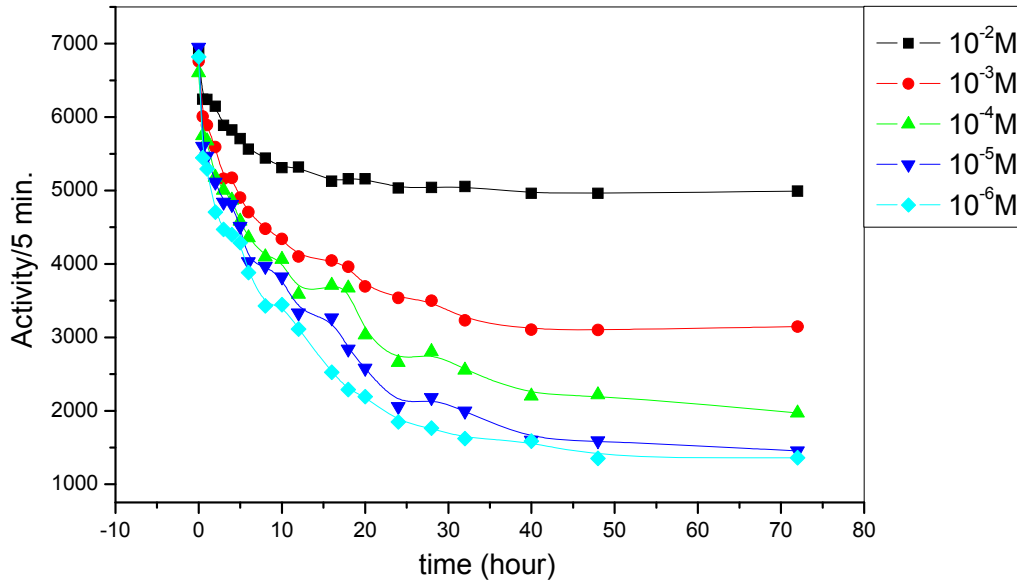


Figure 4.13. Counted activity- time plot of $^{60}\text{Co}^{2+}$ uptake on bentonite. The effect of cation concentration on sorption was investigated at 5°C .

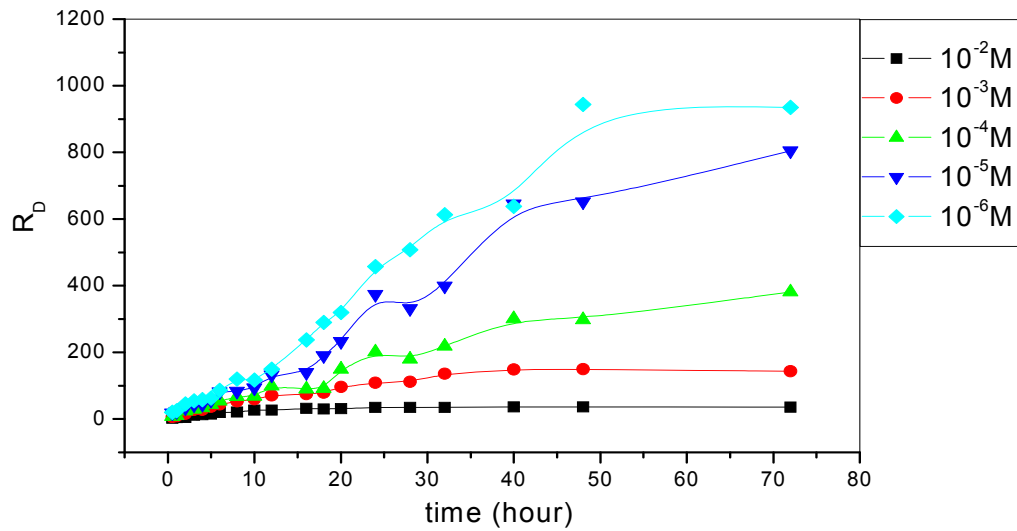


Figure 4.14. $^{60}\text{Co}^{2+}$ uptake on bentonite. The effect of cation concentration on sorption was investigated at 5°C .

Given two cations of equal valence, the more weakly hydrated will tend to partition into the “subaqueous” smectite interlayer phase (Brian and Miller 2006).

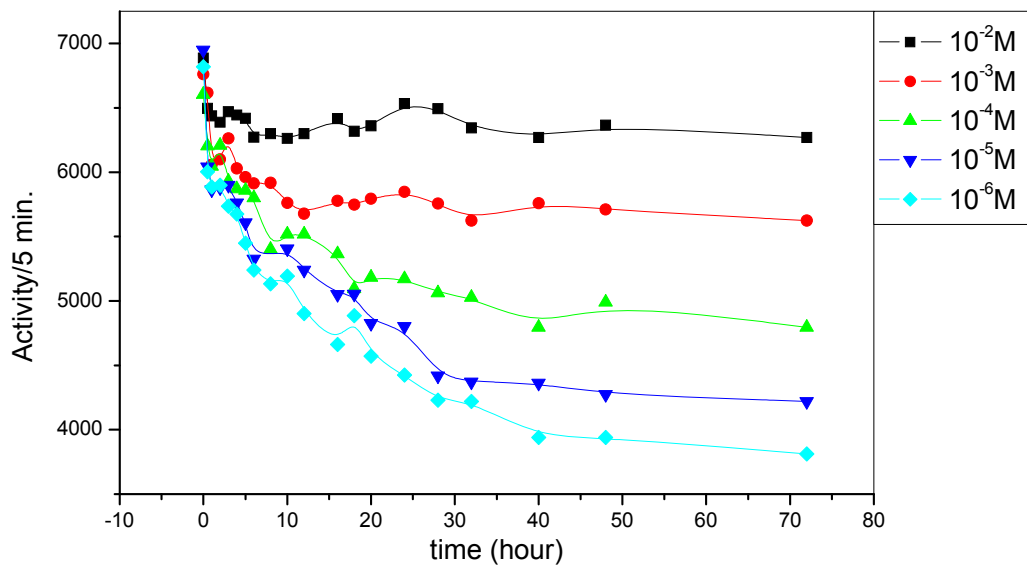


Figure 4.15. Counted activity- time plot of $^{60}\text{Co}^{2+}$ uptake on zeolite. The effect of cation concentration on sorption was investigated at 5°C .

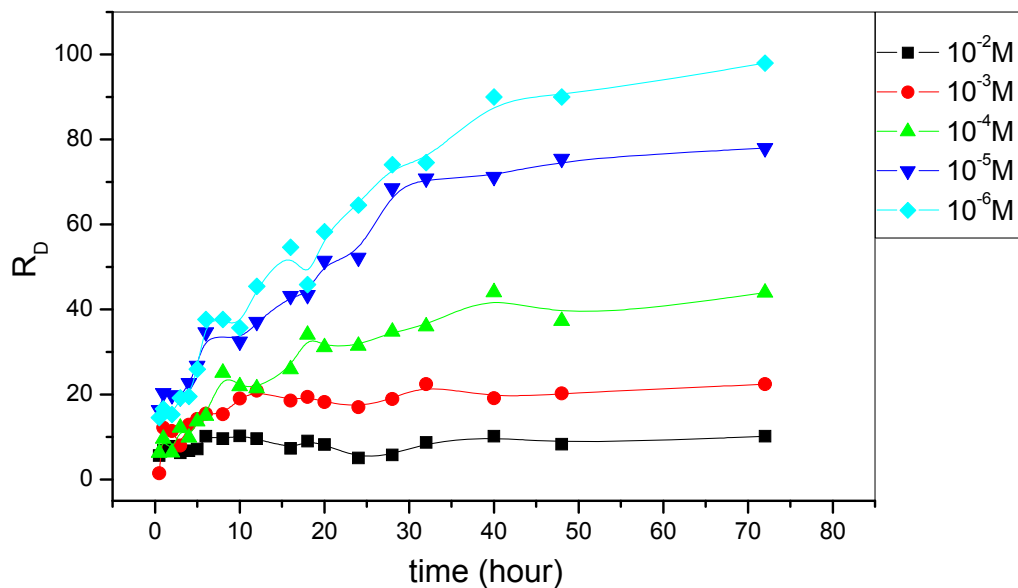


Figure 4.16. $^{60}\text{Co}^{2+}$ uptake on zeolite. The effect of cation concentration on sorption was investigated at 5°C .

Cobalt ions have high hydration energy, see Table 4.a., so tend to be hydrated. Values of the ratios of sorbed cation on the adsorbent to remained in the solution, R_D , are quite low comparing to that of other cations (see at figures 4.4., 4.10. and 4.16.). Especially on zeolite, Fig. 4.16., cobalt ions can not be move freely and

easily in the cavities and channels cause of water molecules around it. Its big spherical form is due to the high hydration energy (Table 4.a.) and surrounded water molecules. The adsorption order is $\text{Co}^{2+} < \text{Zn}^{2+} < \text{Cs}^+$ on zeolite.

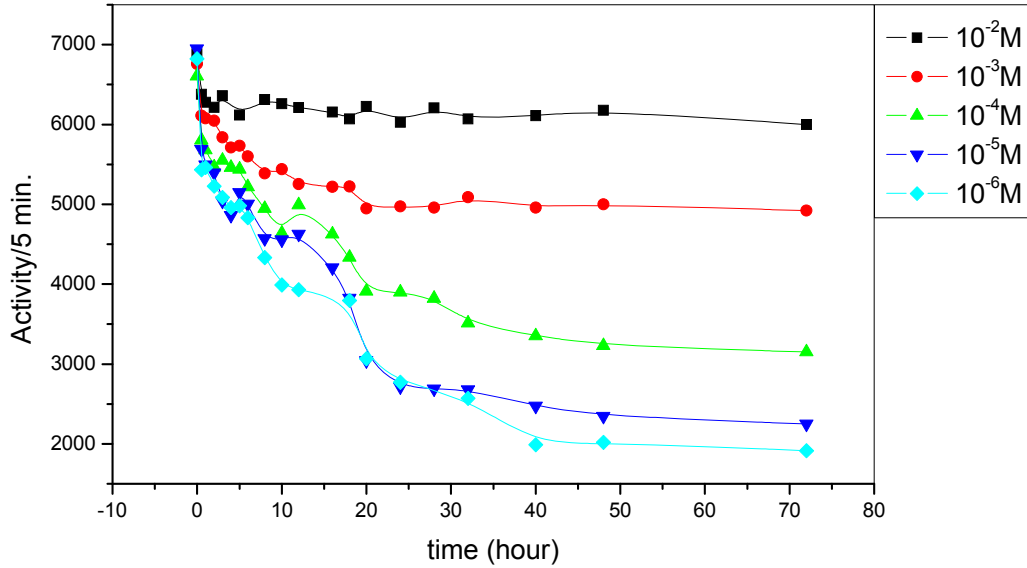


Figure 4.17. Counted activity- time plot of $^{60}\text{Co}^{2+}$ uptake on kaolin. The effect of cation concentration on sorption was investigated at 5°C .

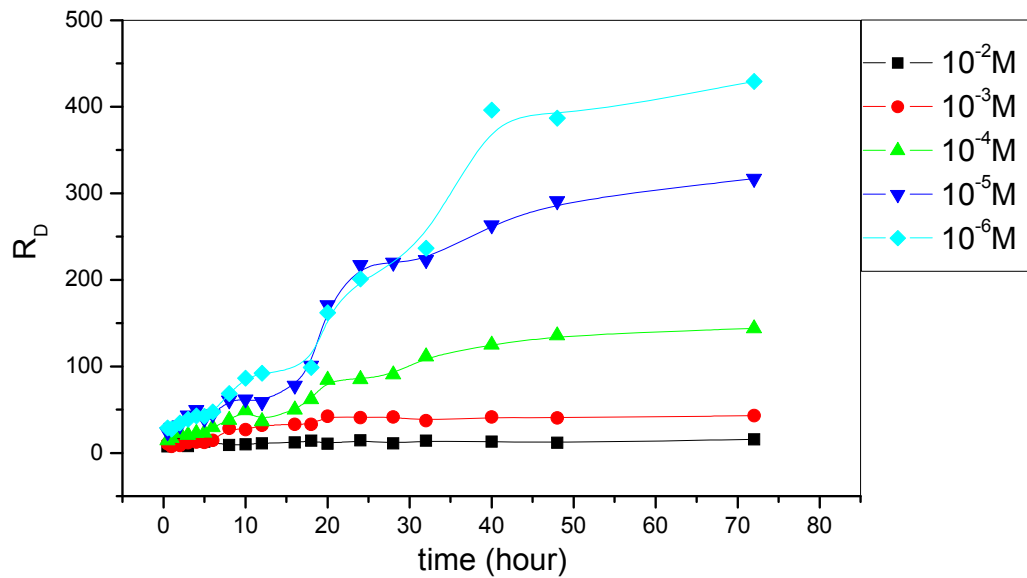


Figure 4.18. $^{60}\text{Co}^{2+}$ uptake on kaolin. The effect of cation concentration on sorption was investigated at 5°C .

Especially, Co^{2+} and Zn^{2+} have same behaviours on kaolin (Figs. 4.18. and 4.6.). Theirs radii are nearly same, and hydration energies are very close to each other. Surface adsorption occurs, but sorption rate is higher by Zn^{2+} than Co^{2+} on kaolin (Figs. 4.17. and 4.5.). Counted radioactivity reached rapidly to the constant value. Erten and Gökmenoğlu (1994) found the value of R_D for adsorption of $^{60}\text{Co}^{2+}$ on kaolinite as 129 mL/g.

In Figures 4.14., 4.16., the difference between the Co^{2+} ions sorptions on bentonite and zeolite is seen. The advance of the Co^{2+} ions in the channels of the structure of zeolite is difficult. Because cobalt ions have higher hydration energy; so ions are surrounded by water molecules, the hydrated ions become larger sized. But in bentonite structure, the main mineral is montmorillonite, the layer consist of three sheets (tetrahedra-octahedra-tetrahedra). The layers are hold by weak van der Waals forces to each other, so there are not so close. Between the layers there are spaces for ion exchange. The ions can pass in these regions easily. By this reason, for bentonite obtained sorption results were higher than that of zeolite. In kaolin, the main mineral is kaolinite, the layer consist of two (tetrahedra-octahedra) sheets. The layers are hold continuously by hydrogen bonds; no any space between them. So layers are closer, without vacancy. Sorption occurs on the surface of kaolin by means of interactions, hydrogen bonding of silica layers and hydrated ions (Fig. 4.c) or in octahedra layers (Fig. 4.b.) by oxygen bonding of alumina groups. For bentonite, either surface bonding and ion-exchange occur, whereas for kaolin sorption takes place only on surface. For Co^{2+} , the order of uptake capacity is bentonite > kaolin > zeolite.

4.4. The results of $^{133}\text{Ba}^{2+}$ barium ion adsorption behaviours on bentonite, kaolin and zeolite

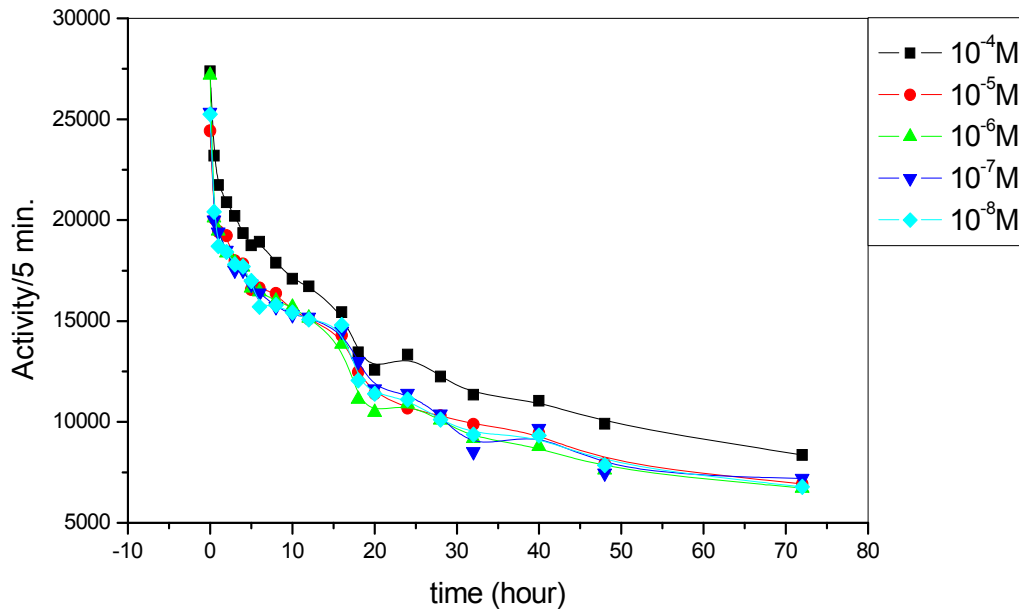


Figure 4.19. Counted activity- time plot of $^{133}\text{Ba}^{2+}$ uptake on bentonite. The effect of cation concentration on sorption was investigated at 5°C .

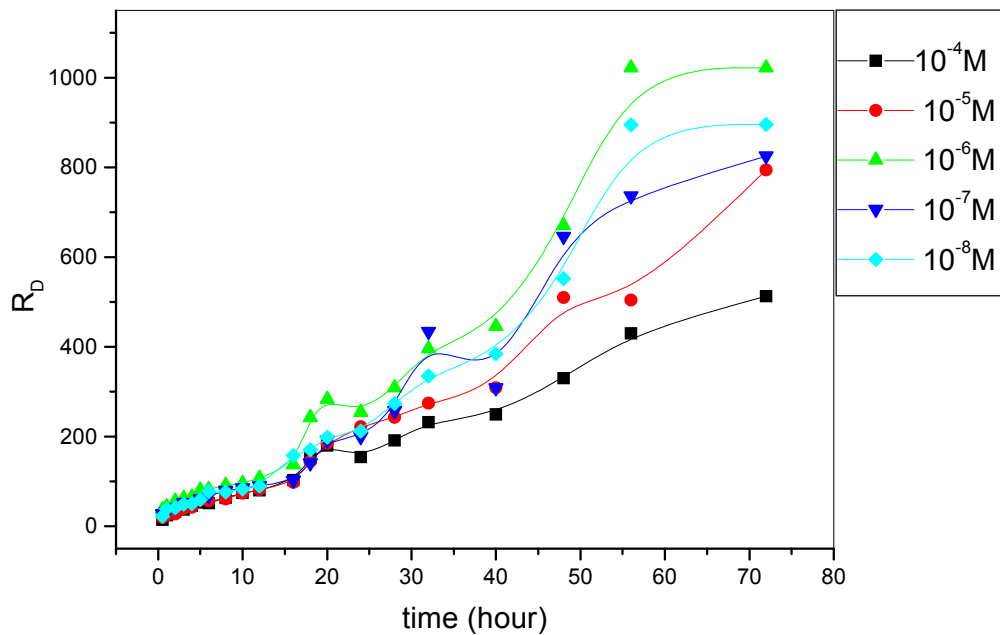


Figure 4.20. $^{133}\text{Ba}^{2+}$ uptake on bentonite. The effect of cation concentration on sorption was investigated at 5°C .

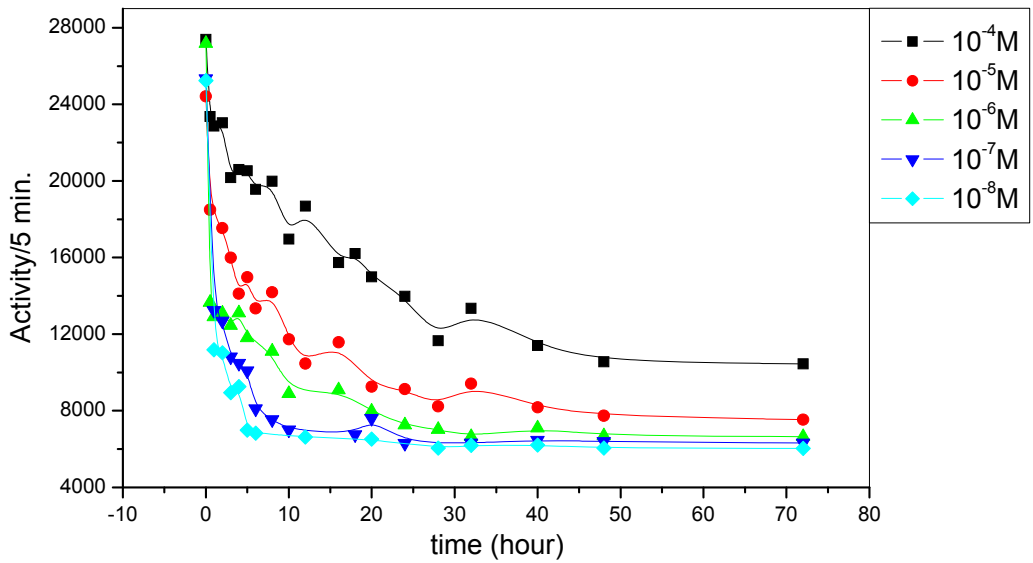


Figure 4.21. Counted activity- time plot of $^{133}\text{Ba}^{2+}$ uptake on zeolite. The effect of cation concentration on sorption was investigated at 5°C .

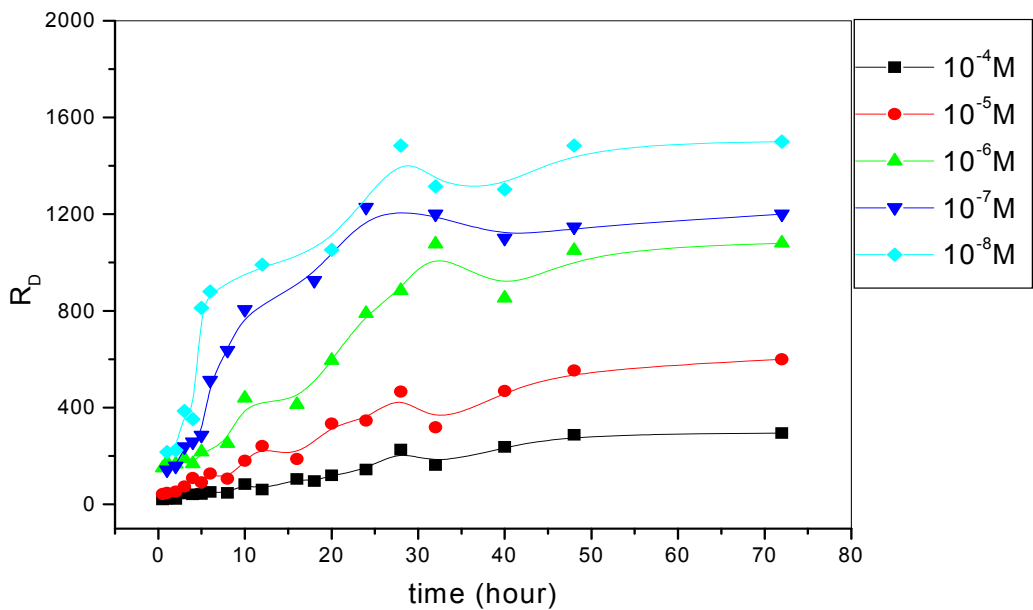


Figure 4.22. $^{133}\text{Ba}^{2+}$ uptake on zeolite. The effect of cation concentration on sorption was investigated at 5°C .

In Barium ion experiments, as different from the other cations, studied concentration interval is $1 \times 10^{-4} \text{ M} - 1 \times 10^{-8} \text{ M}$. For all of the other cations this interval is $1 \times 10^{-2} \text{ M} - 1 \times 10^{-6} \text{ M}$. There is an other experimental difference for barium ion: the

ground water composition is also different from that of the others. NaHCO_3 and $\text{MgSO}_4 \cdot 7\text{H}_2\text{O}$ were not be used. The causes of these changes are due to the precipitation. At high concentrations; 1×10^{-2} M, 1×10^{-3} M, Ba^{2+} ions combine with the HCO_3^- and SO_4^{2-} anions which present in the solution and form precipitates. For the other cations, in general, for the others for 1×10^{-2} M there are no any considerably drop in activity from initial and equilibrium solutions (Figs. 4.1., 4.3., 4.5., 4.11., 4.13., 4.15. and 4.17.), for 1×10^{-2} M the equilibrium adsorption is obtained earlier. But for 1×10^{-6} M there are a big activity drops between the initial solution and after equilibrium. There are considerably big difference in adsorption between studied concentrations. Counted activities depend on the concentration change too much. For barium ions, the initial concentrated solution is for 1×10^{-4} M, equilibrium activity is quite lower than initial activity; so between the for 1×10^{-4} M and for 1×10^{-8} M there is no huge difference as in the other cations in activity drops. The equilibrium activities are close to each other. Because 1×10^{-4} M is quite diluted molarity. Sites on adsorbent materials are completed with ions either with radioactive or nonradioactive at higher molarity; but at diluted molarities the amount of the radioactive ions besides the amount of nonradioactive ions are greater than that of radioactive ions besides nonradioactive ions at concentrated molarities. So the possibility of adsorbing of radioactive cation is high counts of sorbed radioactivity is low at lower concentrations. For 1×10^{-4} M also equilibrium activity is rather low (Figs. 4.19., 4.21. and 4.23.).

In Figs. 4.22. and 4.20., Ba^{2+} uptake on zeolite is higher than that on bentonite.

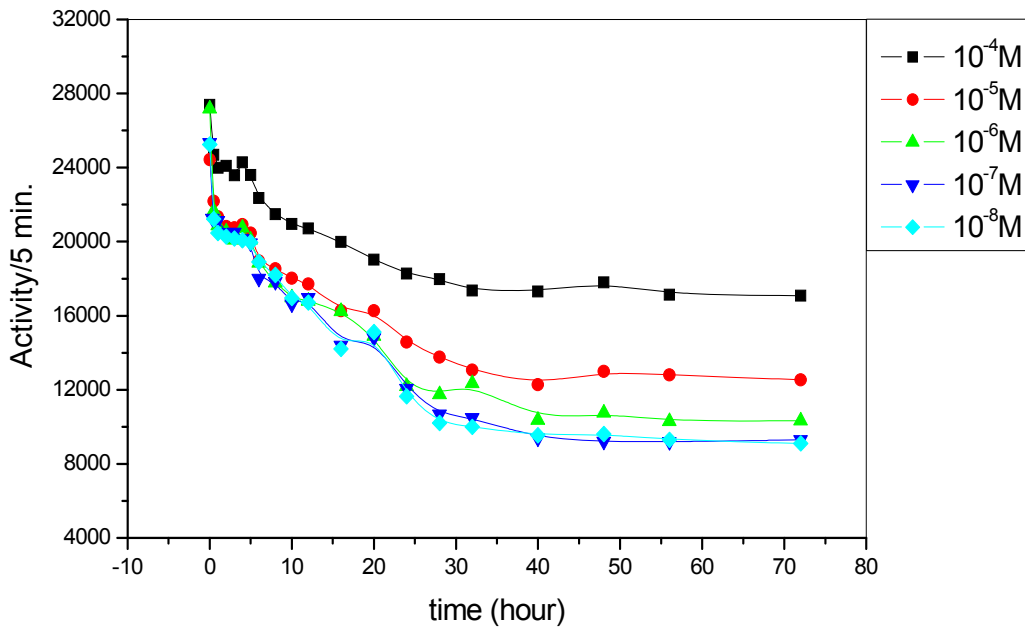


Figure 4.23. Counted activity- time plot of $^{133}\text{Ba}^{2+}$ uptake on kaolin. The effect of cation concentration on sorption was investigated at 5°C .

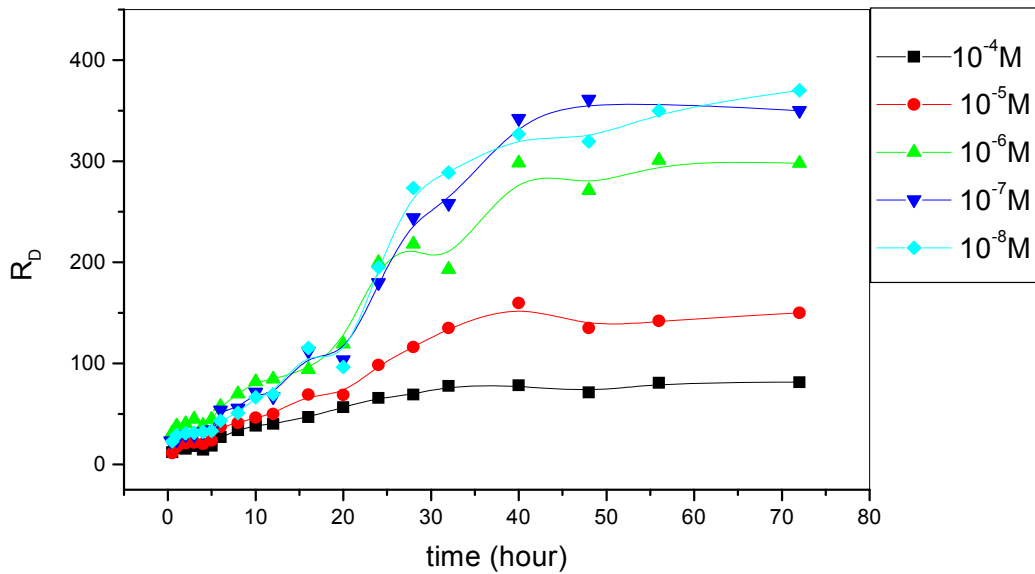


Figure 4.24. $^{133}\text{Ba}^{2+}$ uptake on kaolin. The effect of cation concentration on sorption was investigated at 5°C .

In Fig. 4.23., the lowest equilibrium activity was obtained on kaolin for Ba^{2+} , compared with bentonite and kaolin, Figs. 4.19. and 4.21. the differences are obviously seen. The sorption order of barium ion is: on zeolite>bentonite>kaolin.

In Figs. 4.24., 4.18, and 4.6, on kaolin for Ba^{2+} , Co^{2+} , Zn^{2+} radioisotopes have nearly same behavior according to their adsorbing quantity. In kaolinite, ion exchange between layers can not occur because of tightly arranged layers structure. Ion could not be take place between TO layers, so cation radius is not so important for kaolinite as much as for bentonite and zeolite. Surface bonding occurs by oxygen bonding and hydrogen bonding (Figs. 4.b., 4.c.) or electrostatic interactions. The strength of interactions depends on the distance between the atom of surface and cation; so length of radius is one of the reason of the greatness of these forces. If the cation has higher hydration energy it needs to consider the size of hydrated form. The higher hydration energy means longer radius of hydrated spherical form. But this is not important as much as in bentonite and kaolin. In montmorillonite, in addition of surface bonding, the deficiency of positive charge is supplied by taking place between the layers, which are distant from each other, and in zeolite there are pores and cavities in the structure so cation radius is becoming very important. When the cation can move ahead in the pores the cation exchange can happen. But in kaolin the R_D values are closer to each other, Only Sr^{2+} uptake on Kaolin is quite less than the other. The cation adsorption can take place by means of silanol groups on the surface of kaolinite. There is no cation exchange opportunity between the TO layers in kaolinite, nor specific emptiness or cavities as in zeolite for cation displaying occur. On surface cation bonding occurs by oxygen bonding of alumina octahedra layer, hydrogen bonding of silica tetrahedra layer or electrostatic forces. In respect of dipole moment, the length of radius becomes important; the strength of the bonding force depends on the distance between the center of hydrated cation and the surface of adsorbent material. Degrees of interactions are related to the distance.

4.5. The results of $^{90}\text{Sr}^{2+}$ ion adsorption behaviours on bentonite, kaolin and zeolite

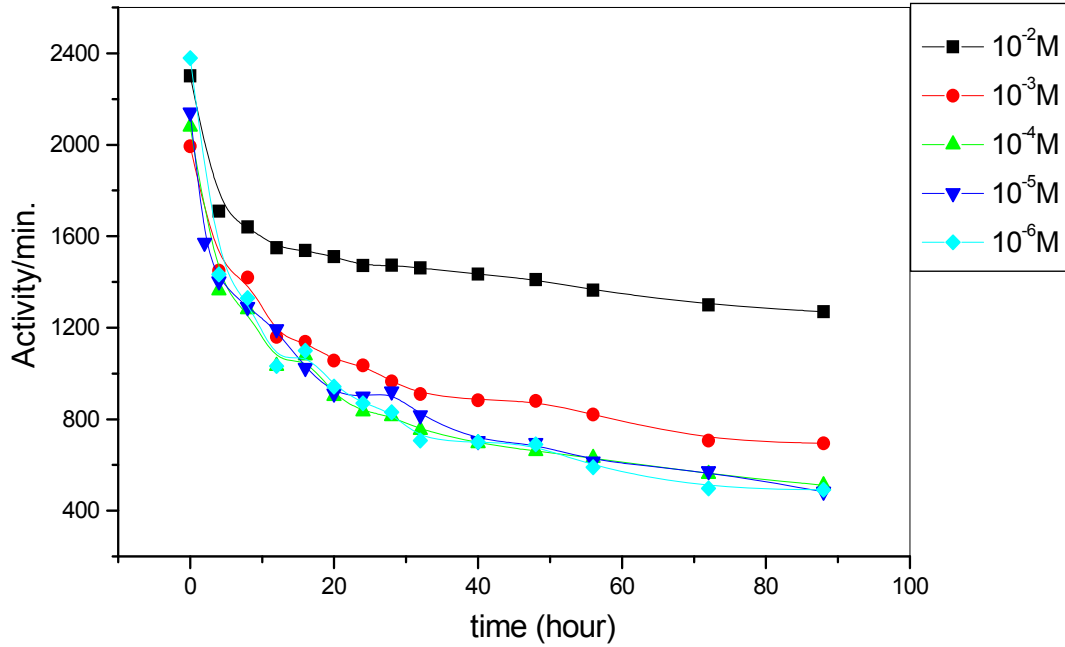


Figure 4.25. Counted activity- time plot of $^{90}\text{Sr}^{2+}$ uptake on bentonite. The effect of cation concentration on sorption was investigated at 5°C .

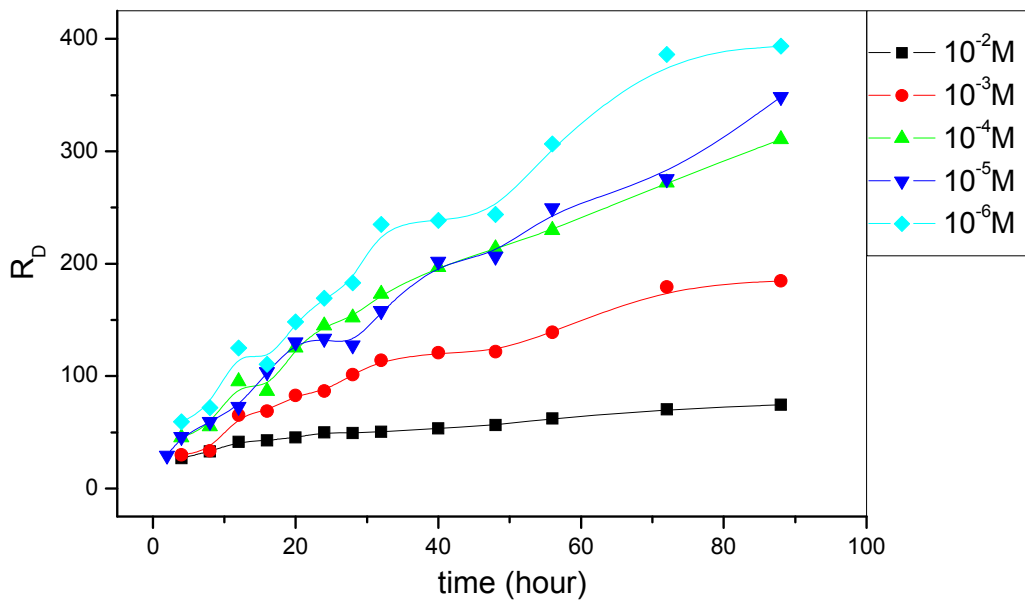


Figure 4.26. $^{90}\text{Sr}^{2+}$ uptake on bentonite. The effect of cation concentration on sorption was investigated at 5°C .

According to (Brian and Miller 2006) Alkaline Earth Cation Selectivity: Divalent alkaline earth cations tend to be selected by smectites in the sequence $Ba^{2+} > Sr^{2+}$. This sequence is consistent with the main hypothesis of Brian and Miller in that the more strongly hydrated cation is always favored in the solution phase as in our results Figs. 4.20 and 4.26. In part 2.2.3., it was mentioned about the information of Swartzen-Allen and Matijević (1974): “Cation exchange selectivity increases with cation charge and for a given charge increases with ionic radius. Thus, the order of increasing affinity for the alkaline earth ions Mg^{2+} , Ca^{2+} , Sr^{2+} and Ba^{2+} .” This statement is showing a good agreement with our experimental results.

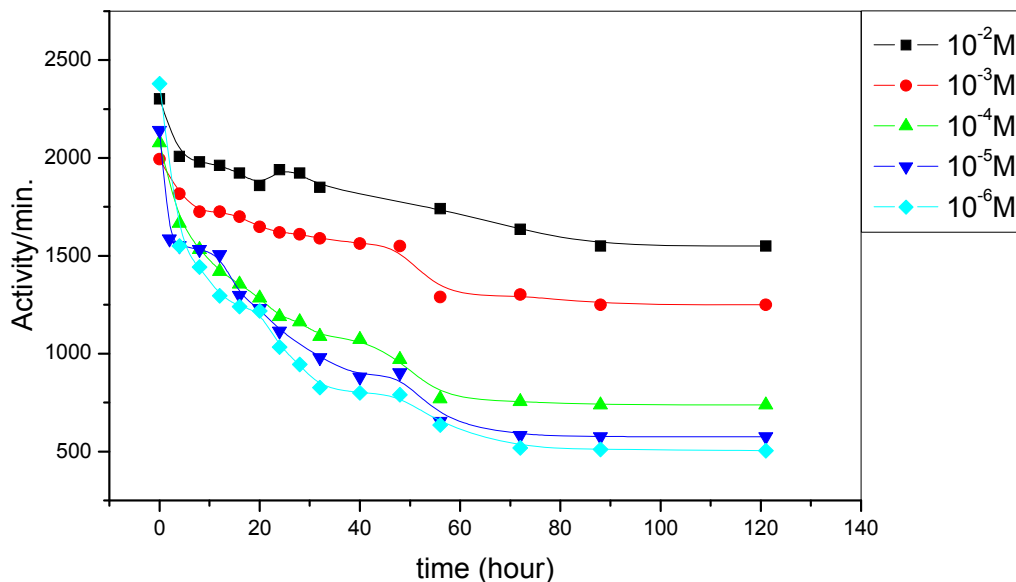


Figure 4.27. Counted activity- time plot of $^{90}Sr^{2+}$ uptake on zeolite. The effect of cation concentration on sorption was investigated at $5^{\circ}C$.

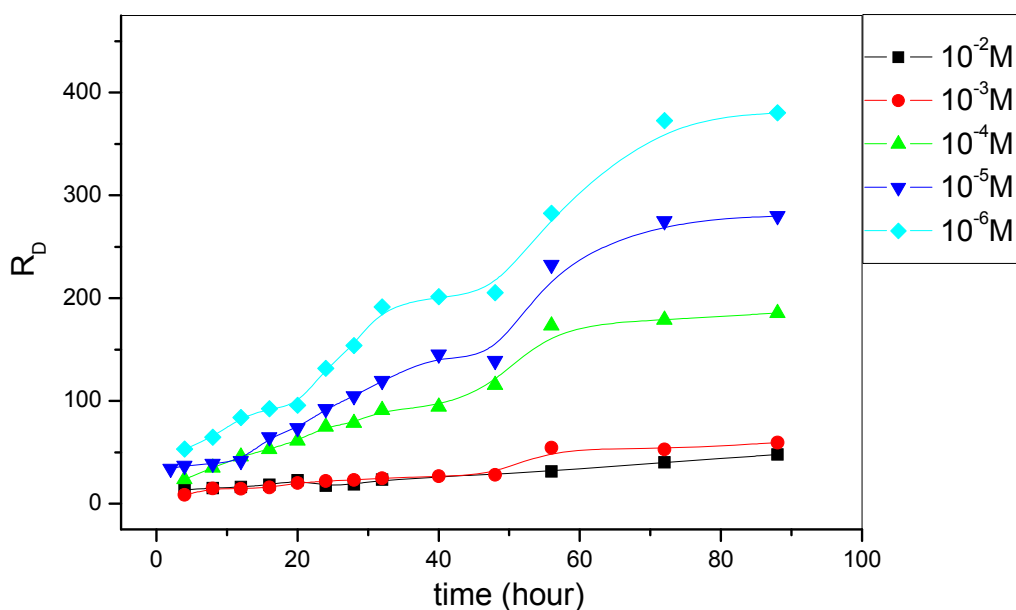


Figure 4.28. $^{90}\text{Sr}^{2+}$ uptake on zeolite. The effect of cation concentration on sorption was investigated at 5°C .

Strontium activity was counted by β -counter (Geiger Müller), activities taken per minute. The average of countings were taken. On kaolin and bentonite, the lowest adsorption capacities were obtained by strontium ions. The equilibrium were reached quite late than the other cations too. Comparing β and γ countings with each other is not exactly true also.

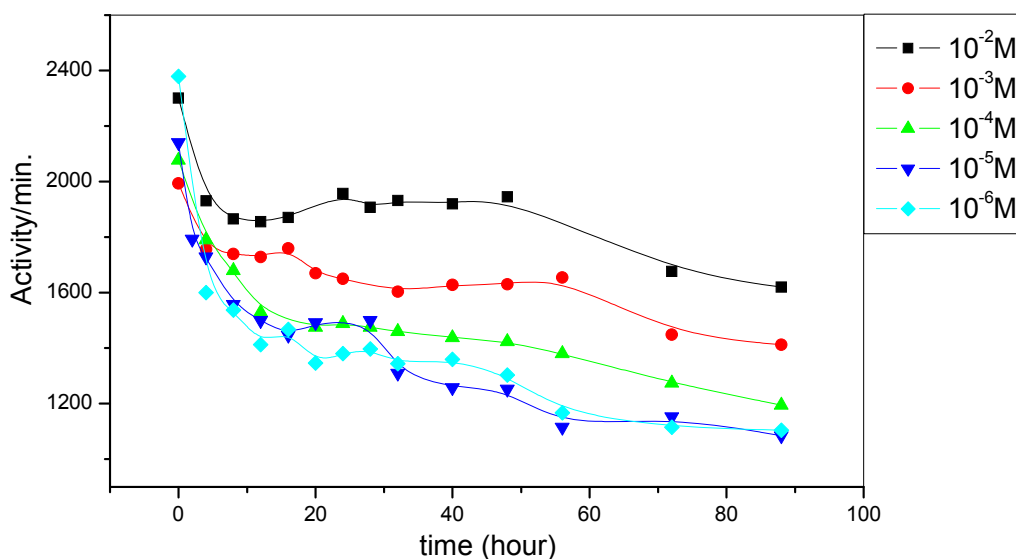


Figure 4.29. Counted activity- time plot of $^{90}\text{Sr}^{2+}$ uptake on kaolin. The effect of cation concentration on sorption was investigated at 5°C .

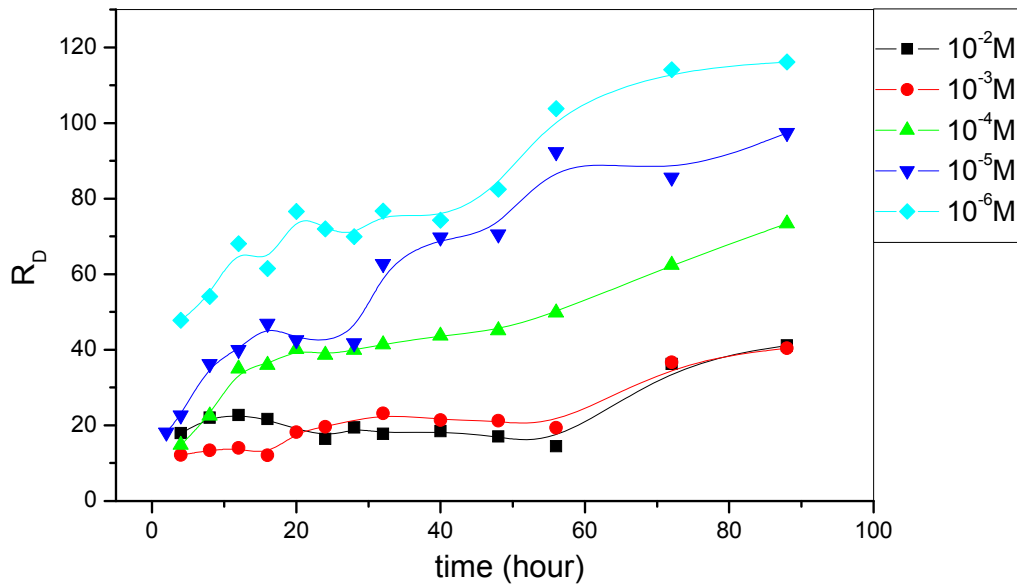


Figure 4.30. $^{90}\text{Sr}^{2+}$ uptake on kaolin. The effect of cation concentration on sorption was investigated at 5°C .

In figures 4.26. and 4.30. it is clear that the strontium sorption on bentonite is higher than that of kaolin as in Başçetin et al.'s studies. Başçetin et al. (2006) used ^{90}Sr as a radiotracer and montmorillonite and kaolinite as minerals. They studied in the concentration range $1 \cdot 10^{-6}$ - $1 \cdot 10^{-2}$ M. They found the distribution coefficients for strontium in montmorillonite are higher than those found in kaolinite. The values of K_d for montmorillonite changed from 823 to 239 mL/g in the increased concentration range of 10^{-6} to 10^{-2} M SrCl_2 , while for kaolinite results decreased from 203 to 72 mL/g in the same range. In our results for $1 \cdot 10^{-6}$ - $1 \cdot 10^{-2}$ M Sr^{2+} on bentonite R_D decreases from 393.5 to 74.5 and on kaolin 116 to 41mL/g at 5°C . Our adsorbents are not pure minerals; instead of montmorillonite mineral we used bentonite as a rock form and instead of kaolinite mineral kaolin was used. Beside this, our experimental temperature was 5°C , theirs was 25°C . By these reasons, directly comparing the results with each other is not exactly true. According to our results, zeolite showed a higher strontium ion sorption capacity than kaolin (Figures 4.28. and 4.30). Akar et al. (2005) also have thermodynamic and kinetic investigations of strontium ions retention by natural kaolinite which is a main mineral of kaolin clay and clinoptilolite mineral of zeolite. They concluded that clinoptilolite has higher strontium ion sorption capacity than kaolin.

The synthetic groundwater's pH is 7 and it is 6 whom is prepared for Ba-133 experiments. Zinc, cobalt, strontium and caesium ions adsorptions on zeolite and kaolin pH were 7, that of on bentonite were 8. In barium ion adsorption experiments on zeolite and kaolin pH were 6 and on bentonite it was 7.

4.6. The effect of temperature on ^{65}Zn ion adsorption behaviours on bentonite, kaolin and zeolite

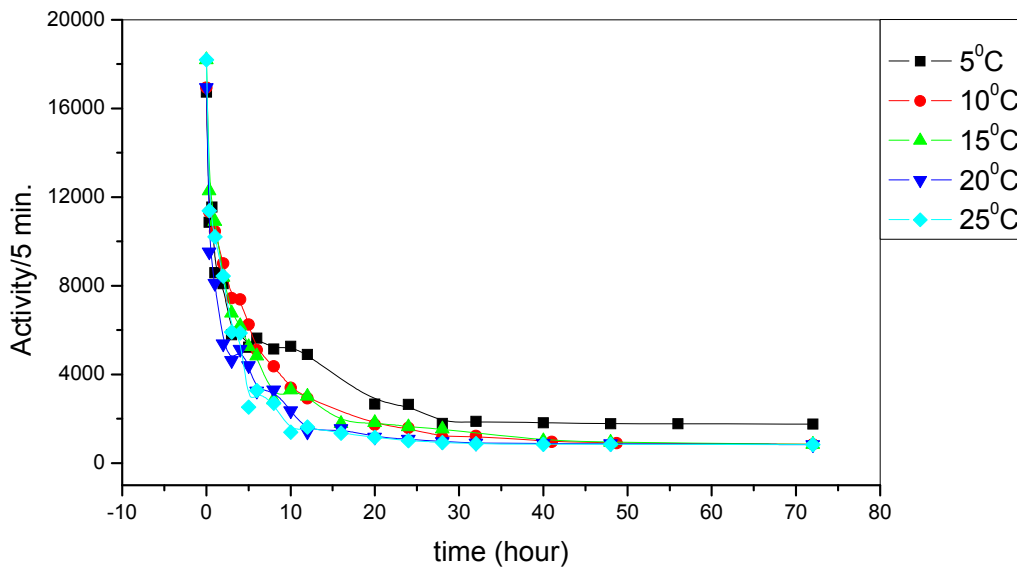


Figure 4.31. Counted activity- time plot of $^{65}\text{Zn}^{2+}$ uptake on bentonite at constant cation concentration ($1 \times 10^{-6}\text{M}$). The effect of temperature on sorption was investigated.

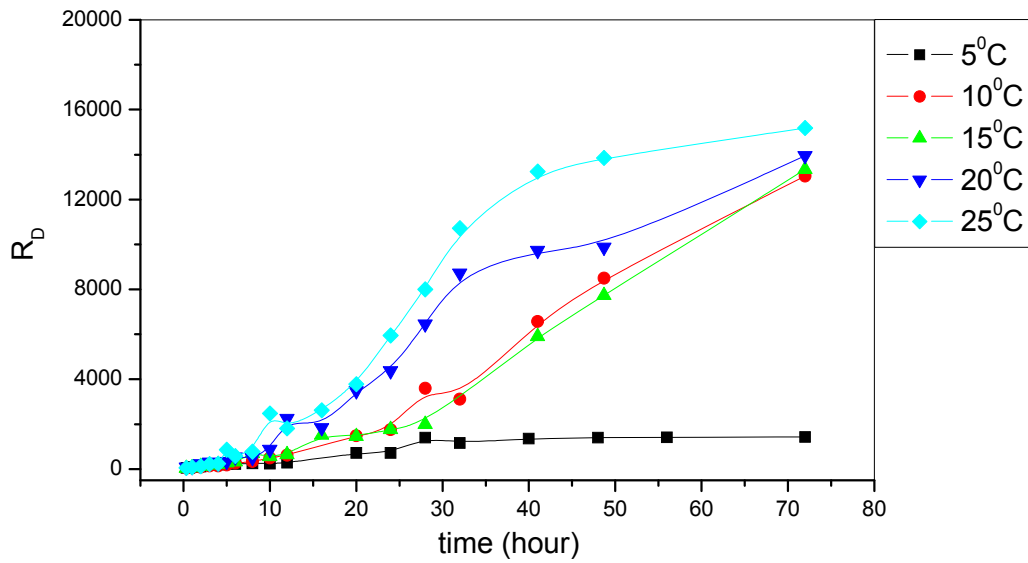


Figure 4.32. $^{65}\text{Zn}^{2+}$ uptake on bentonite at constant cation concentration ($1 \times 10^{-6}\text{M}$). The effect of temperature on sorption was investigated.

In Fig. 4.32. zinc cation uptake of bentonite is very changed with temperature, adsorption is increased to 10.7 times by a change of temperature from 5 to 25°C. This is because of the energy needed in order to overcome the weak van der Waals forces which bond the TOT layers is supported by temperature increase. The forces become weaken. The highest temperature dependency of the adsorption on bentonite and kaolin was seen in zinc ion adsorption. Its adsorptions on bentonite (Fig 4.32.) and kaolin (Fig. 4.36.) increase approximately to 10.7 times and 13 times respectively by an increase from 5 to 25°C.

$$\Delta G^\circ = -RT \ln R_D$$

$$\Delta G^\circ = \Delta H^\circ - T\Delta S^\circ$$

By plotting $\ln R_d$ versus $1/T$, it is possible to determine the value of ΔH° of sorption from the slope and ΔS° of sorption from the intercept of the linear fits.

Table 4.1. Thermodynamic parameters of ⁶⁵Zinc-Bentonite system.

⁶⁵ Zinc-Bentonite			
T(K)	ΔG°(kJ/mol)	ΔH° (kJ/mol)	ΔS° (J/molK)
278	-16.78	67.22	309
283	-22.30		
288	-22.74		
293	-23.25		
298	-23.85		

Zinc ion sorption on bentonite, calculated ΔG° decreases more sharply than that on kaolin and zeolite as temperature increases (Tables 4.1., 4.2., 4.3.), means that sorption increases at high temperatures. It is also in accordance in the adsorption plots at different temperatures.

According to our results; Zn²⁺ uptake on bentonite, among all of cations: Zn²⁺, Cs⁺, Co²⁺, Ba²⁺ and Sr²⁺; has highest (negative) ΔG° (i.e. at 5°C -16.78 kJ/mol) (Tables 4.1., 4.4., 4.7., 4.10., 4.13. respectively) at all temperatures studied; which means highest spontaneity; its high adsorption capacity is seen in the graph (Fig. 4.32.).

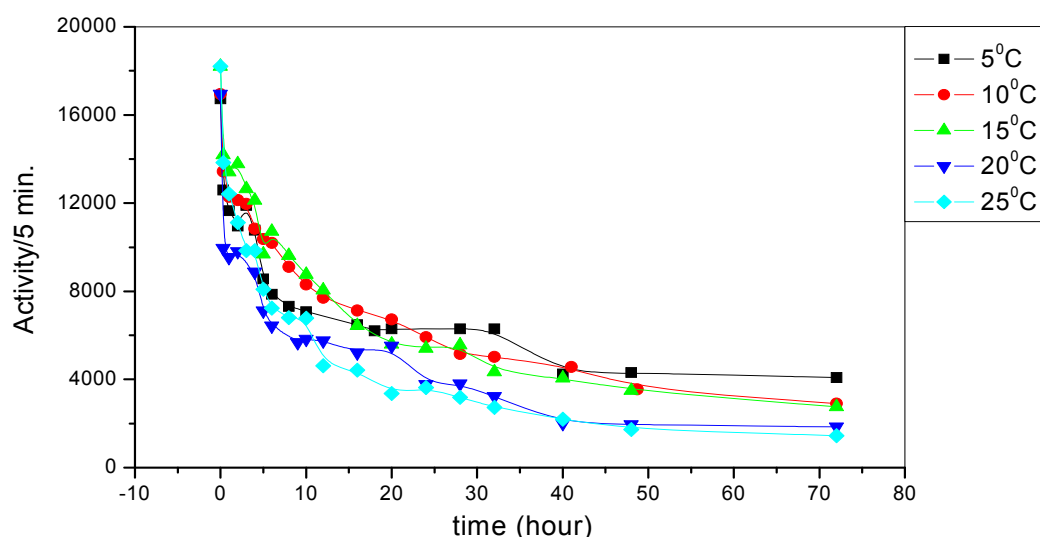


Figure 4.33. Counted activity- time plot of ⁶⁵Zn²⁺ uptake on zeolite at constant cation concentration (1x10⁻⁶M). The effect of temperature on sorption was investigated.

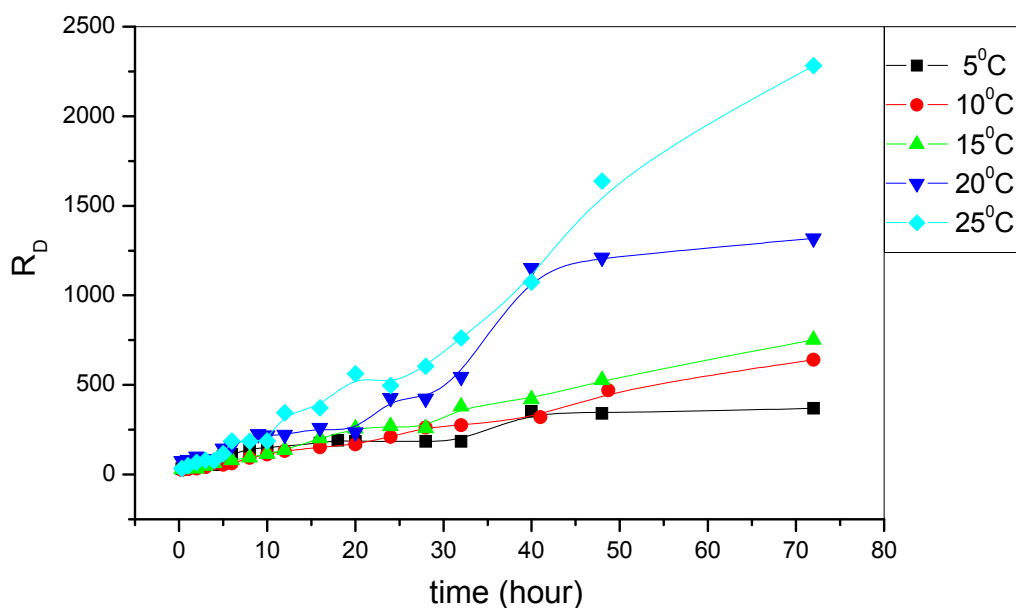


Figure 4.34. $^{65}\text{Zn}^{2+}$ uptake on zeolite at constant cation concentration ($1 \times 10^{-6}\text{M}$). The effect of temperature on sorption was investigated.

Table 4.2. Thermodynamic parameters of $^{65}\text{Zinc-Zeolite}$ system.

$^{65}\text{Zinc-Zeolite}$			
T(K)	ΔG° (kJ/mol)	ΔH° (kJ/mol)	ΔS° (J/molK)
278	-13.67	59.96	265
283	-15.21		
288	-15.86		
293	-17.50		
298	-19.16		

There is an ordered increase in ΔG° values as temperature increases. ΔG° values for Zn^{2+} -zeolite are less negative than that of Zn^{2+} -bentonite. On bentonite the sorption process is more spontaneous than on zeolite because of the difficulties in the structure of zeolite.

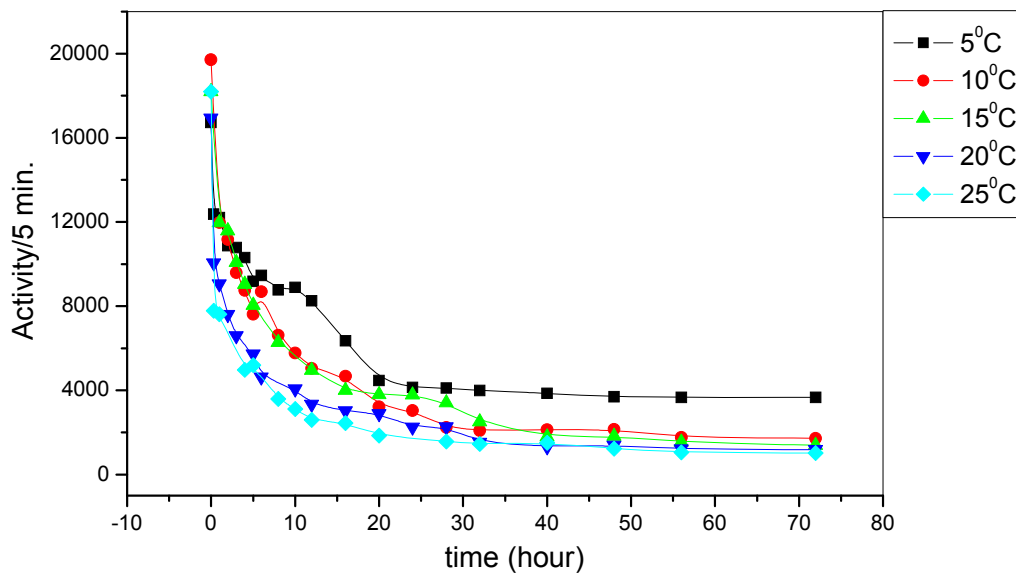


Figure 4.35. Counted activity- time plot of $^{65}\text{Zn}^{2+}$ uptake on kaolin at constant cation concentration ($1 \times 10^{-6}\text{M}$). The effect of temperature on sorption was investigated.

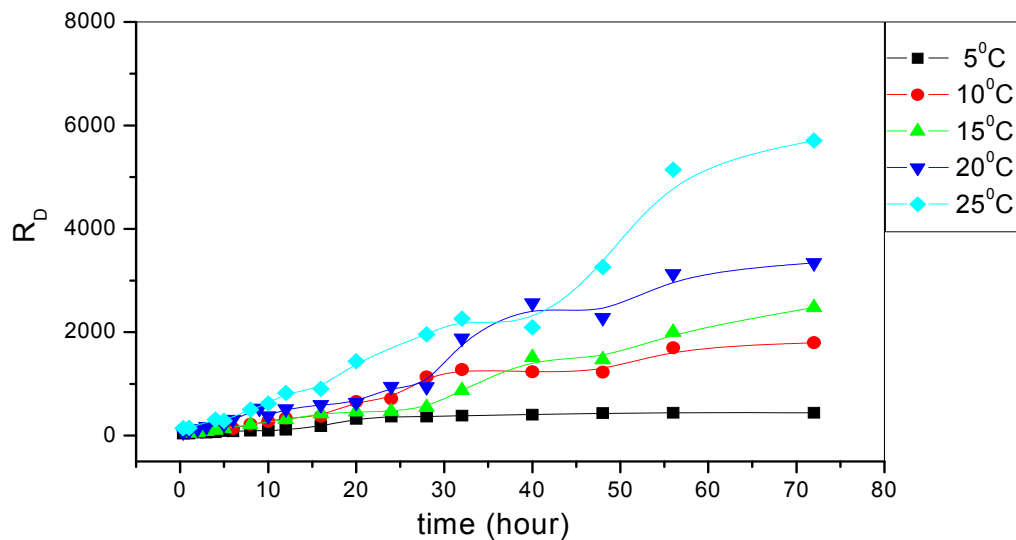


Figure 4.36. $^{65}\text{Zn}^{2+}$ uptake on kaolin at constant cation concentration ($1 \times 10^{-6}\text{M}$). The effect of temperature on sorption was investigated.

In kaolinite the bond of oxygen atom of silanole groups are broken with increasing temperature. As a result adsorption increases by these broken bonds at the surface with temperature. Surface bonding of cation over oxygen atom of silanole groups became easily.

Table 4.3. Thermodynamic parameters of ⁶⁵Zinc-Kaolin system

⁶⁵ Zinc-Kaolin			
T(K)	ΔG° (kJ/mol)	ΔH° (kJ/mol)	ΔS° (J/molK)
278	-14.07	79.53	340
283	-17.64		
288	-18.72		
293	-19.77		
298	-21.43		

According to the ΔG° values, the order of spontaneity of Zn²⁺ on adsorbents is zeolite<kaolin<bentonite. ΔG° results obtained with bentonite are the highest ones comparing the results with kaolin and zeolite obtained at the same temperatures (Tables 4.1., 4.2.,4.3.). Comparing all of the cations sorptions on kaolin, it is zinc ion uptake which is the most effected one by change in temperature (Tables 4.3., 4.6., 4.9., 4.12.,4.15).

4.7. The effect of temperature on ¹³⁷caesium ion adsorption behaviours on bentonite, kaolin and zeolite

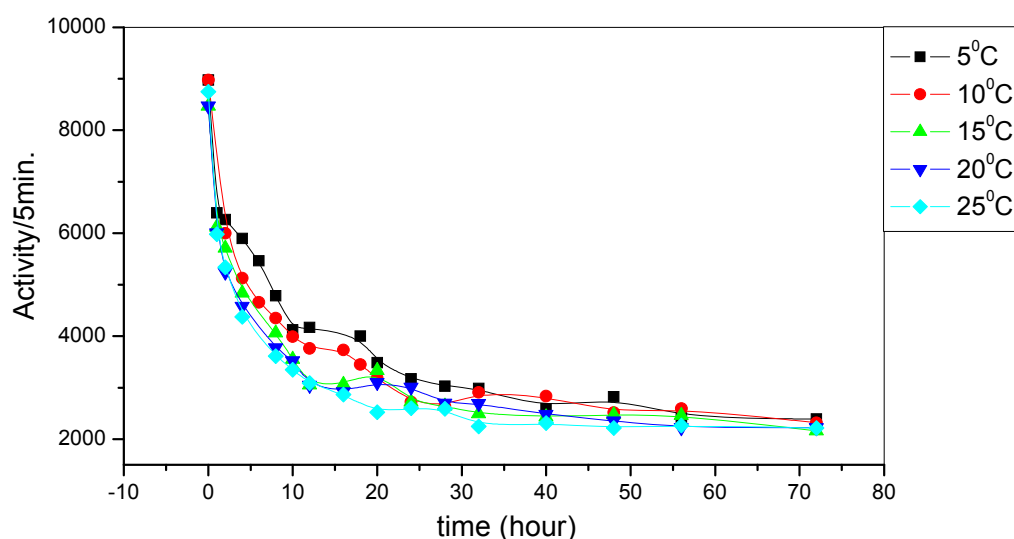


Figure 4.37. Counted activity- time plot of ¹³⁷Cs⁺ uptake on bentonite at constant cation concentration (1x10⁻⁶M). The effect of temperature on sorption was investigated.

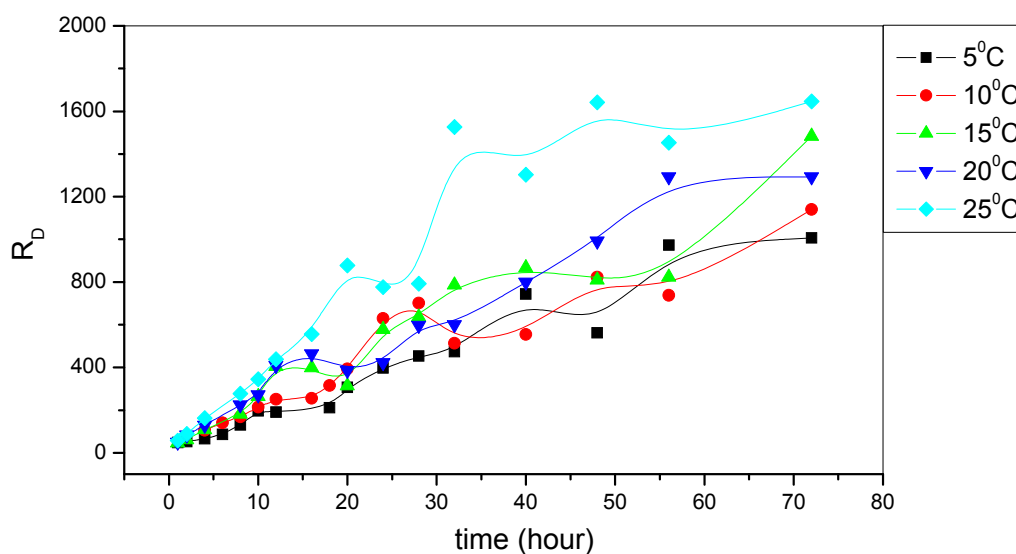


Figure 4.38. $^{137}\text{Cs}^+$ uptake on bentonite at constant cation concentration ($1 \times 10^{-6}\text{M}$). The effect of temperature on sorption was investigated.

Table 4.4. Thermodynamic parameters of $^{137}\text{Caesium-Bentonite}$ system

$^{137}\text{Caesium-Bentonite}$			
T(K)	ΔG° (kJ/mol)	ΔH° (kJ/mol)	ΔS° (J/molK)
278	-15.98	15.33	113
283	-16.56		
288	-17.48		
293	-17.45		
298	-18.35		

The temperature dependence of Cs^+ on bentonite is not high as Zn^{2+} on bentonite (Tables 4.4. and 4.1.). ΔG° values are closer to each other for Cs^+ -bentonite.

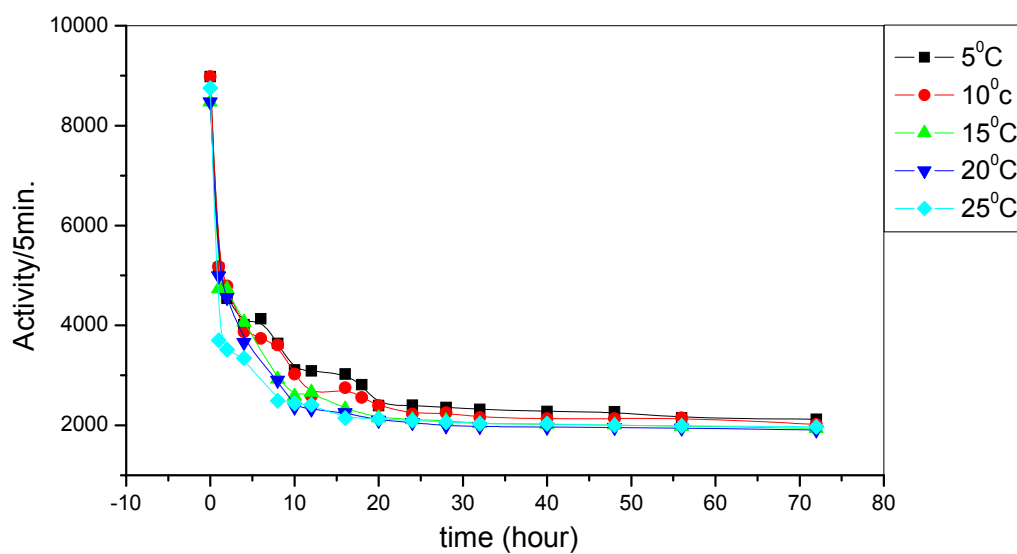


Figure 4.39. Counted activity- time plot of $^{137}\text{Cs}^+$ uptake on zeolite at constant cation concentration ($1 \times 10^{-6}\text{M}$). The effect of temperature on sorption was investigated.

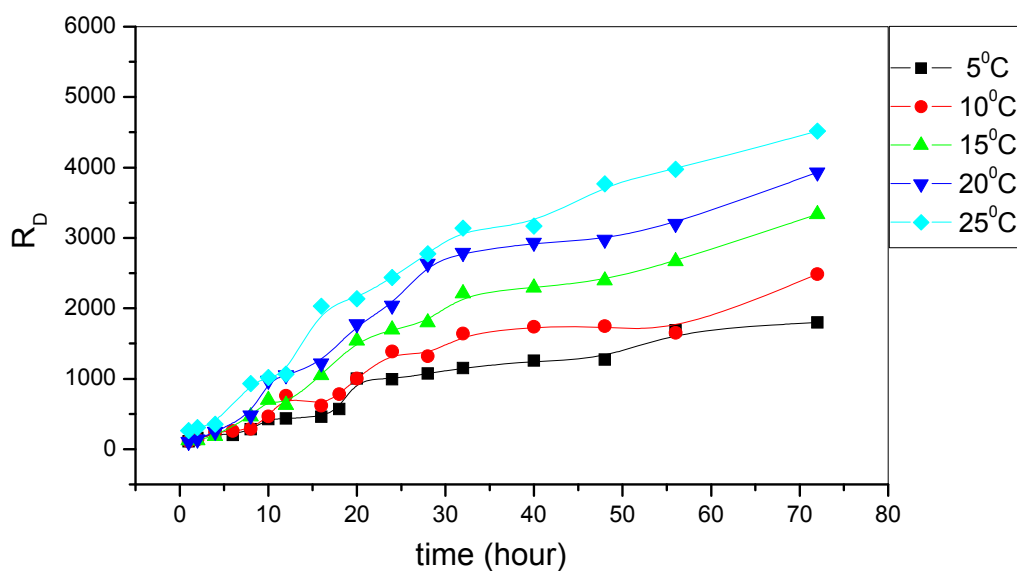


Figure 4.40. $^{137}\text{Cs}^+$ uptake on zeolite at constant cation concentration ($1 \times 10^{-6}\text{M}$). The effect of temperature on sorption was investigated.

Table 4.5. Thermodynamic parameters of ¹³⁷Caesium-Zeolite system

¹³⁷ Caesium-Zeolite			
T(K)	ΔG° (kJ/mol)	ΔH° (kJ/mol)	ΔS° (J/molK)
278	-17.32	31.79	177
283	-18.39		
288	-19.42		
293	-20.16		
298	-20.85		

Comparing the other cations, at 5°C, Cs⁺ has highest (negative) ΔG° on zeolite, (Table 4.5.) (-17.32 kJ/mol at 5°C) which means highest spontaneity. But as temperature increases, caesium does not show high temperature dependence on zeolite. Because Cs⁺ has low hydration energy and does not hydrated so much, its radius is suitable for channels of zeolite.

In Fig. 4.40., it is obviously seen that on zeolite Cs⁺ ion is highly adsorbed, because Cs⁺ has ionic size almost fits for placing to this empty hole in Zeolite. So it is adsorbed tightly in this specific region. The lowest dependence of temperature is observed with cesium uptake. Only a little change occurs by increase in temperature. At 5, 10, 15, 20 and 25°C the adsorptions slightly differs from each other. Because Cs⁺ ionic radius is already suitable for the emptiness of the structure of zeolite. It takes the place there at lower temperature; 5°C. Therefore adsorption is high and rapid even at 5°C, so increase in temperature does not influence the spontaneity so much. Cesium ion is for this special uptake region. So the cesium cation uptake change only to 2 times by an increase from 5 to 25°C.

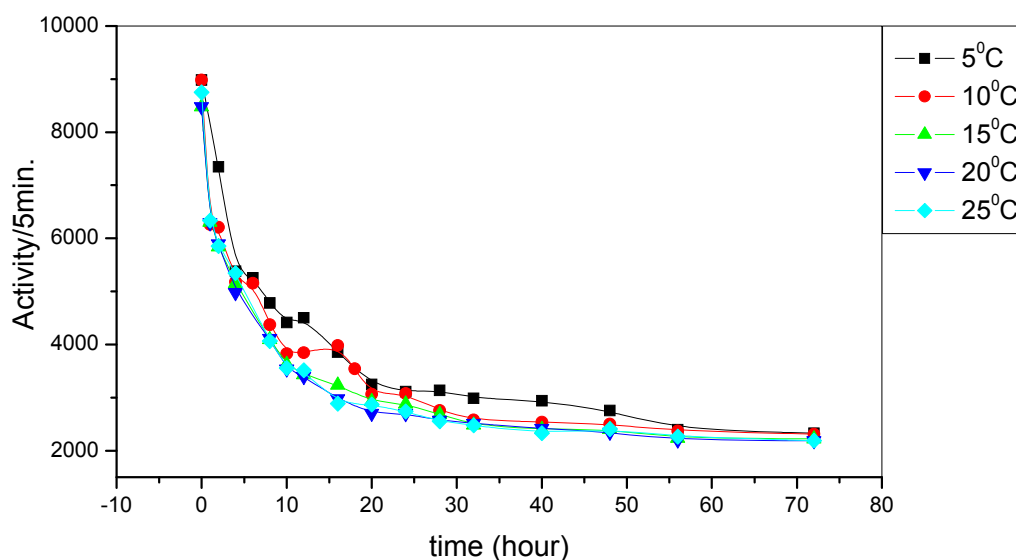


Figure 4.41. Counted activity- time plot of $^{137}\text{Cs}^+$ uptake on kaolin at constant cation concentration ($1 \times 10^{-6}\text{M}$). The effect of temperature on sorption was investigated.

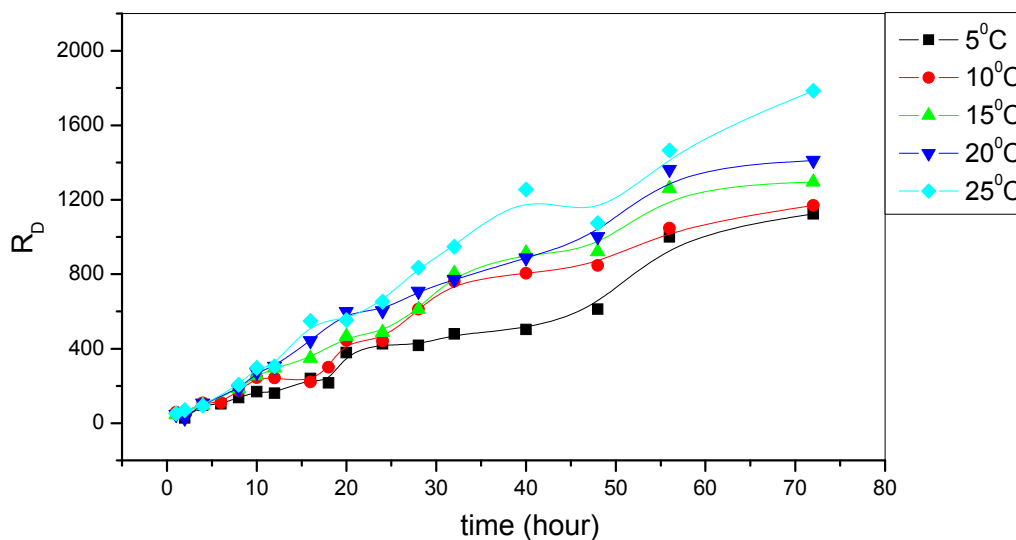


Figure 4.42. $^{137}\text{Cs}^+$ uptake on kaolin at constant cation concentration ($1 \times 10^{-6}\text{M}$). The effect of temperature on sorption was investigated.

Table 4.6. Thermodynamic parameters of ¹³⁷Caesium-Kaolin system

¹³⁷ Caesium-Kaolin			
T(K)	ΔG° (kJ/mol)	ΔH° (kJ/mol)	ΔS° (J/molK)
278	-16.24	17.71	122
283	-16.62		
288	-17.16		
293	-17.67		
298	-18.77		

Spontaneity of Cs⁺ on kaolin increases as the temperature increases.

4.8. The effect of temperature on ⁶⁰cobalt ion adsorption behaviours on bentonite, kaolin and zeolite

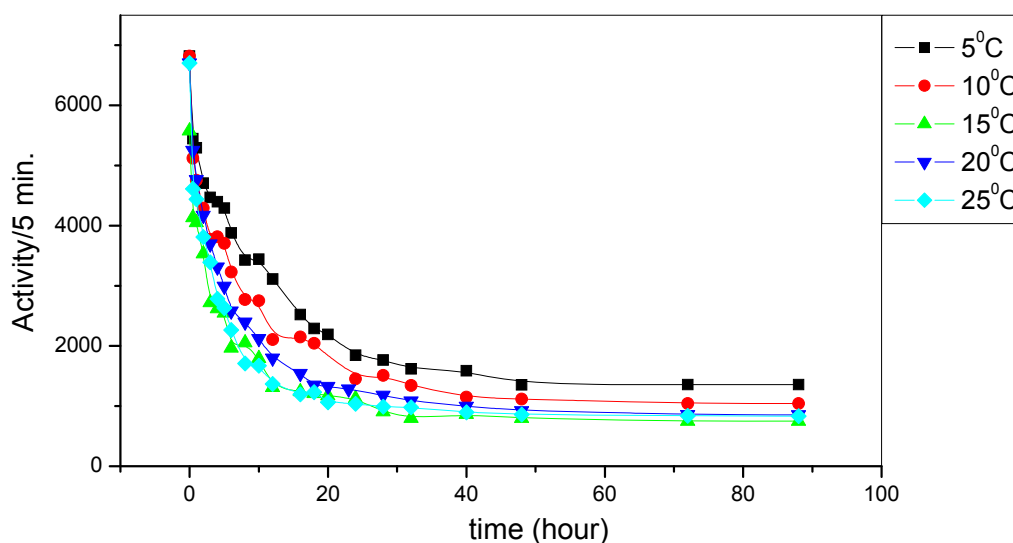


Figure 4.43. Counted activity- time plot of ⁶⁰Co²⁺ uptake on bentonite at constant cation concentration (1x10⁻⁶M). The effect of temperature on sorption was investigated.

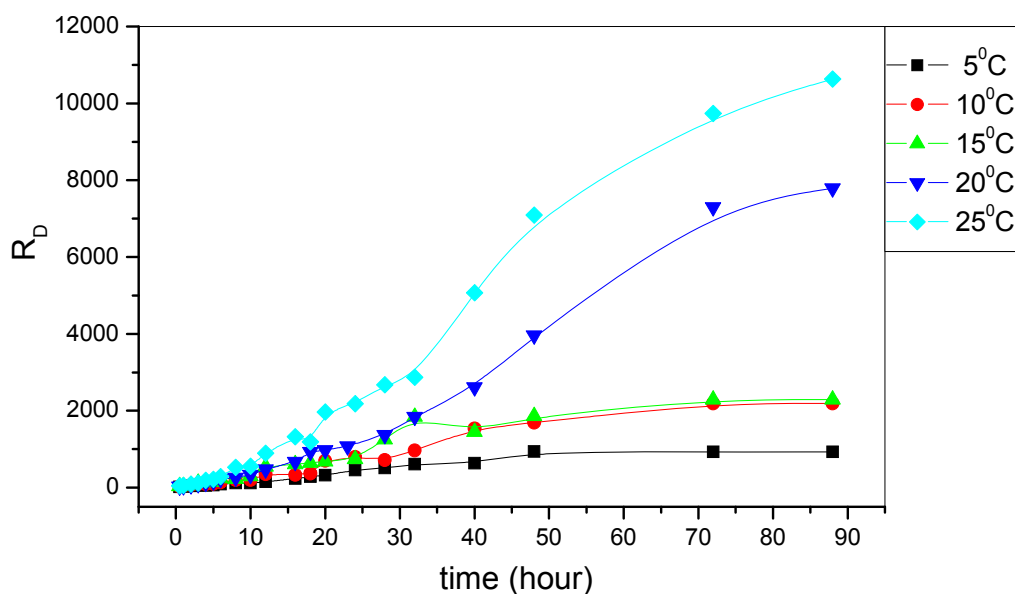


Figure 4.44. $^{60}\text{Co}^{2+}$ uptake on bentonite at constant cation concentration ($1 \times 10^{-6}\text{M}$). The effect of temperature on sorption was investigated.

Table 4.7. Thermodynamic parameters of $^{60}\text{Cobalt-Bentonite}$ system

$^{60}\text{Cobalt-Bentonite}$			
T(K)	ΔG° (kJ/mol)	ΔH° (kJ/mol)	ΔS° (J/molK)
278	-15.81	84.42	361
283	-18.10		
288	-18.52		
293	-21.83		
298	-22.97		

For cobalt ions and zinc ions sorption on Bentonite, calculated ΔG° decreases more sharply as temperature increases (Tables 4.7. and 4.1), it is also in accordance in the adsorption plots at different temperatures. Shahwan et al. (2006) have the experiments at 25°C and 55°C using ^{60}Co as a radiotracer in the adsorption of Co^{2+} ions on natural bentonite clay. They found out for the averages of 1000 and 2500 mg/L $[\text{C}]_0$ values $\Delta H^\circ=13.0$ kJ/mol, at 298 K $\Delta G^\circ=-16.8$ kJ/mol, $\Delta S^\circ=99.7$ J/molK at 328 K $\Delta G^\circ=-13.8$ kJ/mol, $\Delta S^\circ=81.6$ J/molK. But in my thesis the Co^{2+} molarity was $1 \cdot 10^{-6}\text{M}$.

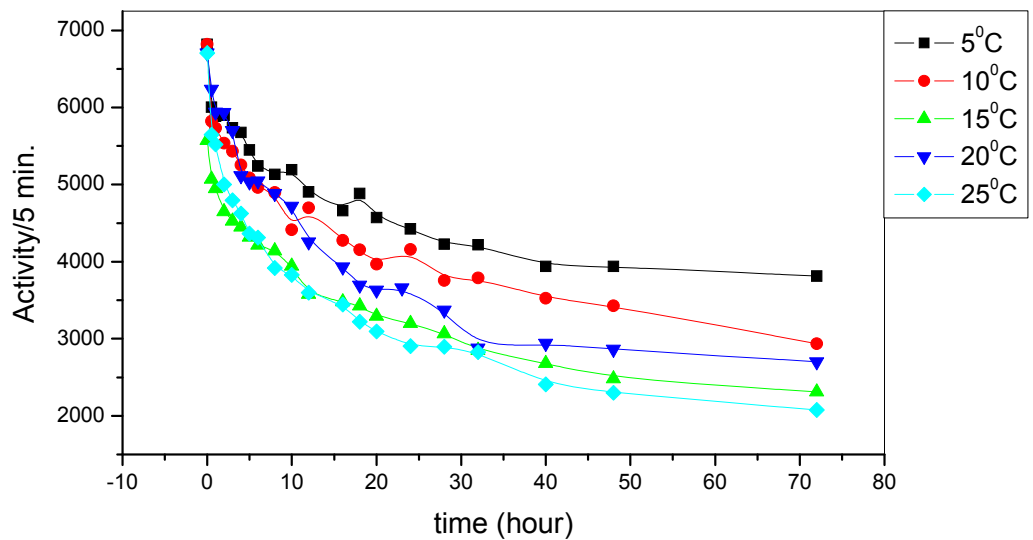


Figure 4.45. Counted activity- time plot of $^{60}\text{Co}^{2+}$ uptake on zeolite at constant cation concentration ($1 \times 10^{-6}\text{M}$). The effect of temperature on sorption was investigated.

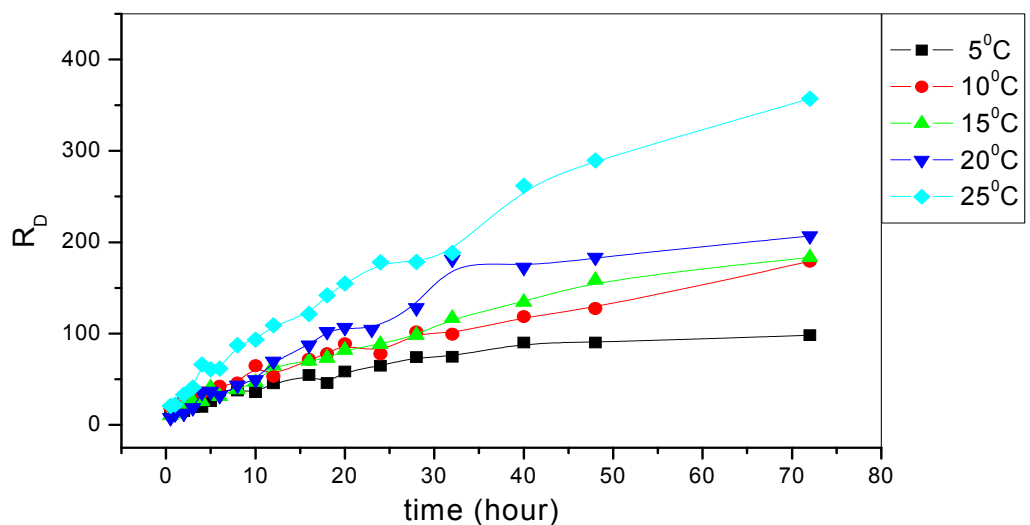


Figure 4.46. $^{60}\text{Co}^{2+}$ uptake on zeolite at constant cation concentration ($1 \times 10^{-6}\text{M}$). The effect of temperature on sorption was investigated.

Table 4.8. Thermodynamic parameters of ^{60}Co -Zeolite system

^{60}Co -Zeolite			
T(K)	ΔG° (kJ/mol)	ΔH° (kJ/mol)	ΔS° (J/molK)
278	-10.60	37.61	174
283	-12.21		
288	-12.48		
293	-12.99		
298	-14.56		

Comparing the cations Zn^{2+} , Cs^+ , Co^{2+} , Ba^{2+} and Sr^{2+} , on zeolite, Tables 4.2., 4.5., 4.8., 4.11. and 4.14., it is clearly seen that Co^{2+} is less spontaneous at all temperatures due to its least negative, in the Table 4.8., ΔG° (i.e. -10.60 kJ/mol at 5°C); it is in accordance with the plots of sorption of cobalt ion (Fig. 4.46.).

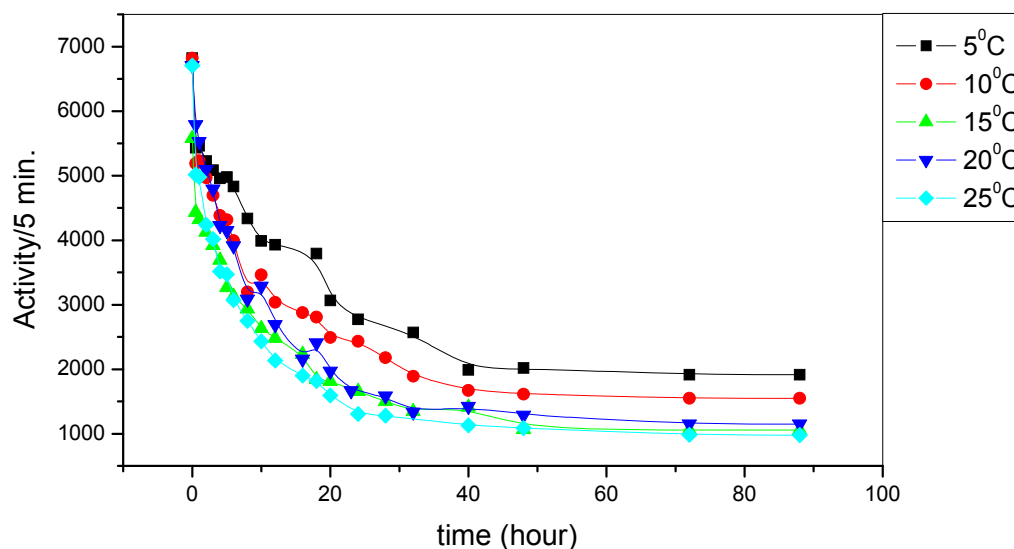


Figure 4.47. Counted activity- time plot of $^{60}\text{Co}^{2+}$ uptake on kaolin at constant cation concentration ($1 \times 10^{-6}\text{M}$). The effect of temperature on sorption was investigated.

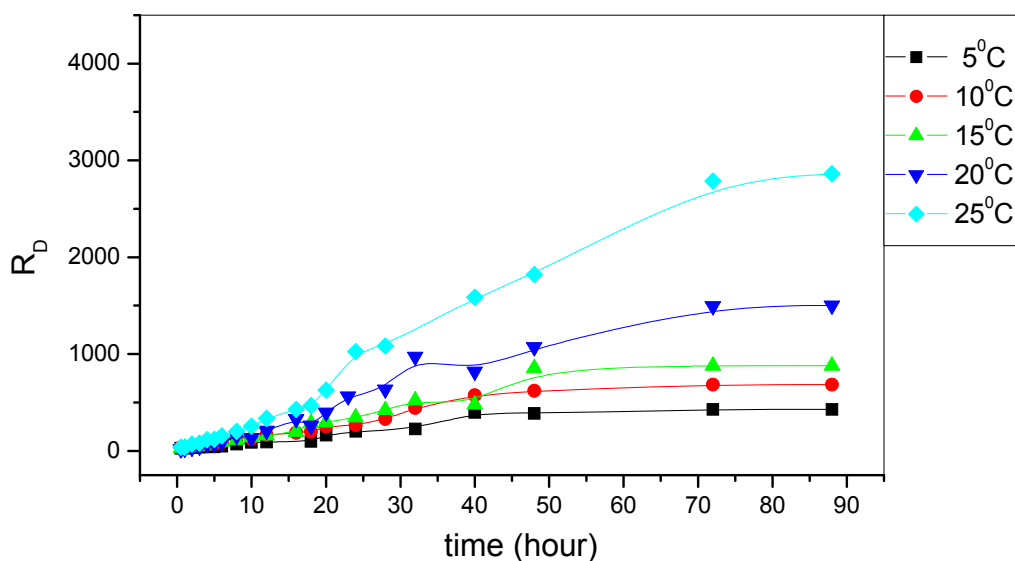


Figure 4.48. $^{60}\text{Co}^{2+}$ uptake on kaolin at constant cation concentration ($1 \times 10^{-6}\text{M}$). The effect of temperature on sorption was investigated.

The adsorption of cobalt ion on bentonite Fig. 4.44. and kaolin Fig. 4.48. increases to 11 times and 7 times respectively by an increase from 5 to 25°C.

Table 4.9. Thermodynamic parameters of $^{60}\text{Cobalt-Kaolin}$ system

$^{60}\text{Cobalt-Kaolin}$			
T(K)	ΔG° (kJ/mol)	ΔH° (kJ/mol)	ΔS° (J/molK)
278	-14.01	62.90	276
283	-15.36		
288	-16.23		
293	-17.82		
298	-19.72		

The order of spontaneity of Co^{2+} on adsorbents is Zeolite < Kaolin < Bentonite according to the ΔG° values.

Yavuz et al. (2003), found that for Co(II)-kaolinite system; mean ΔH° as 21.52 kJ/mol between at 25°C and 40°C.

4.9. The effect of temperature on $^{133}\text{Ba}^{2+}$ barium ion adsorption behaviours on bentonite, kaolin and zeolite

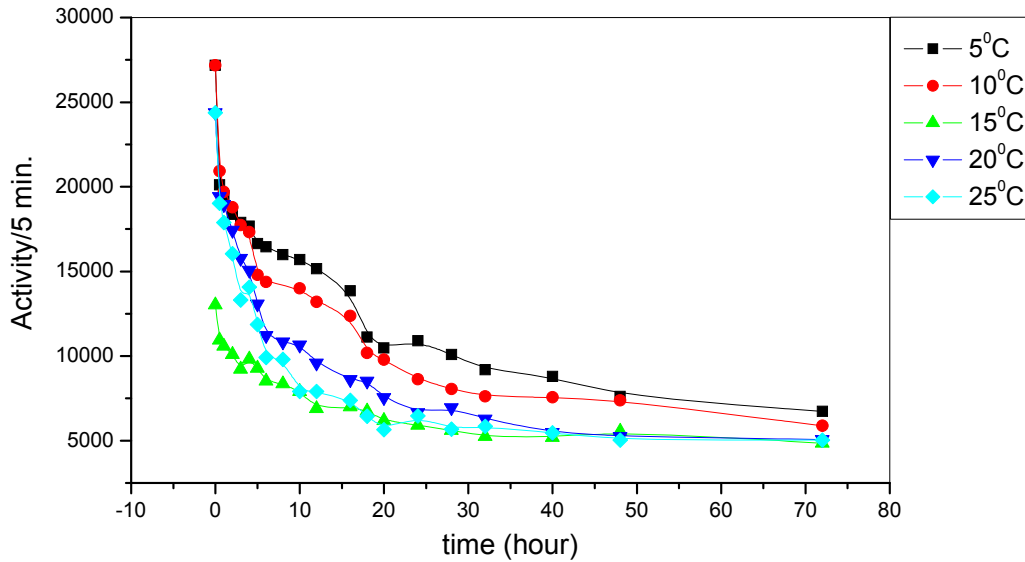


Figure 4.49. Counted activity- time plot of $^{133}\text{Ba}^{2+}$ uptake on bentonite at constant cation concentration ($1 \times 10^{-6}\text{M}$). The effect of temperature on sorption was investigated.

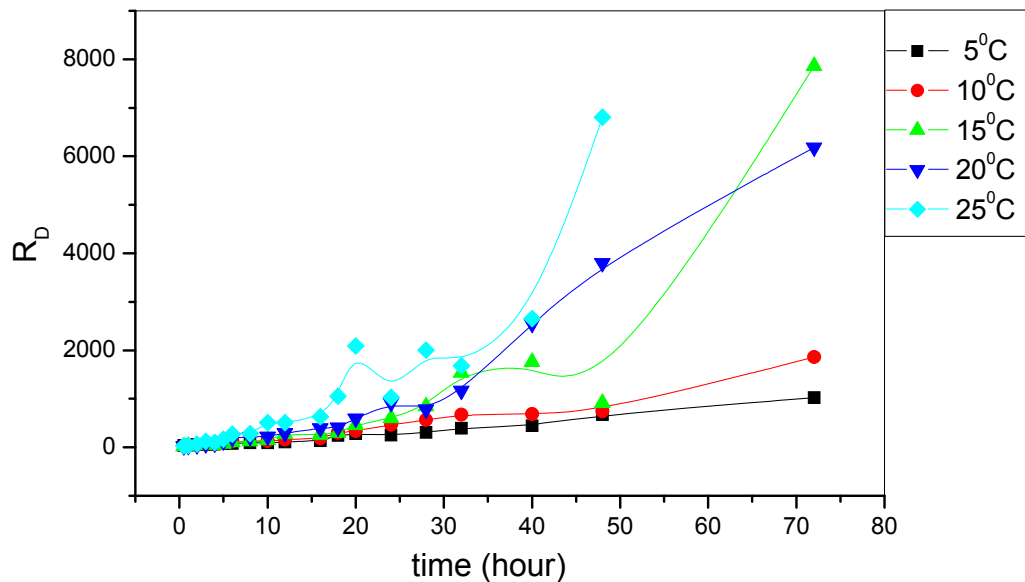


Figure 4.50 $^{133}\text{Ba}^{2+}$ uptake on bentonite at constant cation concentration ($1 \times 10^{-6}\text{M}$). The effect of temperature on sorption was investigated.

Table 4.10. Thermodynamic parameters of ^{133}Ba -Bentonite system

^{133}Ba -Bentonite			
T(K)	ΔG° (kJ/mol)	ΔH° (kJ/mol)	ΔS° (J/molK)
278	-16.73	59.36	279
283	-21.29		
288	-21.44		
293	-22.41		
298	-23.02		

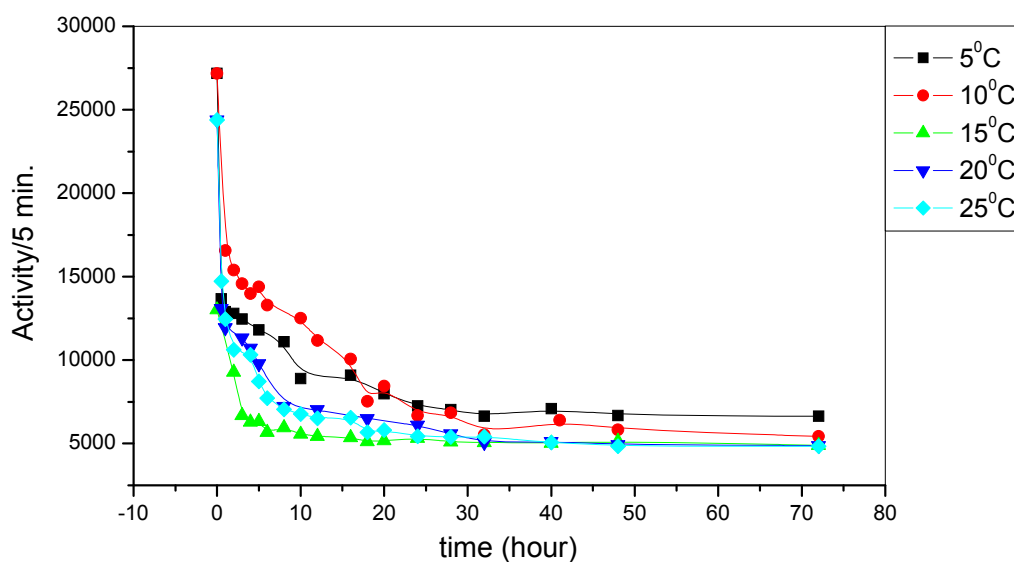


Figure 4.51. Counted activity- time plot of $^{133}\text{Ba}^{2+}$ uptake on zeolite at constant cation concentration ($1 \times 10^{-6}\text{M}$). The effect of temperature on sorption was investigated.

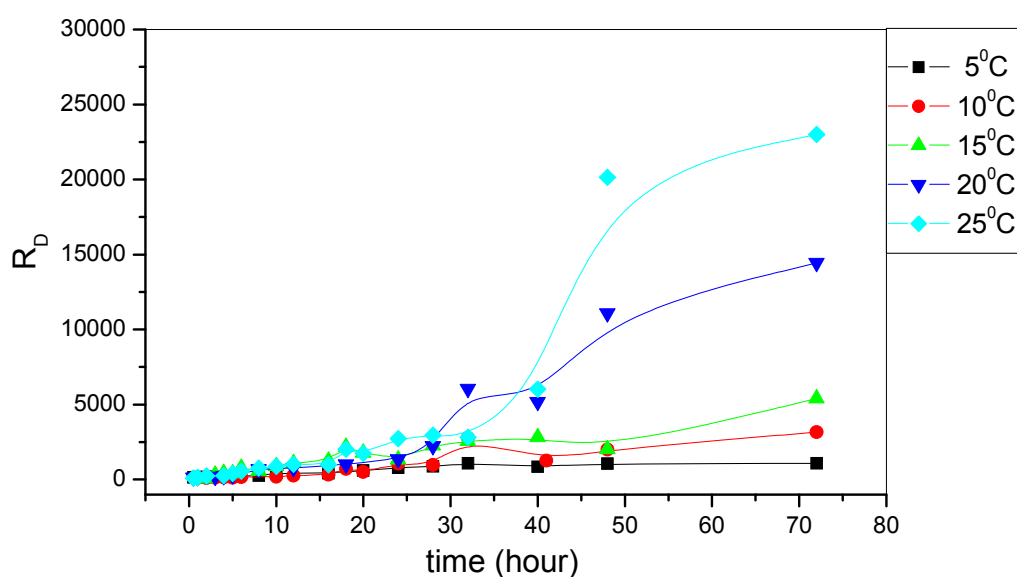


Figure 4.52. $^{133}\text{Ba}^{2+}$ uptake on zeolite at constant cation concentration ($1 \times 10^{-6}\text{M}$). The effect of temperature on sorption was investigated.

Table 4.11. Thermodynamic parameters of $^{133}\text{Barium-Zeolite}$ system

$^{133}\text{Barium-Zeolite}$			
T(K)	ΔG° (kJ/mol)	ΔH° (kJ/mol)	ΔS° (J/molK)
278	-16.14	105.31	438
283	-18.97		
288	-20.58		
293	-23.33		
298	-24.88		

In the case of zeolite-cation systems, Ba^{2+} is the cation which shows the maximum change in ΔG° by rise in temperature.

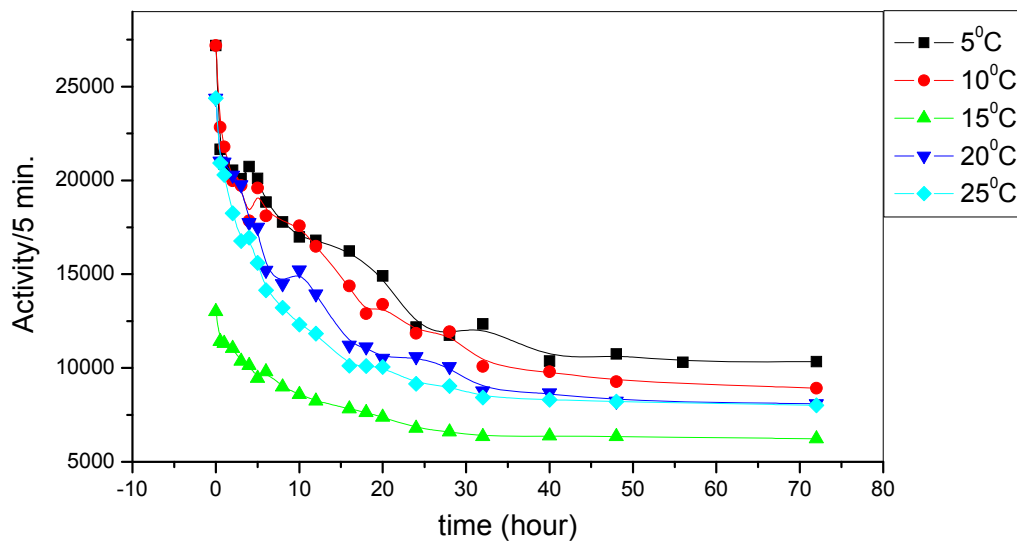


Figure 4.53. Counted activity- time plot of $^{133}\text{Ba}^{2+}$ uptake on kaolin at constant cation concentration ($1 \times 10^{-6}\text{M}$). The effect of temperature on sorption was investigated.

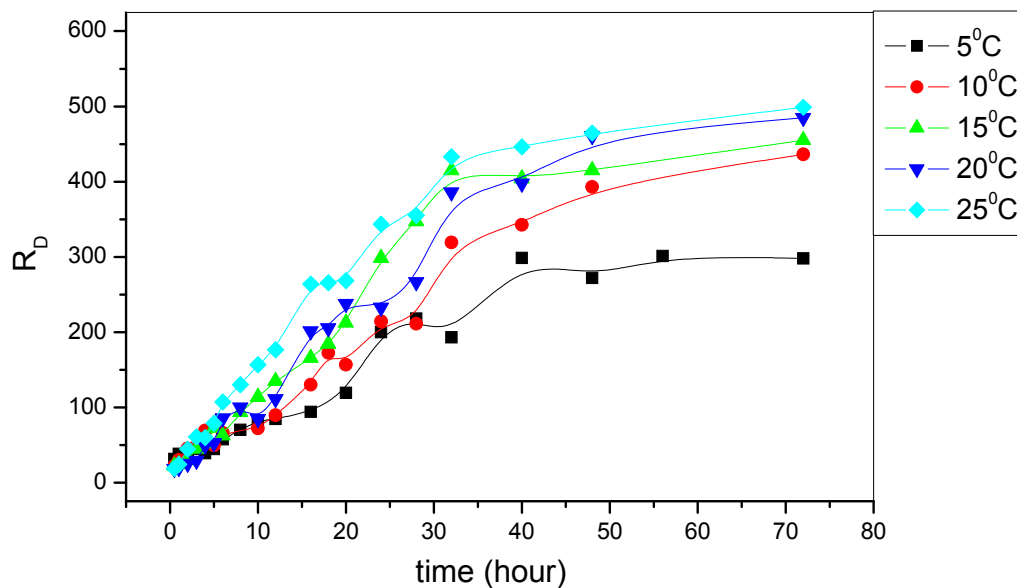


Figure 4.54. $^{133}\text{Ba}^{2+}$ uptake on kaolin at constant cation concentration ($1 \times 10^{-6}\text{M}$). The effect of temperature on sorption was investigated.

The layers are held together tightly in kaolinite. Surface bondings of cations are over oxygen atom of silanole groups of kaolinite. Breaking of O-H bond occurs

easily at high temperatures. On surface of kaolinite there is no any significant increase in adsorptions of Cs^+ , Ba^{2+} and Sr^{2+} by the increase of temperature from 5°C to 25°C ; approximately 1.6, 1.7, 2 times respectively (Figs. 4.42., 4.54., 4.60.). By increase in temperature, weakening of van der Waals forces between the layers of montmorillonite structure are much easier than weakening of O-H bonds in Si tetrahedra and Al octahedra groups. The transition metals, Co^{2+} and Zn^{2+} adsorption effected much more than the others; in Figs. 4.48., and 4.32., approximately 7 times and 10.7 times respectively. The metal which shows the greatest temperature effect on adsorption on bentonite and kaolin is zinc ion. After zinc ion, cobalt is coming secondly which shows a significant increase on adsorption.

Table 4.12. Thermodynamic parameters of ^{133}Ba Barium-Kaolin system

^{133}Ba Barium-Kaolin			
T(K)	ΔG° (kJ/mol)	ΔH° (kJ/mol)	ΔS° (J/molK)
278	-13.17	15.82	105
283	-14.30		
288	-14.66		
293	-15.07		
298	-15.39		

The order of spontaneity of Ba^{2+} ions on adsorbent is kaolin < bentonite < zeolite (Tables 4.10, 4.11., 4.12). (At higher temperatures bentonite and zeolite change their places).

4.10. The effect of temperature on ^{90}Sr ion adsorption behaviours on bentonite, kaolin and zeolite

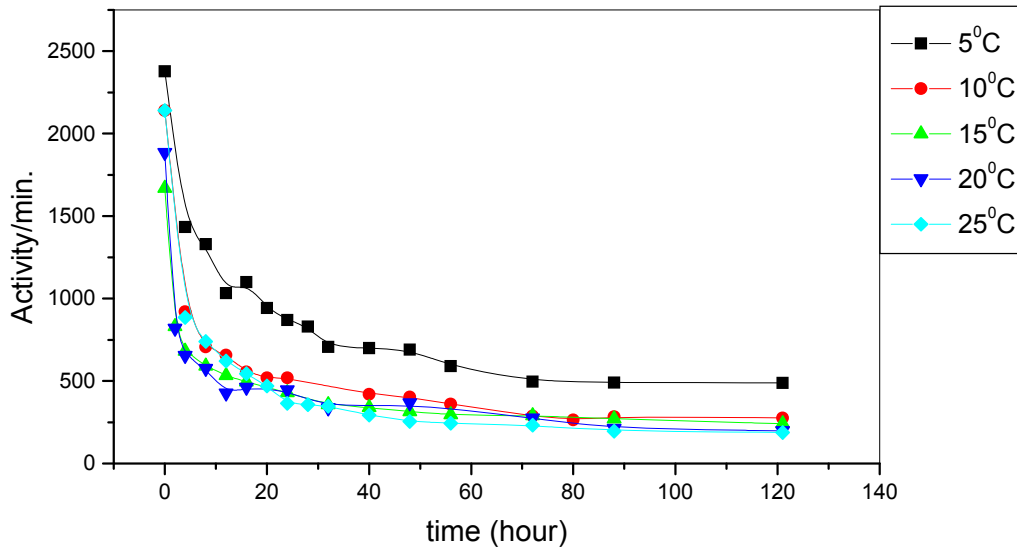


Figure 4.55. Counted activity- time plot of $^{90}\text{Sr}^{2+}$ uptake on bentonite at constant cation concentration ($1 \times 10^{-6}\text{M}$). The effect of temperature on sorption was investigated.

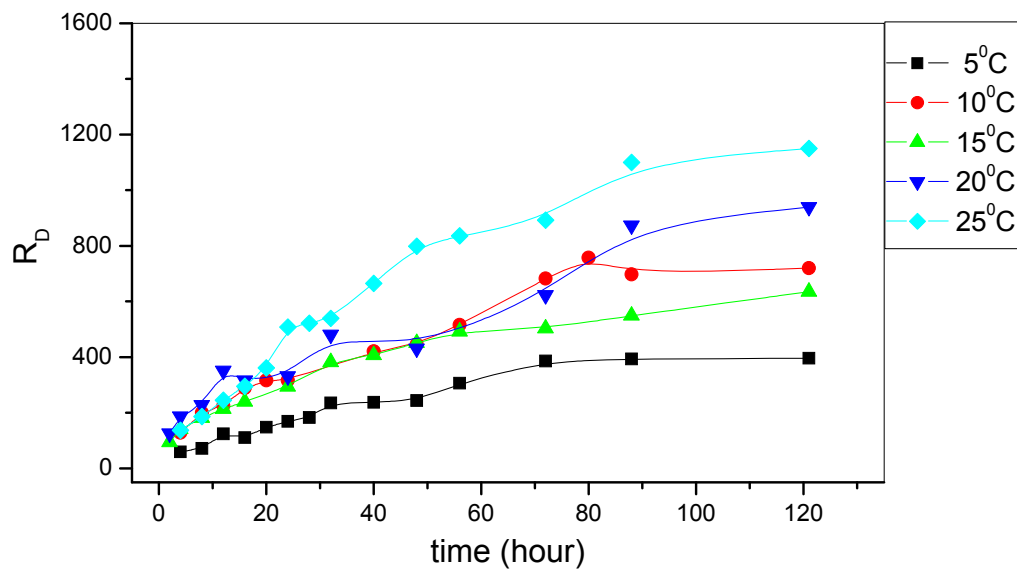


Figure 4.56. $^{90}\text{Sr}^{2+}$ uptake on bentonite at constant cation concentration ($1 \times 10^{-6}\text{M}$). The effect of temperature on sorption was investigated.

Table 4.13. Thermodynamic parameters of $^{90}\text{Strontium-Bentonite}$ system

$^{90}\text{Strontium-Bentonite}$			
T(K)	ΔG° (kJ/mol)	ΔH° (kJ/mol)	ΔS° (J/molK)
278	-13.83	33.09	170
283	-15.48		
288	-15.45		
293	-16.67		
298	-17.46		

According to the Tables 4.1., 4.4., 4.7., 4.10. and 4.13 among all cations strontium ion has the lowest spontaneity on bentonite (i.e. at 5°C -13.83 kJ/mol) means that less negative ΔG° values at all temperatures. Khan et al. (1995) investigated the sorption of Sr on bentonite at different experimental conditions. They also pointed out that the negative value of the free energy of sorption, $\Delta G^\circ = -10.69$ kJ/mol at 298 K, showing the spontaneity. ΔG° becomes more negative with increasing temperature. They determined the heat of sorption as 30.62 kJ/mol at 298 K. They found out the positive sign for ΔS° ; which means increase of disorder, as in our results. They explain the increase in entropy on the basis of an ion-exchange process of the ions that displace to the places of each other. In this process more translational entropy is gained by the ions that are transferred from the sorbent surface to the solution comparing with the decrease in entropy due to removal of ions from solution and their sorption on the sorbent.

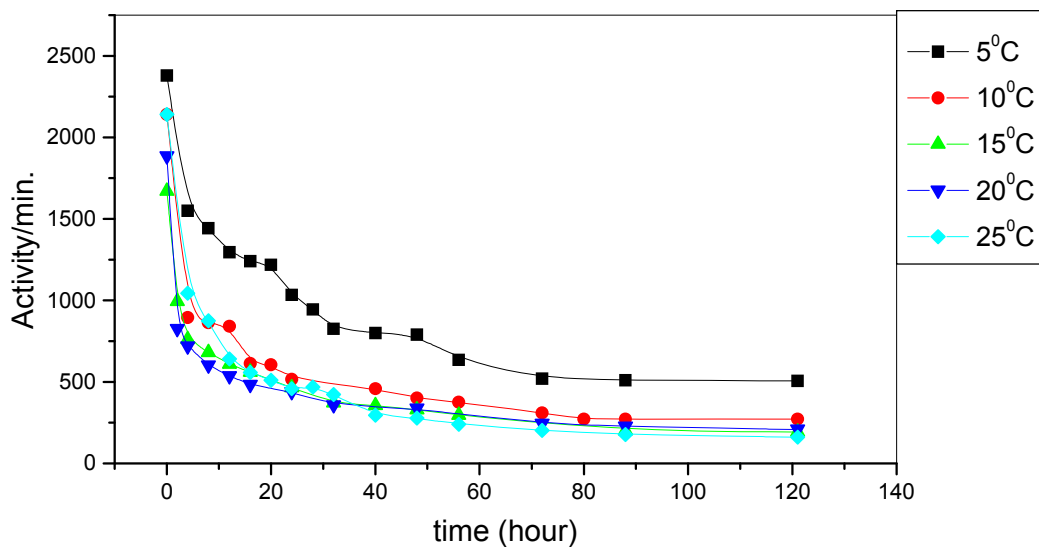


Figure 4.57. Counted activity- time plot of $^{90}\text{Sr}^{2+}$ uptake on zeolite at constant cation concentration ($1 \times 10^{-6}\text{M}$). The effect of temperature on sorption was investigated.

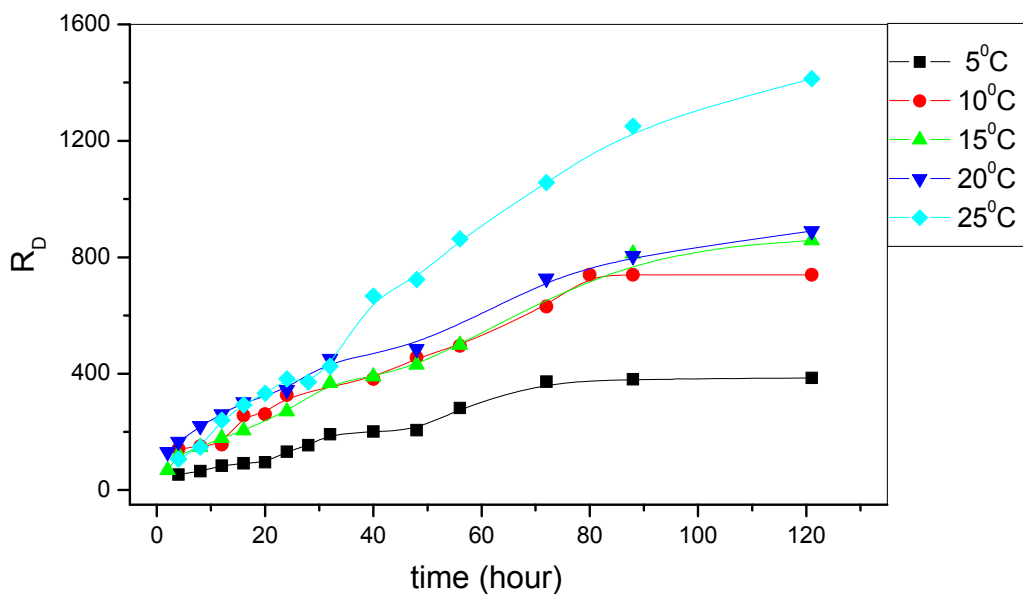


Figure 4.58. $^{90}\text{Sr}^{2+}$ uptake on zeolite at constant cation concentration ($1 \times 10^{-6}\text{M}$). The effect of temperature on sorption was investigated.

Table 4.14. Thermodynamic parameters of ^{90}Sr -Zeolite system

^{90}Sr -Zeolite			
T(K)	ΔG° (kJ/mol)	ΔH° (kJ/mol)	ΔS° (J/molK)
278	-13.76	38.48	189
283	-15.55		
288	-16.17		
293	-16.54		
298	-17.97		

Sr^{2+} uptakes on zeolite and bentonite have nearly same spontaneity (Tables 4.13. and 4.14.).

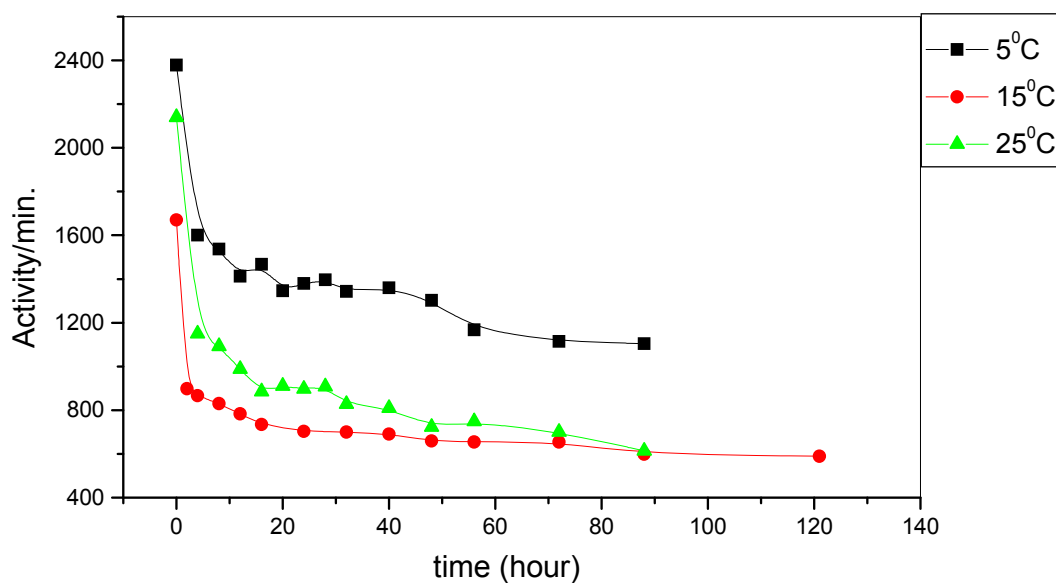


Figure 4.59. Counted activity- time plot of $^{90}\text{Sr}^{2+}$ uptake on kaolin at constant cation concentration ($1 \times 10^{-6}\text{M}$). The effect of temperature on sorption was investigated.

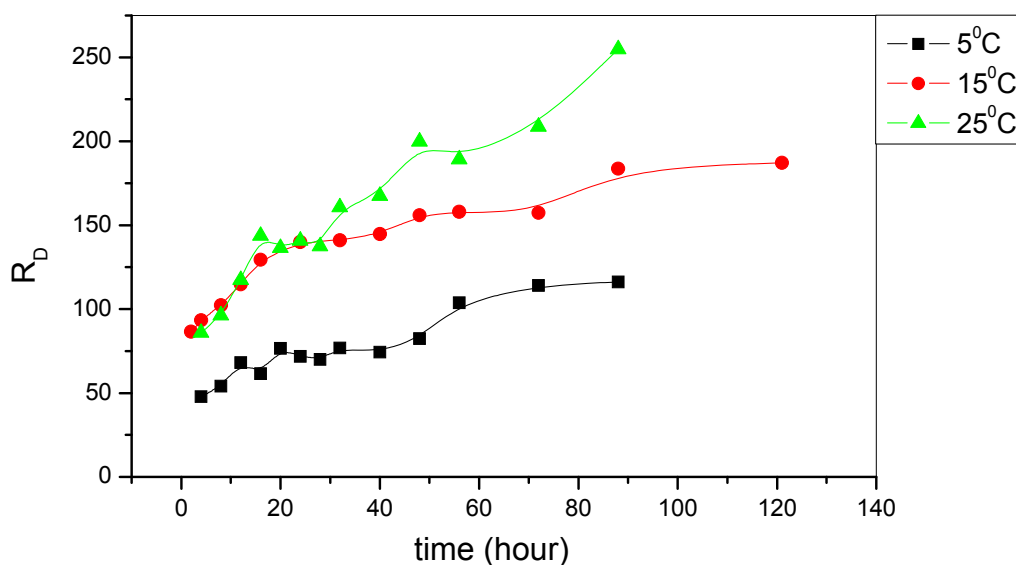


Figure 4.60. $^{90}\text{Sr}^{2+}$ uptake on kaolin at constant cation concentration ($1 \times 10^{-6}\text{M}$). The effect of temperature on sorption was investigated.

Table 4.15. Thermodynamic parameters of $^{90}\text{Strontium-Kaolin}$ system

$^{90}\text{Strontium-Kaolin}$			
T(K)	ΔG° (kJ/mol)	ΔH° (kJ/mol)	ΔS° (J/molK)
278	-10.99	27.05	137
283			
288	-12.53		
293			
298	-13.72		

The order of spontaneity of Sr^{2+} on Kaolin is the lowest in the adsorbents (Table 4.15.). Sr^{2+} ions show approximately same behavior on zeolite and on bentonite (Tables 4.14. and 4.13.).

In the Table 4.15., comparing to the ΔG° values of the other cations on kaolin in the Tables 4.3., 4.6., 4.9., 4.12. Sr^{2+} uptake has highest ΔG° (for kaolin -10.99 kJ/mol at 5°C) which means lowest spontaneity. Its low adsorption capacity is seen also in the plots of R_d -time (Fig. 4.60.). According to the results of Akar et al. (2005) the sorption process on both kaolinite which is the mineral of kaolin clay

and clinoptilolite which is the mineral of zeolite was spontaneous and endothermic. This conclusion shows the accordance with our results (Table 4.14. and 4.15.). But comparing the numerical values is not true cause of our samples are in their natural form, not pure mineral.

The calculated thermodynamic parameters are presented in the tables for sorption of Zn^{2+} , Ba^{2+} , Co^{2+} , Sr^{2+} and Cs^+ on bentonite, zeolite and kaolin. For the

* Bentonite- Zn^{2+} , Bentonite- Ba^{2+} , Bentonite- Co^{2+} , Bentonite- Sr^{2+} , Bentonite- Cs^+

* Zeolite- Zn^{2+} , Zeolite- Ba^{2+} , Zeolite- Co^{2+} , Zeolite- Sr^{2+} , Zeolite- Cs^+ ,

* Kaolin- Zn^{2+} , Kaolin- Ba^{2+} , Kaolin- Co^{2+} , Kaolin- Sr^{2+} , Kaolin- Cs^+ systems:

Table 4.16. The evaluation of the thermodynamic results which are obtained.

$\Delta G^\circ < 0$; indicates the spontaneity of the process, adsorptions are spontaneous over the range 278–298K.

ΔG° becomes more negative \downarrow as temperature \uparrow ; shows that sorption is favoured at high temperatures,

$\Delta H^\circ > 0$; shows that the adsorption process is endothermic,

$\Delta S^\circ > 0$; more disorder is generated in the system upon adsorption.

In the tables of thermodynamic parameters it is seen that Gibbs energy, ΔG° , is negative for all adsorbent-cation systems that means that sorptions of all cations on adsorbent surfaces are spontaneous. An other common behaviour; as temperature increases negative value of ΔG° increases that means that sorption process favors high temperatures. ΔG° has more negative values at higher temperatures for all investigated systems that indicates the spontaneity of the sorptions. The other common properties are positive enthalpy of sorption, ΔH , which means that all of sorptions are endothermic and positive entropy change, ΔS° , gaining more mobility during the sorption for all systems.

In general, for all systems high temperatures are more favorable for sorption.

4.11. Freundlich isotherms of zinc adsorption at 5°C.

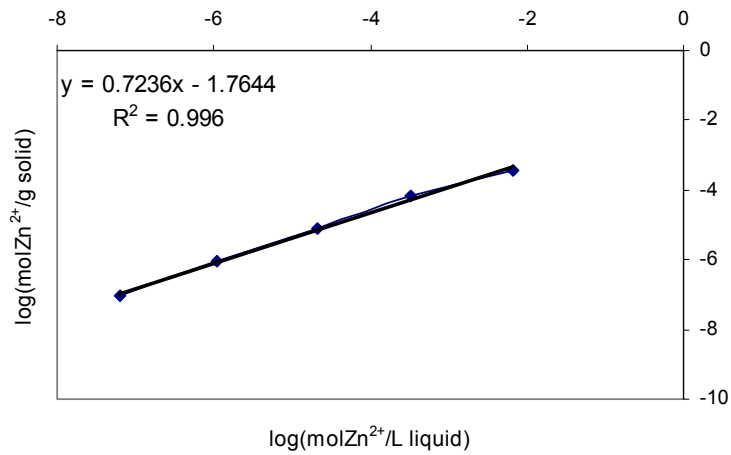


Figure 4.61. $^{65}\text{Zn}^{2+}$ -Bentonite system: $n=0.7236$, $k=0.0172$.

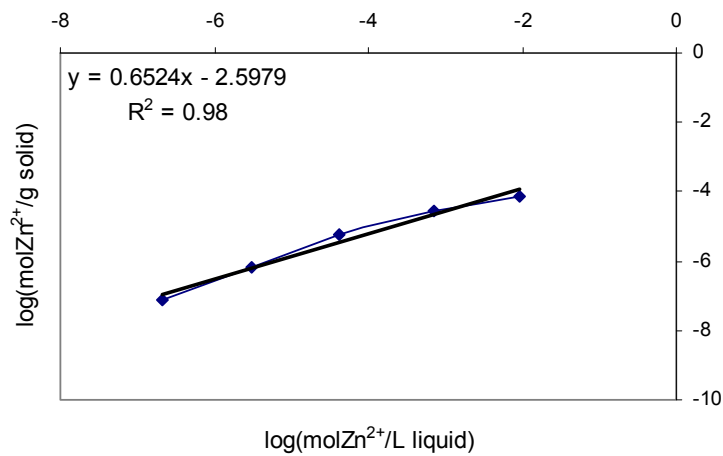


Figure 4.62. $^{65}\text{Zn}^{2+}$ -Zeolite system: $n=0.6524$, $k=0.0025$.

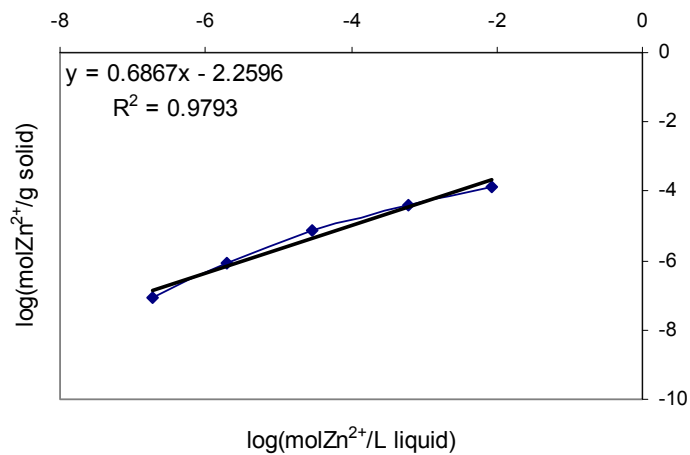


Figure 4.63. $^{65}\text{Zn}^{2+}$ -Kaolin system: $n=0.6867$, $k=0.0055$.

4.12. Freundlich isotherms of barium adsorption at 5°C.

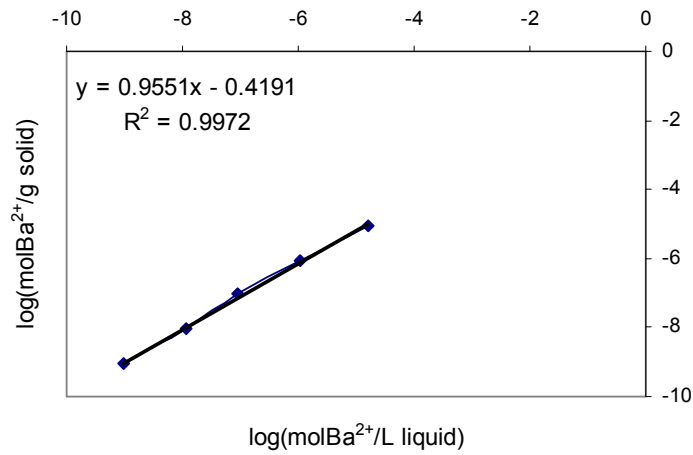


Figure 4.64. $^{133}\text{Ba}^{2+}$ -Bentonite system: $n=0.9551$, $k=0.381$.

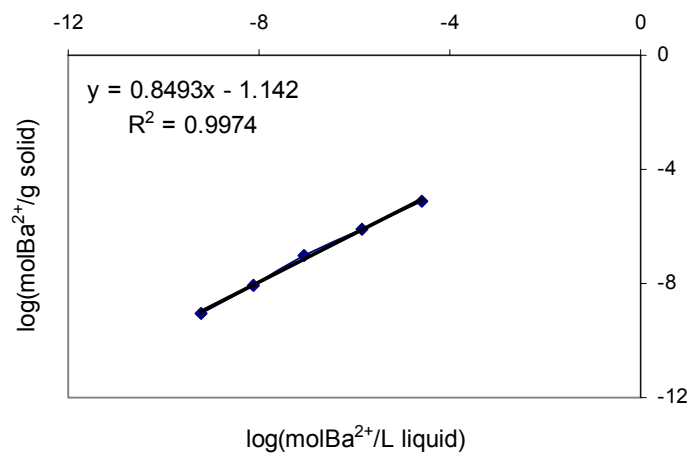


Figure 4.65. $^{133}\text{Ba}^{2+}$ -Zeolite system: $n=0.8493$, $k=0.072$.

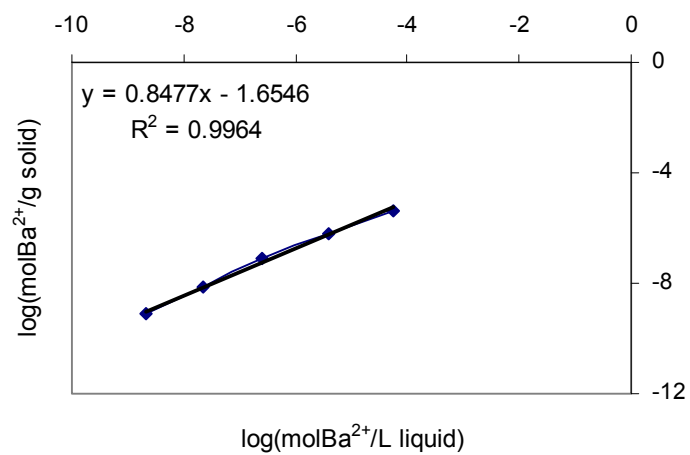


Figure 4.66. $^{133}\text{Ba}^{2+}$ -Kaolin system: $n=0.8477$, $k=0.02215$.

4.13. Freundlich isotherms of cobalt adsorption at 5°C.

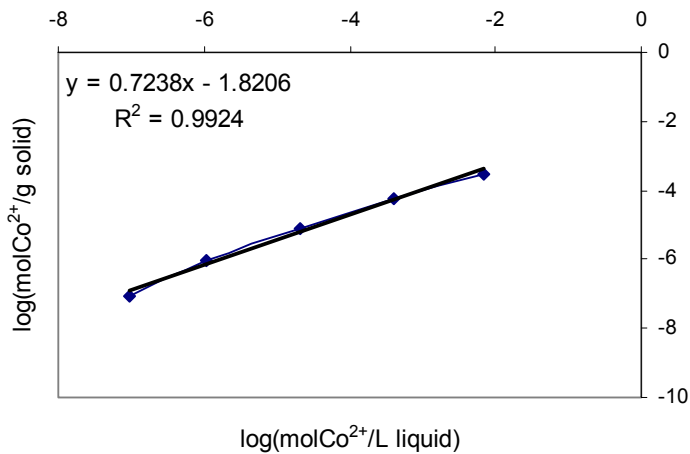


Figure 4.67. $^{60}\text{Co}^{2+}$ -Bentonite system: $n=0.7238$, $k=0.0151$.

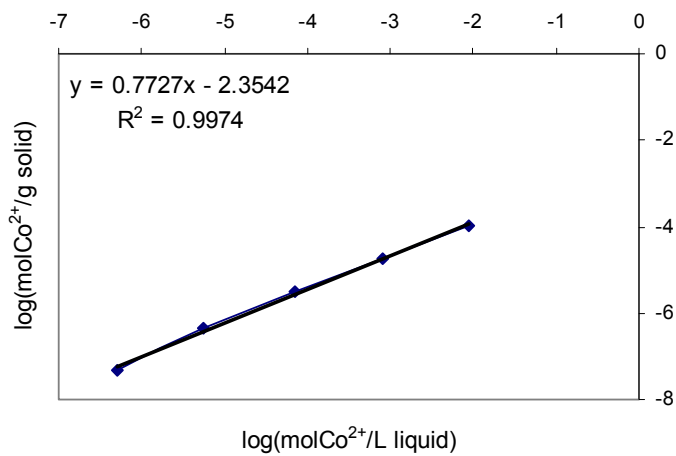


Figure 4.68. $^{60}\text{Co}^{2+}$ -Zeolite system: $n=0.7727$, $k=0.00442$.

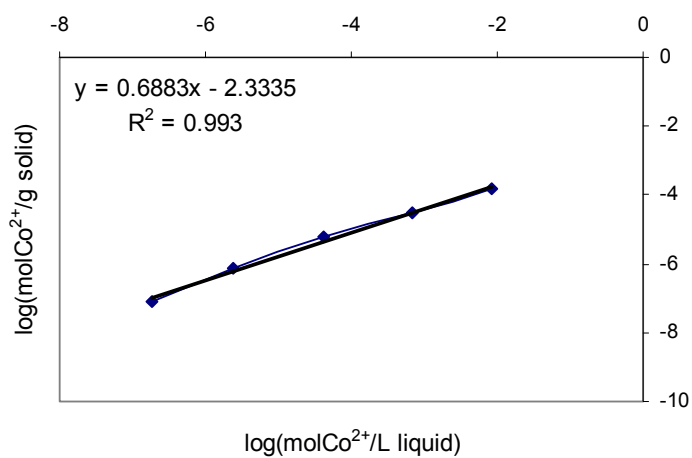


Figure 4.69. $^{60}\text{Co}^{2+}$ -Kaolin system: $n=0.6883$, $k=0.00464$.

4.14. Freundlich isotherms of caesium adsorption at 5°C.

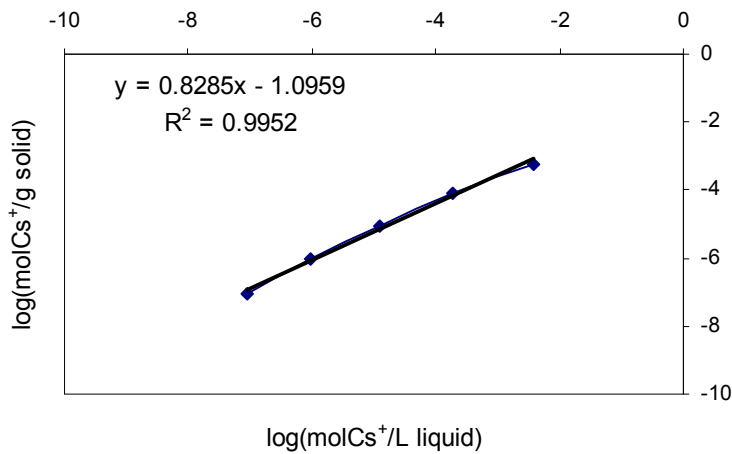


Figure 4.70. $^{137}\text{Cs}^+$ -Bentonite system: $n=0.8285$, $k=0.0802$.

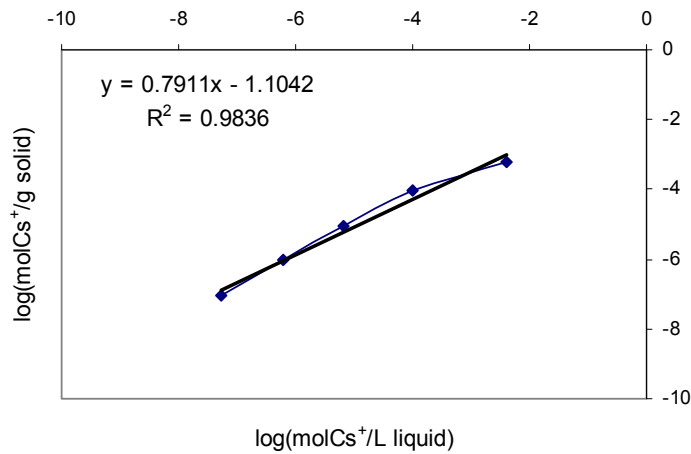


Figure 4.71. $^{137}\text{Cs}^+$ -Zeolite system: $n=0.7911$, $k=0.07867$.

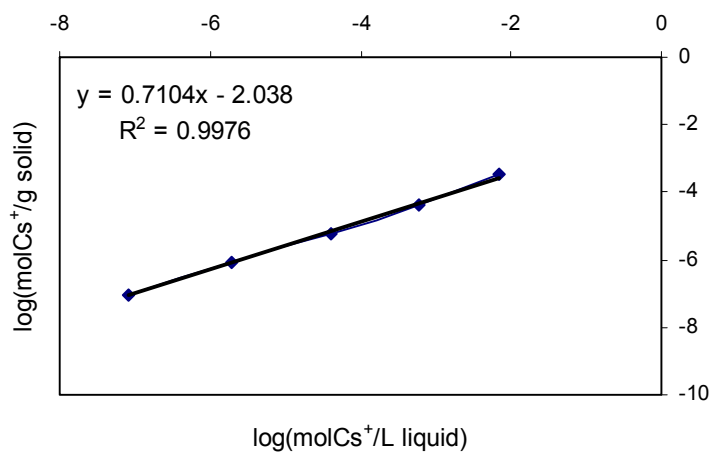


Figure 4.72. $^{137}\text{Cs}^+$ -Kaolin system: $n=0.7104$, $k=0.00916$.

4.15. Freundlich isotherms of strontium adsorption at 5°C.

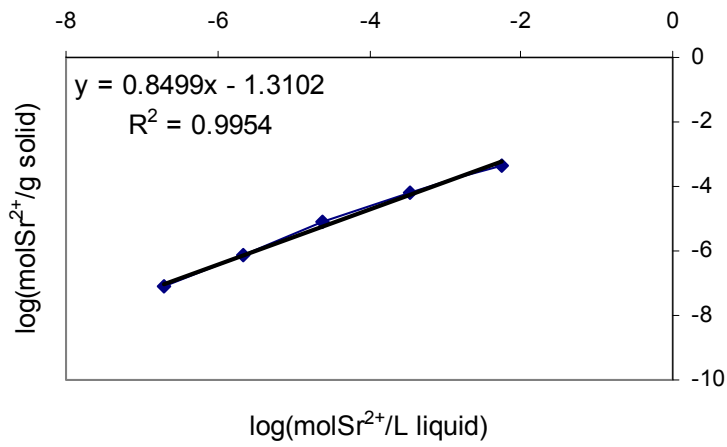


Figure 4.73. $^{90}\text{Sr}^{2+}$ -Bentonite system: $n=0.8499$, $k=0.049$.

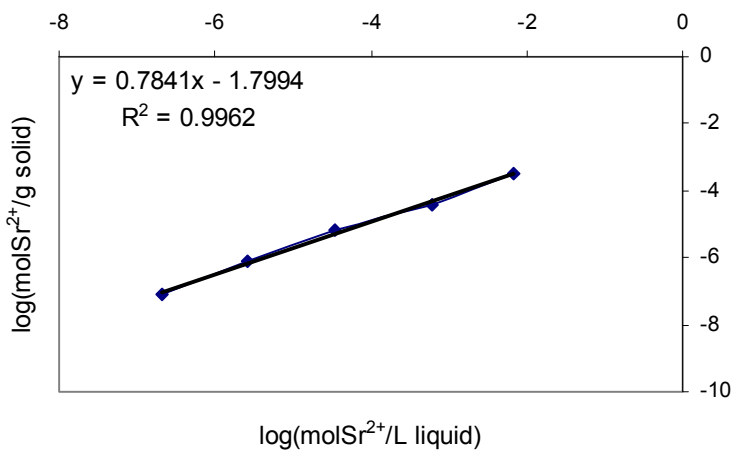


Figure 4.74. $^{90}\text{Sr}^{2+}$ -Zeolite system: $n=0.7841$, $k=0.0159$.

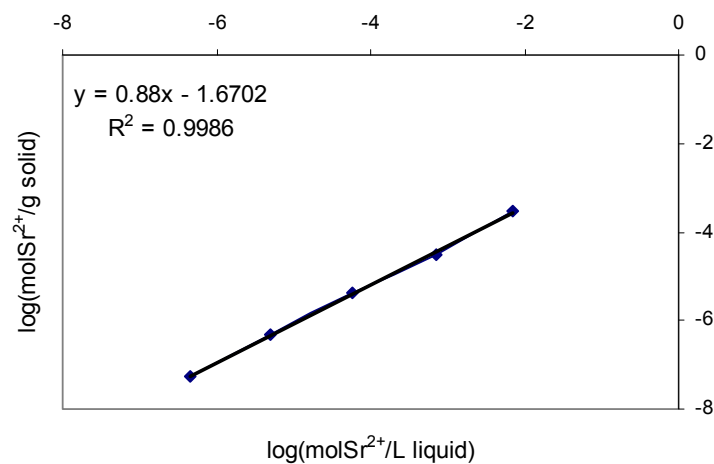


Figure 4.75. $^{90}\text{Sr}^{2+}$ -Kaolin system: $n=0.88$, $k=0.0214$.

It was found that the sorption isotherms fitted to Freundlich model. All of the sorption isotherms can be considered to be linear. The minimum R^2 is 0.9793.

Table 4.17. Freundlich parameters.

Bentonite					
	Zn-65	Ba-133	Co-60	Cs-137	Sr-90
n	0.7236	0.9551	0.7238	0.8285	0.8499
k	0.0172	0.381	0.0151	0.08019	0.049
Zeolite					
	Zn-65	Ba-133	Co-60	Cs-137	Sr-90
n	0.6524	0.8493	0.7727	0.7911	0.7841
k	0.0025	0.072	0.00442	0.07867	0.0159
Kaolin					
	Zn-65	Ba-133	Co-60	Cs-137	Sr-90
n	0.6867	0.8477	0.6883	0.7104	0.88
k	0.0055	0.02215	0.00464	0.00916	0.0214

4.16. Desorption behaviours of zinc ion 5°C, 25°C on bentonite, kaolin and zeolite

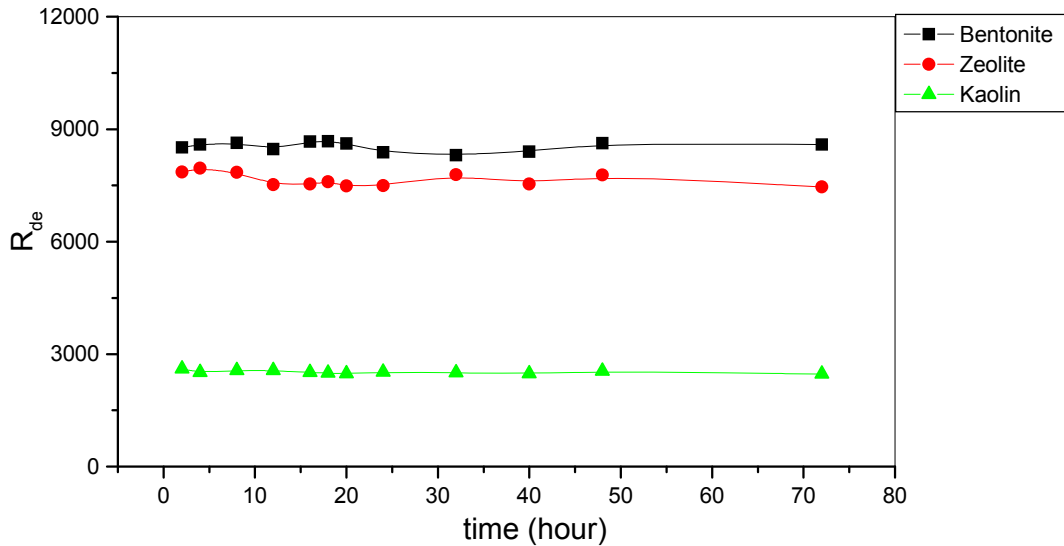


Figure 4.76. $^{65}\text{Zn}^{2+}$ desorption behaviours at 5°C (constant cation concentration $1 \times 10^{-6}\text{M}$).

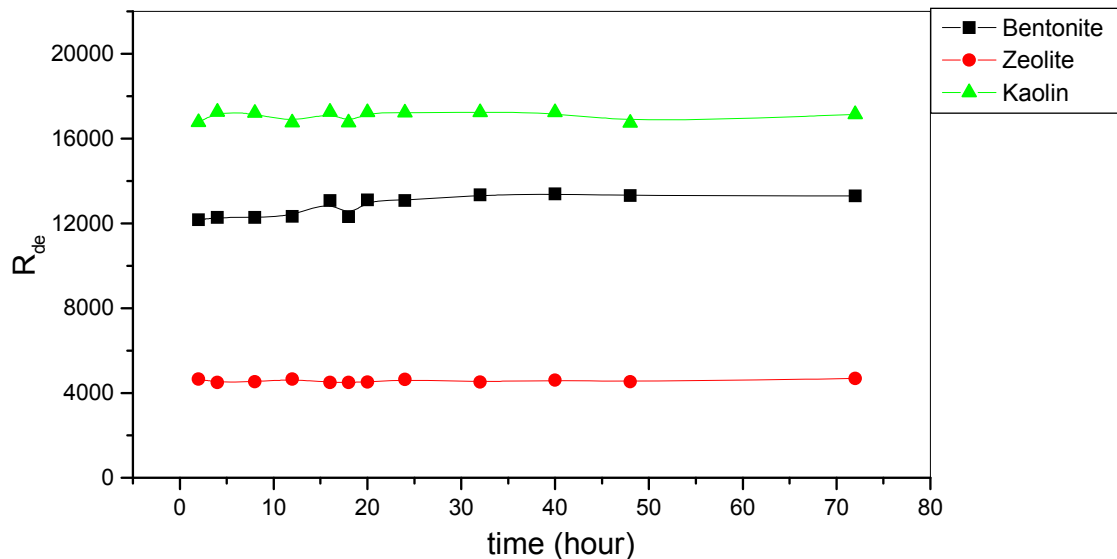


Figure 4.77. $^{65}\text{Zn}^{2+}$ desorption behaviours at 25°C (constant cation concentration $1 \times 10^{-6}\text{M}$).

After sorption for 72 hours, the adsorbents were put into groundwater. Desorption ratio was defined as the amount of cation sorbed on clay / released cation from the solid to the groundwater. The higher R_{de} value is the lower desorption. For

example, in Figure 4.76 distribution ratio for desorption of zinc ion on kaolin is about 2900; it means the amount of cation on kaolin is 2900 times of the released amount to the groundwater. In Figures 4.76. and 4.77. as the temperature increases especially on kaolin desorption decreases, means that desorption ratio, R_{de} , increases, 2900 increase to about 17000, desorption decreases. In other words, kaolin doesn't release the amount of Zn^{2+} sorbed on it. It was evaluated in the sorption experiments, Zn^{2+} is the most effected by the temperature changes on kaolin (part 4.1). This is true also for the desorption results (Figures 4.76. and 4.77.). At 25°C desorption is lower than that of 5°C. The ratio of zinc ion on kaolin to the released amount is very higher at 25°C than that of 5°C.

4.17. Desorption behaviours of barium ion at 5°C, 25°C on bentonite, kaolin and zeolite

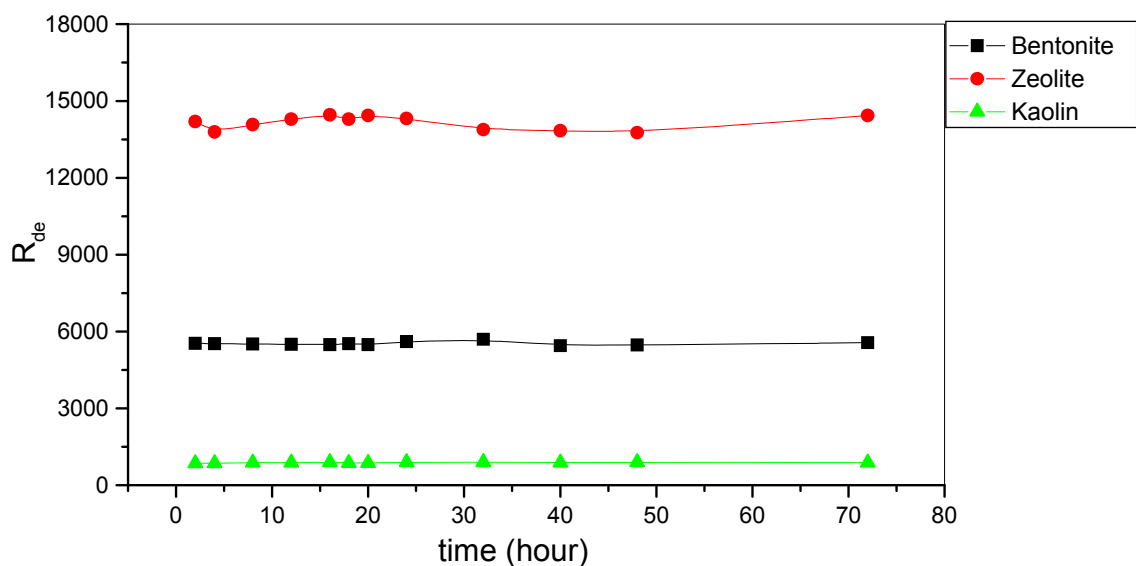


Figure 4.78. $^{133}Ba^{2+}$ desorption behaviours at 5°C (constant cation concentration $1 \times 10^{-6} M$).

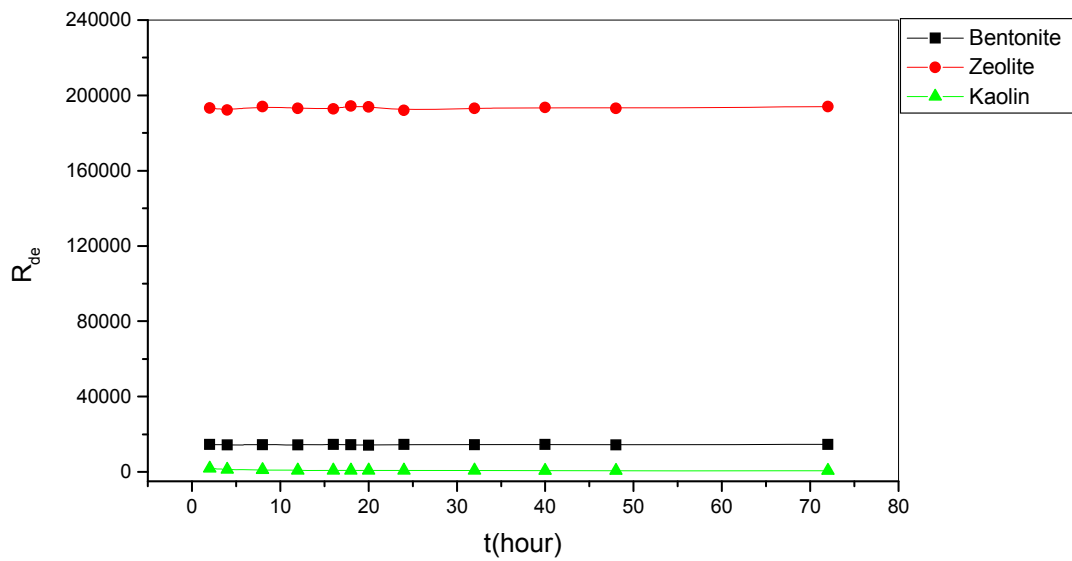


Figure 4.79. $^{133}\text{Ba}^{2+}$ desorption behaviours at 25°C (constant cation concentration $1 \times 10^{-6}\text{M}$).

Solid adsorbent were put into pure groundwater after 72 hours sorption time. At different time intervals samples were taken from groundwater in order to check whether solid release sorbed cation to the solution or not. R_{de} is the ratio of cation remained on the solid / cation passed into the solution. In desorption behaviours Ba^{2+} does not be desorbed. The sorption order was Zeolite>Bentonite>Kaolin, it is the same for opposit to the desorption: Zeolite does not release Ba^{2+} ions at all. The lowest desorption is on zeolite. As temperature increases, desorption decreases considerably, the ratio of cation on solid / cation passed to the solution increases.

4.18. Desorption behaviours of cobalt ion at 5°C, 25°C on bentonite, kaolin and zeolite

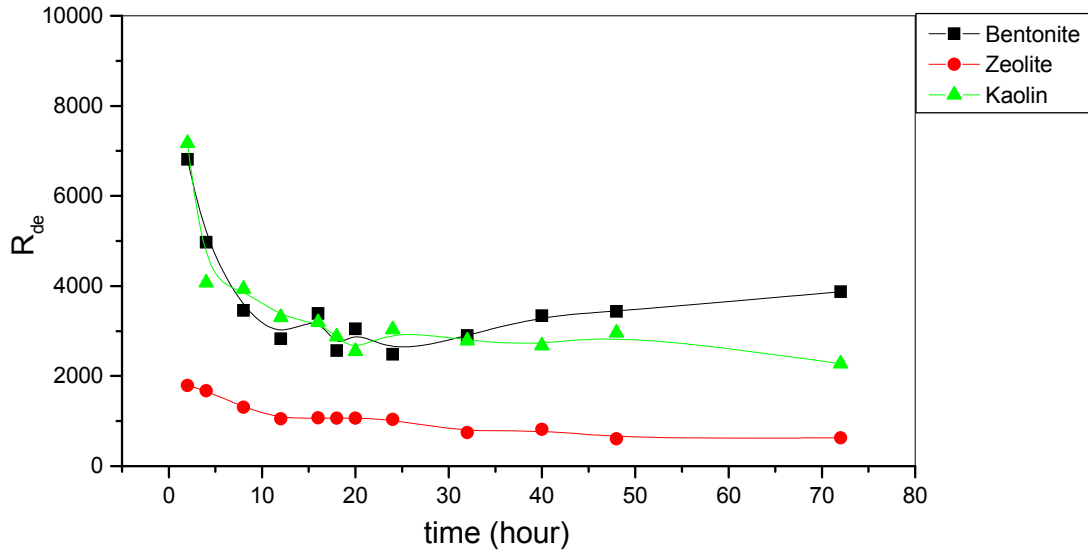


Figure 4.80. $^{60}\text{Co}^{2+}$ desorption behaviours at 5°C (constant cation concentration $1 \times 10^{-6}\text{M}$).

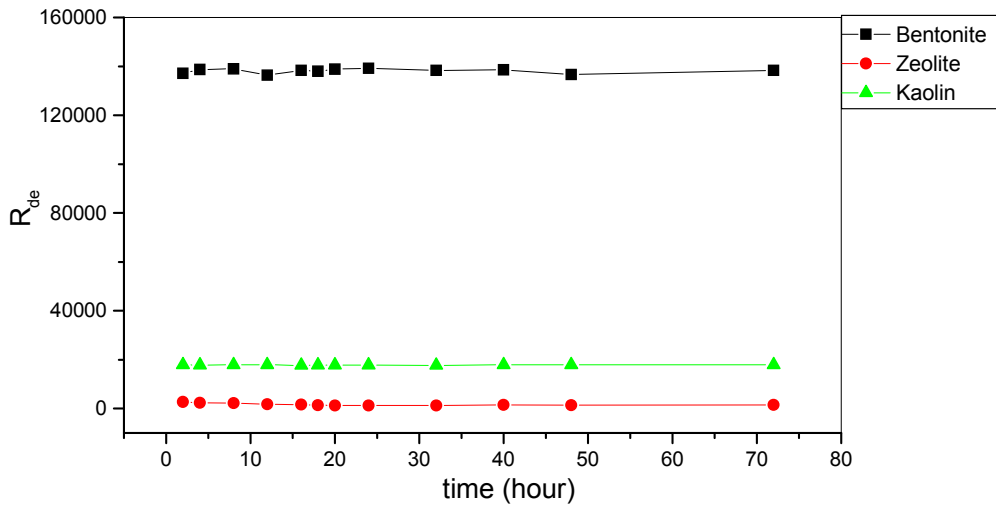


Figure 4.81. $^{60}\text{Co}^{2+}$ desorption behaviours at 25°C (constant cation concentration $1 \times 10^{-6}\text{M}$).

Graetest R_{de} means that; solid does not release the sorbed amount of cation. R_{de} : cation sorbed on solid / cation released to the solution.

For cobalt ion, there is a common property of sorption and desorption behaviours; the resistance to desorption order is the same of sorption order either 5 and 25°C; on Bentonite>Kaolin>Zeolite. Desorption results of cobalt ion are closer to each other at 5°C in Figure 4.80 as in sorption results (Figures 4.14., 4.16. and 4.18.). But at 25°C; desorption results are quite different from each other in Figure 4.81. as in sorption results in Figures 4.44, 4.46. and 4.48. Besides this, at 5°C, in Figure 4.80., there is a decrease in the distribution ratios of desorptions: activity sorbed by the adsorbent / activity of solution. The decrease of this ratio means activity passes from solid to the solution medium. In the other words, adsorbent releases the uptaken cation on it. But at 25°C, sorption capacity increases as temperature increases, sorption is quite high. At 25°C desorption conditions are the groundwater at 25°C. So the adsorbed amount of cation does not be released from the solid to the liquid. The desorption amount does not change with time at 25°C we see this linearity. As temperature increases desorption decreases. R_{de} indicates cation uptaken / cation released to the solution. The higher R_{de} the lower desorption, means good uptake.

4.19. Desorption behaviours of strontium ion bentonite, kaolin and zeolite

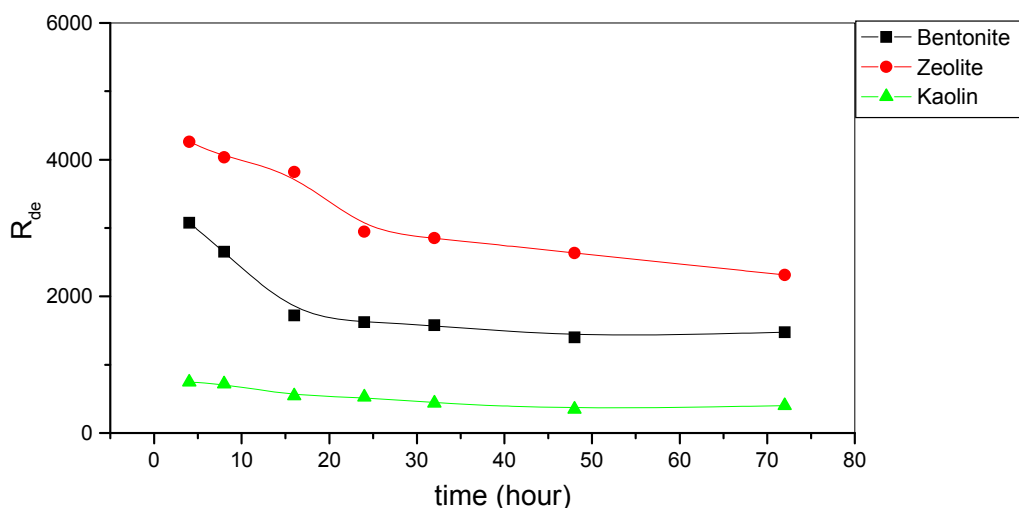


Figure 4.82. $^{90}\text{Sr}^{2+}$ desorption behaviours at 5°C (constant cation concentration $1 \times 10^{-6}\text{M}$).

The desorption behaviour of Sr^{2+} is seen in Figure 4.82. Sr^{2+} was desorbed in the first 24 hours but after this period adsorbents stopped to release the cation.

4.20. Desorption behaviours of caesium ion at 5°C on bentonite, kaolin and zeolite

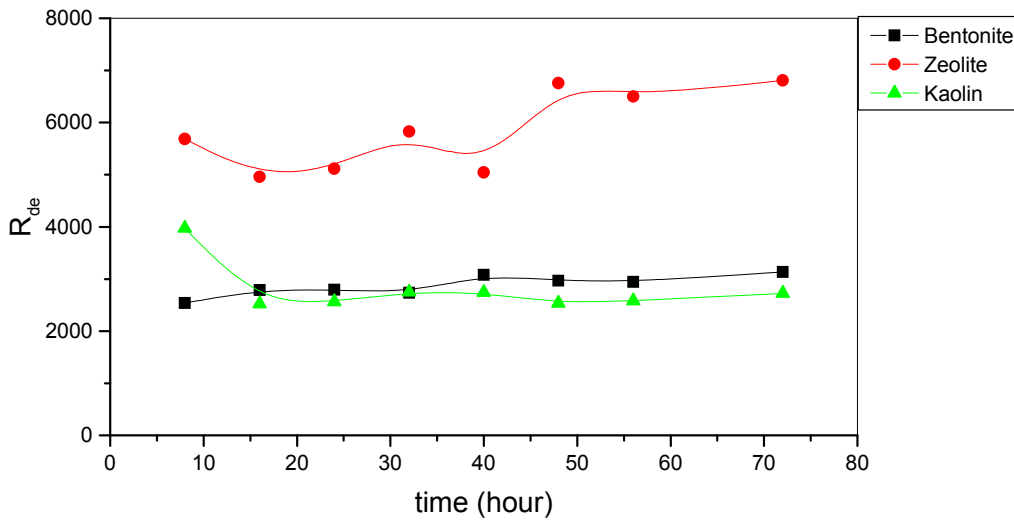


Figure 4.83. $^{137}\text{Cs}^+$ desorption behaviours at 5°C (constant cation concentration $1 \times 10^{-6}\text{M}$).

In sorption studies zeolite showed maximum distribution ratio value for Cs^+ uptake (part 4.2.). The same behaviour was observed in desorption results. Zeolite showed good and strong uptake capacity to caesium; higher R_{de} means it does not release. The amount on solid is 6000 times greater than the amount passed into the groundwater at 10. hour. The cause of the increase in the R_{de} values of Cs^+ is that zeolite re-adsorbed the released cation.

5. CONCLUSION

→ According to the results of the experiments, as the hydration energy increases adsorption decreases. Cs^+ ion behaves likely to be adsorbed rather than be hydrated by water molecules cause of its lower hydration energy. It can move in the channels and vacancies in the structure. But cobalt ion adsorption on zeolite is lowest one due to the very high hydration energy. The more hydrated ion is the largest one; it means that difficult to penetrate and to interact with surface and very hard to displace. For Co^{2+} , the order of uptake capacity is **bentonite > kaolin > zeolite**. The difference between the radiuses reflects in adsorption. For Cs^+ , the order of uptake capacity, in the respect of used adsorbents, is on **zeolite > bentonite > kaolin**. On zeolite, Cs^+ has greteast ΔG° (-17.32 kJ/mol at 5°C) which means highest spontaneity, between the cations, Co^{2+} is less spontaneous due to the its least negative ΔG° (-10.60 kJ/mol at 5°C); it is in accordance with the plots of sorptions.

→ The adsorption of all cations on kaolin is quite less than that on bentonite because of there is no any opportunity of cation exchange between the layers in kaolinite structure. They bonded together very tightly. But montmorillonite layers are bonded to each other weakly; by means of van der Waals bonds. On kaolinite, cation bonding occurs on surface. On montmorillonite exchange achieves mainly between layers rather than on surface. This is valid for all cations.

→ On kaolin and bentonite, the lowest adsorption capacities were obtained by strontium ions. The equilibrium were reached quite late than the other cations too. Comparing β and γ countings with each other is not exactly true also.

→ Caesium does not show high temperature dependence as temperature increases, Cs^+ takes the place in the channels and holes in the structure of zeolite even at 5°C due to the low hydration energy.

According to the thermodynamic parameters:

Zn²⁺- Bentonite, Ba²⁺-Bentonite, Co²⁺ -Bentonite, Sr²⁺- Bentonite, Cs⁺- Bentonite

Zn²⁺- Zeolite, Ba²⁺- Zeolite, Co²⁺- Zeolite, Sr²⁺- Zeolite, Cs⁺- Zeolite

Zn²⁺- Kaolin, Ba²⁺- Kaolin, Co²⁺-Kaolin, Sr²⁺-Kaolin, Cs⁺-Kaolin.

$\Delta G < 0$; indicates the spontaneity of the process, adsorptions are spontaneous over the range 278–298K,

$\Delta G \downarrow$ as temp. \uparrow ; shows that sorption is favoured at high temperatures,

$\Delta H > 0$; shows that the adsorption process is endothermic,

$\Delta S > 0$; fixation cation by clay comes out as positive indicating that more disorder is generated in the system upon. More translational entropy is gained by the ions that are transferred from the sorbent surface to the solution comparing with the decrease in entropy due to removal of ions from solution and their sorption on the sorbent.

→ In general, for all systems high temperatures are more favorable for sorption.

→ In the tables of thermodynamic parameters it is seen that Gibbs enthalpy, ΔG° , is negative for all adsorbent-cation systems that means that sorptions of all cations on adsorbent surface are spontaneous.

→ An other common behavior; as temperature increases ΔG° decreases that means that sorption process favors high temperatures. ΔG° has more negative values at higher temperatures for all investigated systems that indicates the spontaneity of the sorptions.

→ Comparing all of the cations sorptions on kaolin, it is zinc ion uptake which is the most effected one by change in temperature. Its adsorption on bentonite and kaolin increases approximately to 11 times and 13 times respectively by an increase from 5 to 25°C. After zinc, cobalt is coming secondly which shows a

significant increase of adsorption on bentonite. Their hydration energies are very high. This is because of the energy needed in order to overcome the weak van der Waals forces which hold the TOT layers in bentonite is supported by temperature increases. The forces become weakened.

→ The order of spontaneity of Sr^{2+} on adsorbent is kaolin < zeolite < bentonite,
(at higher temperatures bentonite and zeolite change their places),
that of Ba^{2+} is kaolin < zeolite < bentonite,
(at higher temperatures bentonite and zeolite change their places),
that of Co^{2+} is zeolite < kaolin < bentonite,
that of Cs^+ is bentonite < kaolin < zeolite,
that of Zn^{2+} is zeolite < kaolin < bentonite according to the ΔG° values.

→ The other common properties are positive enthalpy of sorption, ΔH° , which means that all of sorptions are endothermic and positive entropy change, ΔS° , gaining more mobility during the sorption for all systems. In this process more translational entropy is gained by the ions that are transferred from the sorbent surface to the solution comparing with the decrease in entropy due to removal of ions from solution and their sorption on the sorbent. It can be concluded that the sorptions are chemically, spontaneous (highly negative Gibbs energy), which means sorptions prefer high temperatures and the sorption process are endothermic (positive enthalpy of sorption).

→ The higher R_{de} value indicates that the lower desorption, which means it does not release. As the temperature increases especially on kaolin desorption decreases, means that desorption ratio, R_{de} , increases, for zinc ion especially, 2900 to about 17000. In other words, kaolin doesn't release the amount of Zn^{2+} sorbed on it at high temperatures. Both sorption and desorption experiments zinc ion results show the maximum temperature dependence on kaolin and barium ion results show the maximum temperature dependence on zeolite.

REFERENCES

- Akar, D., Shahwan, T. and Erođlu, A.E., 2005, Kinetic and thermodynamic investigations of strontium ions retention by natural kaolinite and clinoptilolite minerals, *Radiochimica Acta*, 93(8), 477-485.
- Andrews J. N. And Hornsey D. H., 1972, *Basic Experiments with Radioisotopes*, Pitman Publishing, 18.
- Armbruster, T., 2001, Clinoptilolite-heulandite: applications and basic research, *Studies in Surface Science and Catalysis*, 135, 13-27.
- Atomic Energy of Canada, 1994, Environmental impact statement on the concept for disposal of Canada's nuclear fuel waste, AECL-10711, COG-93-1.
- Atun, G., Bařçetin, E., 2003, Adsorption of barium on kaolinite, illite and montmorillonite at various ionic strengths, *Radiochimica Acta*, volume 91(4), 223-228.
- Bařçetin, E. and Atun, G., 2006, Adsorption behaviour of strontium on binary mineral mixtures of montmorillonite and kaolinite, *Applied Radiation and Isotopes*, 64(8), 957-964.
- Bors, J., Dultz, St. and Riebe, B., 1999, Retention of radionuclides by organophilic bentonite, *Engineering Geology*, 195-206.
- Börgesson, L., Johannesson, L.E. and Gunnarsson, D., 2003, Influence of soil structure heterogeneities on the behaviour of backfill materials based on mixtures of bentonite and crushed rock, *Applied Clay Science*, Volume 23(1-4), 1.
- Chmielewská-Horvátová, E., 1998, The interaction mechanisms between aqueous solutions of ^{137}Cs and ^{134}Ba radionuclides and local natural zeolites for an deactivation scenario, *Journal of Radioanalytical and Nuclear Chemistry*, 227(1-2), 151-155.
- Cole, T., Bidoglio G., Soupioni M., O'Gorman, M., and Gibson, N., 2000, Diffusion mechanisms of multiple strontium species in clay, *Geochimica et Cosmochimica Acta*, Volume 64(3), 385-396.
- Ebina, T., Iwasaki, T., Onodera, Y. and Chatterjee, A., 1999, A comparative study of DFT and XPS with reference to the adsorption of caesium ions in smectites, *Computational Materials Science*, Volume 14(1-4), 254-260.
- Elizondo, N.V., Ballesteros, E. and Kharisov, B.I., 2000, Cleaning of liquid radioactive wastes using natural zeolites, *Applied Radiation and Isotopes*, 52, 27-30.
- Ericsson, L.O., 1999, Geoscientific R&D for high level radioactive waste disposal in Sweden-current status and future plants, *Engineering Geology*, 52, 305-317.
- Ersoy, B. and Çelik, M.S., 2002, Electrokinetic properties of clinoptilolite with mono-and multivalent electrolytes, *Microporous and Mesoporous Materials*, 55(3), 305-312.
- Erten, H.N. and Gokmenoglu, Z., 1994, Sorption behavior of Co^{2+} , Zn^{2+} , and Ba^{2+} ions on alumina, kaolinite and magnesite, *Journal of Radioanalytical and Nuclear Chemistry*, 182(2), 375-384.

- Erten, H.N., Aksoyoglu, S. and Göktürk, H., 1988, Sorption/desorption of Cs on clay and soil fractions from various regions of Turkey, *The Science of the Total Environment*, 69, 269-296.
- Eylem, C., Erten, H.N. and Göktürk, H., 1989, Sorption of barium on kaolinite, montmorillonite and chlorite, *Analyst*, 114, 351-353.
- Fernández, A. M., Baeyens, B., Bradbury, M., Rivas, P., 2004, Analysis of the porewater chemical composition of a Spanish compacted bentonite used in an engineered barrier_files, *Physics and Chemistry of the Earth*, Vol. 29(1), 105-118.
- Garney, B.W., 1995, Zeolites, US Patent 5470557.
- Gonzales-Pradas, E., Villafranca-Sanchez, M., Canton-Cruz, F., Socias-Viciano, M., Fernandez-Perez, M., 1994, Adsorption of cadmium and zinc from aqueous solution on natural and activated bentonite, *J. Chem. Tech. Biotechnol.* 59, 289–295.
- Grim, R.E., 1953, *Clay Mineralogy*, 1st Ed., McGraw-Hill, New York, 384 p.
- Gupta, G.C. and Harrison, F.L., 1980, Effect of kaolin concentration on distribution coefficient of copper, *Water, Air, and Soil Pollution*, 13(2), 247-250.
- Güray, Şebnem, 1997, Master S. Thesis, Removal of lead from water by natural clinoptilolite, 75.
- Hall, P.L., 1987, Clays: their significance, properties, origins and uses, in *A Handbook of Determinative Methods in Clay Mineralogy*, M.J. Wilson (ed.), Blackie & Son Ltd., London, 1-25.
- Ikhsan, J., Johnson, B. B. and Wells, J. W., 1999, A comparative study of the adsorption of transition metals on kaolinite”, *Journal of Colloid and Interface Science* 217, 403-410.
- International Atomic Energy Agency, 1994, A Publication Within the Radwaste Programme, Classification of Radioactive Waste, A Safety Guide.
- Jedinakova-Krizova, V., 1996, Radionuclides migration in the geosphere and their sorption on natural sorbents, *Journal of Radioanalytical and Nuclear Chemistry*, 208(2), 559-575.
- Jeong, C.H., 2001, Mineralogical and hydrochemical effects on adsorption removal of cesium-137 and strontium-90 by kaolinite, *Journal of Environmental Science and Health: Part A - Toxic/Hazardous Substances & Environmental Engineering*, 36(6), 1089-1099.
- Kapoor, A., Viraraghavan, T., 1998, Use of immobilized bentonite in removal of heavy metals from wastewater, *J. Environ. Eng.* 124 (10) 1020–1024.
- Kaya, A. and Ören, A. H., 2005, Adsorption of zinc from aqueous solutions to bentonite, *Journal of Hazardous Materials*, Volume 125(1-3), 18
- Kaya, A., Durukan, S., 2004, Utilization of bentonite-embedded zeolite as clay liner, *Applied Clay Science* 25, 83-91.
- Khan, S. A., Rehman, R. and Khan, M.A., 1995, Sorption of strontium on bentonite, *Waste Management*, Volume 15, Issue 8, 641-650.

- Khan, S.A., Rehman, R. and Khan, M. A., 1995, Adsorption of chromium (III), chromium (VI) and silver (I) on bentonite, *Waste Management*, Vol. 15(4), 271-282.
- Komine, H., 2004, Simplified evaluation for swelling characteristics of bentonites, *Engineering Geology*, 71(3-4), 265-279.
- Konan Koffi Léon, Peyratout Claire, Bonnet Jean-Pierre, Smith Agnès, Jacquet Alain, Magnoux Patrick and Ayrault Philippe, 2007, Surface properties of kaolin and illite suspensions in concentrated calcium hydroxide medium, *Journal of Colloid and Interface Science*, 307 (1), 101-108.
- Krumhansl, J.L., Brady, P.V. and Anderson, H.L., 2001, Reactive barriers for ¹³⁷Cs retention, *Journal of Contaminant Hydrology*, 47, 233-240.
- Liu, J., Kozaki T., Horiuchi, Y., Sato, S., 2003, Microstructure of montmorillonite/silica sand mixture and its effects on the diffusion of strontium ions, *Applied Clay Science* 23, 89-95.
- Marinin, D.V. and Brown, G.N., 2000, Studies of sorbent/ion-exchange materials for the removal of radioactive strontium from liquid radioactive waste and high hardness groundwaters, *Waste Management*, 20, 545-553.
- Martin, R.T., 1991, Report of the Clay Minerals Society Nomenclature Committee: Revised Classification of Clay Minerals, *Clays and Clay Miner.*, 39(3), 333-335.
- Mellah, A. and Chegrouche, S., 1997, The removal of zinc from Aqueous Solutions By Natural Bentonite, *Wat. Res.* 31(3), 621-629.
- Mishra, S.P., and Tiwary, D., 1999, Ion exchangers in radioactive waste management: Part XI. Removal of barium and strontium ions from aqueous solutions by hydrous ferric oxide, *Applied Radiation and Isotopes*, 51, 359-366.
- Missana, T. and Adell, A., 2000, On the applicability of DLVO theory to the prediction of clay colloids stability, *Journal of Colloid and Interface Science* 230, 150–156.
- Missana, T., Turrero, M. J. and Melon A., 1999, *Mater. Res. Soc. Symp. Proc.* 556, 647.
- Montes-H, G., Fritz, B., Clement, A. and Michau, N., 2005, A simplified method to evaluate the swelling capacity evolution of a bentonite barrier related to geochemical transformations, *Applied Geochemistry*, 20(2), 409-422.
- Murray, H.H., 2002, Clays, in Ullmann's Encyclopedia of Industrial Chemistry, 6th Ed.
- Naseem, R. and Tahir, S. S., 2001, Removal of Pb(II) from aqueous/acidic solutions by using bentonite as an adsorbent, *Water Research*, 35(16), 3982-3986.
- Nilchi, A., Maalek, B., Khanchi, A., Maragheh, M.G., Bagheri, A. and Savoji, K., 2006, Ion exchangers in radioactive waste management: Natural Iranian zeolites, *Applied Radiation and Isotopes*, 64(1), 138-143.
- Ören, A. H. and Kaya, A., 2006, Factors affecting adsorption characteristics of Zn²⁺ on two natural zeolites, *Journal of Hazardous Materials*, volume 131(1-3), 59-65.

- Parkman, R. H., Charnock, J. M., Livens, F. R., and Vaughan, D. J., 1998, A study of the interaction of strontium ions in aqueous solution with the surfaces of calcite and kaolinite, *Geochimica et Cosmochimica Acta*, Vol. 62(9), 1481-1492.
- Plecas, I., Pavlovic, R. and Pavlovic, S., 2004, Leaching behaviour of ^{60}Co and ^{137}Cs from spent ion exchange resins in cement-bentonite clay matrix, *Journal of Nuclear Materials*, 327, 171-174.
- Rafferty, P., Shiao, S.-Y., Binz, C. M. and Meyer, R.E., 1981, Adsorption of Sr(II) on clay minerals: Effects of salt concentration, loading, and pH, *Journal of Inorganic and Nuclear Chemistry*, Volume 43(4), 797-805.
- Reyes, S. C., Sinfelt, J. H., DeMartin, G.J., Ernst, R. H., 1999, The role of adsorption on the observed temperature dependencies of diffusion coefficients, *Catalysis Today*, 53, 339-342.
- Roland, E. and Kleinschmit, P., 2002, Zeolites, in Ullmann's Encyclopedia of Industrial Chemistry, 6th Ed.
- Salles Fabrice, Henry Marc, Douillard Jean-Marc, Determination of the surface energy of kaolinite and serpentine using PACHA formalism—Comparison with immersion experiments, 2006, *Journal of Colloid and Interface Science* 303, 617–626.
- Shahwan, T., Erten, H.N. and Unugur, S., 2006, A characterization study of some aspects of the adsorption of aqueous Co^{2+} ions on a natural bentonite clay, *Journal of Colloid and Interface Science*, Volume 300(2), 447-452.
- Shahwan, T. and Erten, H.N., 2002, Thermodynamic parameters of Cs^+ sorption on natural clays, *Journal of Radioanalytical and Nuclear Chemistry*, 253(1), 115-120.
- Shahwan, T., Atesin, A.C., Erten, H.N. and Zararsiz, A., 2002, Uptake of Ba^{2+} ions by natural bentonite and CaCO_3 : A radiotracer, EDXRF and PXRD study, *Journal of Radioanalytical and Nuclear Chemistry*, 254(3), 563-568.
- Shahwan, T., Sayan, S., Erten, H.N., Black, L., Hallam, K.R. and Allen, G.C., 2000, Surface spectroscopic studies of Cs^+ , Ba^{2+} sorption on chlorite-illite mixed clay, *Radiochimica Acta*, 88, 681-686.
- Shelef, M., 1995, Selective catalytic reduction of NO_x with N-free reductants, *Chemical Reviews*, 95(1), 209-225.
- Sheta, A. S., Falatah, A. M., Al-Sewailem, M. S., Khaled, E. M. and Sallam, A. S. H., 2003, Sorption characteristics of zinc and iron by natural zeolite and bentonite, *Microporous and Mesoporous Materials*, Volume 61(1-3), 127-136.
- Singh, R., Dutta, P.K., 1999, Use of surface-modified zeolite Y for extraction of metal ions from aqueous to organic phase, *Microporous and Mesoporous Materials*, 32, 29-35.
- Swartzen-Allen, S.L. and Matijević, E., 1974, Surface and colloid chemistry of clays, *Chemical Reviews*, 74(3), 385-400.
- Swedish Nuclear Fuel and Waste Management, 1992, SKB91 final disposal of spent nuclear fuel, Importance of the bedrock for safety. SKB Technical Report 92-20.

- Tahir, S.S., Naseem, R., 2003, Thermodynamic studies of Ni(II) adsorption onto bentonite from aqueous solution, *J. Chem. Thermodynamics*, 35, 2003–2009.
- Teppen Brian J. and Miller David M., 2006, Hydration Energy Determines Isovalent Cation Exchange Selectivity by Clay Minerals, *Soil Science Society of America*, 70:31-40.
- Tsai, S.C., Juang, K.W., 2000, Comparison of linear and nonlinear forms of isotherm models for strontium sorption on a sodium bentonite, *J. Radioanal. Nucl. Chem.*, 243 (3), 741.
- Tsai, S.-C., Ouyang, S. and Hsu, C.-N., 2001, Sorption and diffusion behaviour of Cs and Sr on Jih-Hsing bentonite, *Applied Radiation and Isotopes*, 54, 209-215.
- van Olphen, H., 1977, *An introduction to clay colloids chemistry*, Wiley Interscience, New York.
- Warnecke, E. and Brennecke, P., 2002, Radioactive Waste Management, Section 5.5., in *Ullmann's Encyclopedia of Industrial Chemistry*, 6th Ed.
- Xu, Y. F., Sun, D. and Yao, Y., 2004, Surface fractal dimension of bentonite and its application to determination of swelling properties, *Chaos, Solitons & Fractals*, Volume 19(2), 347-35.
- Yavuz, Ö., Altunkaynak, Y. and Güzel, F., 2003, Removal of copper, nickel, cobalt and manganese from aqueous solution by kaolinite, *Water Research*, 37(4), 948-952.

CURRICULUM VITAE

Name & Surname : BERNA YILDIZ

Place of Birth : ANKARA

Date of Birth : 07.07.1973

Marital Status : Single

Education and Academic Life

High School : 1984-1991 Ankara Anadolu High School, French Division

B.Sc. : 1992-1997 Hacettepe University, Department of Chemistry

M.Sc. : 1998-2001 Hacettepe University, Department of Chemistry

PhD. : 2001- 2007 Hacettepe University, Department of Chemistry

PhD. Apprenticeship : 12.03.2007-11.05.2007 Radiochemistry Group of the Nuclear Physics Institute in Orsay University (Paris-Sud XI)

Foreign Language : English, French

Work Experience

1996 Summer stage : Turkish Standards Institute, Textile and Detergent Laboratories

1999-2007 : Research Assistant, Hacettepe University, Chemistry Department